Three-Dimensional Stress Analysis of Single Lap Adhesive Joints with and without a Hole

by

Rajat Bansal

A thesis submitted in partial fulfilment
of the requirements for the degree of
Master of Science in Engineering
(Automotive Systems Engineering)
in the University of Michigan–Dearborn
2018

Master's Thesis Committee:

Professor Pankaj K. Mallick, Chair
Lecturer Vivek Bhise
Assistant Professor Tanjore V. Jayaraman

To my Parents

and Friends

ACKNOWLEDGMENTS

I would like to express my gratitude to Prof. P. K. Mallick for the guidance and support he gave me during this project. His advice and insights were crucial in my completion of the project.

I would like to thank Prof. Vivek Bhise and Prof. Tanjore V. Jayaraman for taking time to serve on my thesis committee. Their valuable suggestions are much appreciated.

I would also like to thank my friends and family members for the support they provided me during my studies.

Finally, I would like to thank Sherry Boyd for helping me with administrative issues that made my work on the project run a lot smoother.

TABLE OF CONTENTS

LIST OF FIGURES

LIST OF TABLES

ABSTRACT

Conventional joining techniques, such as resistance spot welding and gas metal arc welding are commonly used for sheet metal steel parts in automotive applications. While there is a rising need for utilizing light weight metals, such as aluminum alloys, magnesium alloys and fiber reinforced composites in body in white (BIW) applications, finding joining technologies compatible with properties of these new materials without compromising on the joint strength is very challenging. Unlike steels, welding techniques are not suitable for most lightweight materials; so there is a major need to explore other joining techniques such as adhesive bonding, that can provide for high joint strength and long term structural integrity.

This study focuses on determining stresses in an adhesive bonded lap joint between two magnesium substrates with and without a hole. The prime motivation for this work is to investigate if the stresses in the adhesive layer can be reduced by either applying lateral pressure in the overlap area or by combining the adhesive joint with a mechanical fastener. Since mechanical fastening using a bolted connection requires drilling a hole through the substrates and the adhesive layer, the effect of a hole on the stresses in the adhesive layer is also of interest in this study.

A linear elastic three-dimensional finite element stress analysis was performed to determine stresses in a single lap adhesive joint of two magnesium substrates under a tensile force. Stress distributions in the length, thickness and width directions of the adhesive layer were determined and the effect of substrate thickness difference on the maximum stresses were examined. In an adhesive joint without a hole, high tensile peel stress and high in-plane shear stress are present at the lap ends, both of which are known to contribute to joint failure. The difference in substrate thicknesses increases both peel and shear stresses. The lateral pressure in the overlap area creates compressive stresses that can be beneficial in preventing failure due to high peel and shear stresses at the lap ends. With a hole at the center of the overlap, high tensile stresses are created at the hole boundary. If a clamping pressure is applied around the hole, these stresses are reduced substantially and can even become compressive in nature, which is also beneficial for improved joint strength.

CHAPTER I

Introduction

Growing industry standards and challenging fuel economy targets in the mobility industry are greatly increasing the need for new and innovative lightweight solutions. Engineers and researchers in the automotive industry are trying to develop advanced solutions directed toward developing lightweight vehicle body structures to meet the fuel economy targets. Reduction in vehicle weight is becoming crucial for improving fuel efficiency and reducing exhaust gas emissions. Alternative materials being developed as potential lightweight solutions for vehicle body shells are advanced high strength steels, aluminum and magnesium alloys, and fiber reinforced composites. Another parallel research area is the joining technologies which can be used to join these new lightweight materials without compromising on the joint strength requirements as per the FMVSS and other regulatory standards. In recent years, sheet material joining techniques have been developed rapidly for joining advanced lightweight materials that are dissimilar, coated and relatively hard to weld [1, 2]. Thus, to obtain light-weight vehicle body shells having strength of conventional body exteriors, joining of dissimilar materials becomes one of the critical design issues that must be addressed for safe and long-term use of the vehicle structure.

Figure 1.1 shows various joining techniques currently used to assemble vehicle exterior shells. Since steel is the principal material of construction in today's automobiles, the most common joining technique is resistance spot welding (mainly due to the high strength of spot welds and availability of reliable and cost-effective industrial equipment/robots). As the use of aluminum, magnesium and fiber reinforced composites in vehicle today increases, joining techniques that are gaining increasing attention are adhesive bonding followed by mechanical fastening, especially for joining dissimilar materials in high-strength applications [4]. A

combination of these two joining techniques is also of interest, since such a combination can provide improved performance in some applications requiring long-term durability in fatigue.

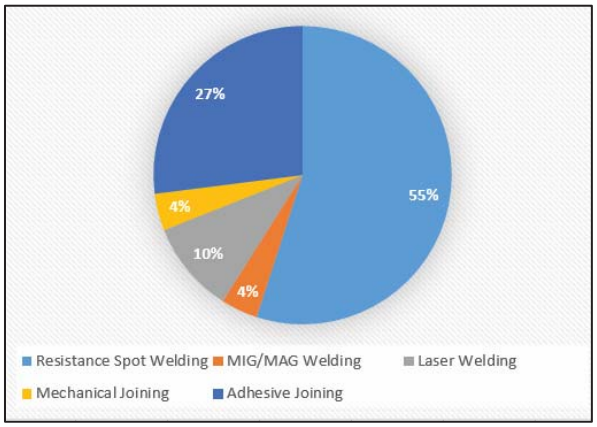

Figure 1.1: Joining techniques used in the automotive industry [3, 39]

1.1 Literature Review on Adhesive Bonding

Various sections in this chapter highlight key concepts and brief reviews of selected past research in the context of adhesive bonding which is the core interest area of this study. Concepts ranging from types of adhesive bonds, their failure mechanisms and strength improvement techniques are discussed. This chapter also highlights the new research concepts in the field of adhesive bonding that align with the objectives of this study.

Adhesive bonding has been traditionally used as a joining method in vast number applications over many centuries. However, only in the last seventy years, the science and technology behind adhesive bonding has progressed significantly [5, 6]. Scientific literature defines adhesive as a polymeric material which, when applied to two or more surfaces, can join them and resist their separation or relative motion against application of forces. The technique of joining materials by the application of adhesives which solidify to produce an adhesive bond is known as adhesive bonding. Adhesively bonded joints are increasing alternatives to mechanical joints in automotive applications providing many advantages over conventional mechanical fastening techniques.

The advantages in adhesive joining over other conventional joining methods include (a) weight reduction and material cost savings (by elimination of fasteners), (b) reduction in number

of parts to be designed and managed (screws, washers etc. can be eliminated from the assembly process), (c) reduction in complexity of machinery and machining operations (hole drilling machines, torqueing equipment for screws), (d) better overall surface finish, (e) higher strength to weight ratio than conventional joining techniques, (f) good electrical and thermal insulation, and (g) higher fatigue resistance [7].

1.1.1 Mechanisms of Adhesion

Adhesive bonding is known to occur due to a combination of the following mechanisms.

(a) Mechanical Interlocking: Adhesive penetrates the surface of the substrate, displacing the trapped air at the interface. The effects of mechanical interlocking, clean surface, formation of a reactive surface and improvement is surface area [8].

(b) Adsorption: Adsorption occurs due to contact at molecular levels and corresponding surface forces. Good wetting (the continuous contact between adhesive and adherent) develops when the adhesive flows into the valleys and crevices on the substrate surface as shown in Figure 1.2 [8]. Once wetting is achieved, permanent adhesion results through molecular attraction. These could be electrostatic bonds, covalent bonds, metallic bonds and van der Waals's forces.

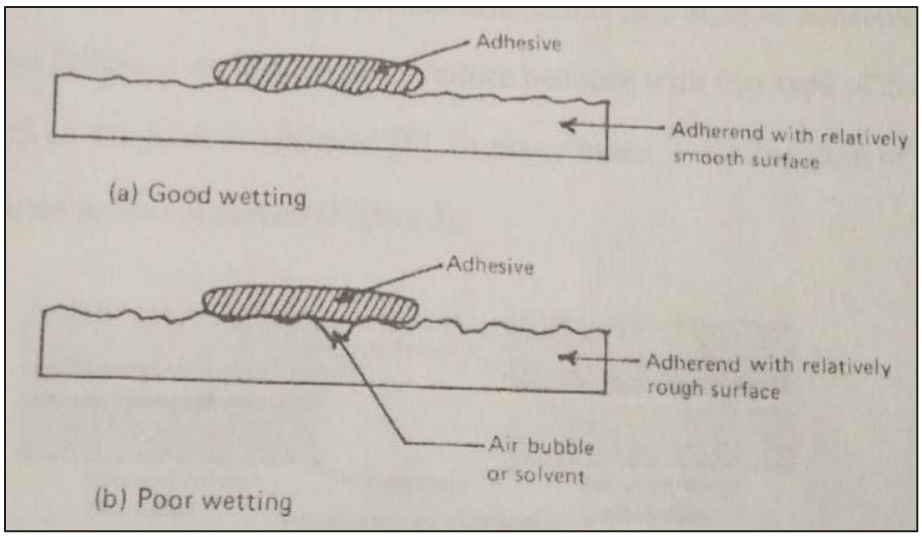

Figure 1.2: Wetting conditions of adhesives

(c) Electrostatic Forces: The electrostatic forces in an adhesive bonding unit form an electrical double layer at the adhesive-adherent interface. Presence of electrical discharges observed during peeling of the adhesive from the substrate form the basis of this adhesion mechanism [8].

(d) Diffusion: This mechanism depends on the inter-diffusion of molecules in the adhesive and the adherent. It is applicable when both the adhesive and adherents are long-chain polymers [8].

(e) Weak-Boundary Layer: Sometimes bond failure results of a cohesive break or a weak boundary layer. The weak layer occurs due to impurity concentrations near the interface. This results in the formation of weak attachment to the surface and an early failure at the adhesive-adherent interface [8].

1.1.2 Joint Configurations

Maintaining strength of joints represent one of the greatest challenges in the design of structures, since they entail geometric discontinuities of the structure and/or material properties, and may result in high local stress concentrations. A wide variety of joints available to a structural designer is discussed by Adams and Wake [9]. Commonly analyzed joint configurations in the literatures are single-lap joints, double-lap joints, scarf joints, and stepped-lap joints. Figure 1.3 shows these four joint configurations pictorially [10].

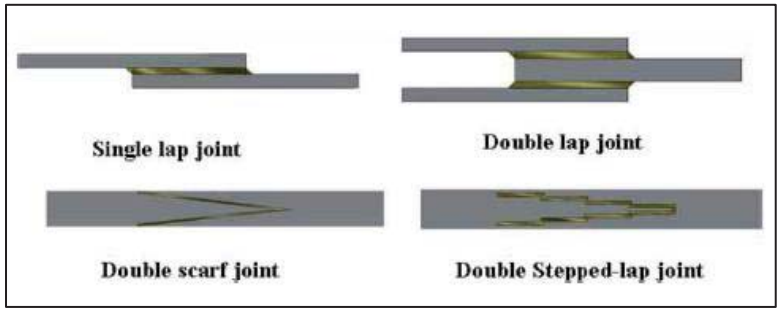

Figure 1.3: Adhesive bonded joint configurations [10]

1.1.3 Failure Mechanisms

Adhesive joints undergo failure either adhesively or cohesively [8]. Adhesive failure occurs when the interfacial bond between the adhesive and adherent fails. Cohesive failure occurs when the adhesive fails away from the interface and leaves a layer of adhesive on both surfaces. Cohesive failures are ideal when considered for structural applications because with this type of failure, the

maximum strength of the joint is achieved [8]. In many cases, a combination of cohesive and adhesive failures is also observed. Figure 1.4 shows the concepts of cohesive, adhesive and a combination of the two failures pictorially.

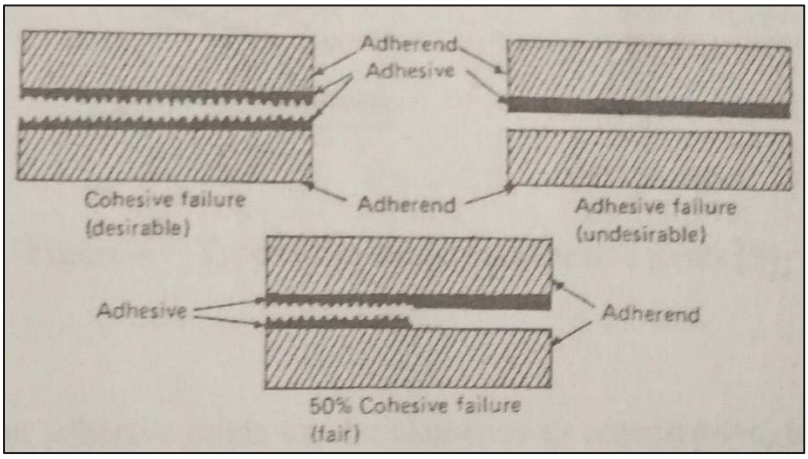

Figure 1.4: Cohesive, adhesive and combination of cohesive/adhesive failures [11]

Cohesive failure usually occurs when low strength adhesives are used. The other causes of bond failure include poor wetting, presence of voids, internal stresses due to the shrinkage of the adhesive during curing and differences in thermal expansion coefficients of the adhesive and the substrates. The type of loading, loading rate and operating environment are also important in determining the strength and durability of adhesive bonds. Adhesive joints often display reduction in strength with aging. Sustained loading can cause premature failure.

1.1.4 Loadings on Adhesive Joints

Figure 1.5 shows different types of loadings on adhesive joints. They can be classified as compressive, tensile, shear, peel and cleavage. A combination of these loadings may also occur in many practical applications. Figure 1.5(a) shows a joint in compression where forces act towards the joint interface. Such joints are less likely to fail; however they are limited in applications. Tensile loading on adhesive joints Figure 1.5(b) is not desirable, since it can cause early failure. Figure 1.5(c) shows shear loading which is generally recommended for load transmission from one substrate to the other. Peel loading depicted in Figure 1.5(d) is more common in flexible

materials. Figure 1.5(e) shows cleavage loading which is caused by offset tensile loads. To accommodate offset loads sufficiently large bonding area is required resulting in an expensive joint.

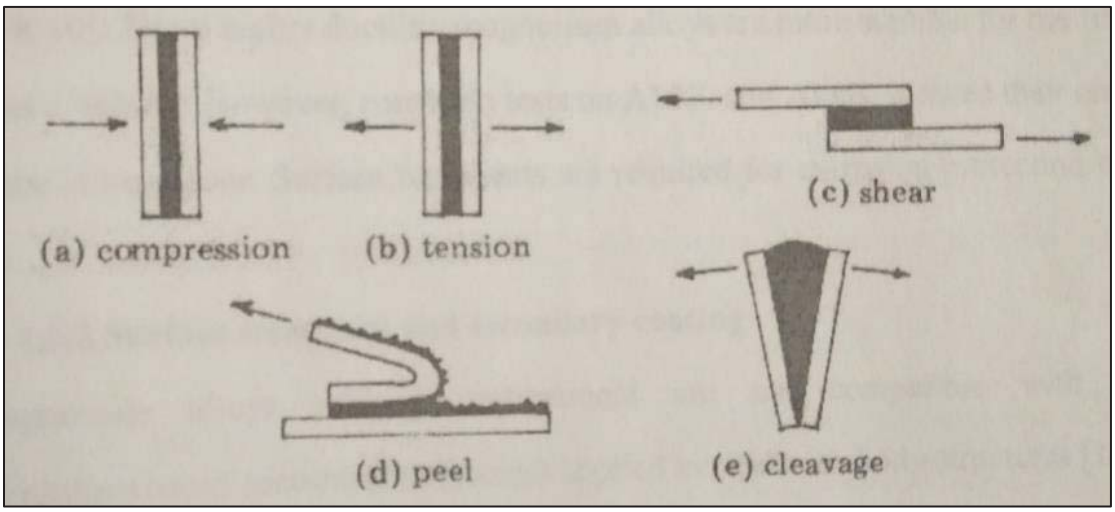

Figure 1.5: Types of loadings on adhesive joints [8]

1.1.5 Analysis of Adhesive Joints

The adhesively bonded single-lap joint has been studied extensively with most of the analytical and theoretical work being focused on predicting the state of stress within the thin adhesive layer. The Finite Element Method (*FEM*) is increasingly being used since it has proven to be an effective tool for obtaining either two- or three-dimensional stress and strain distributions along a loaded joint of complex geometry.

Early theoretical works by Volkersen [29], Goland and Reissner [30] and Hart-Smith [31], which were based on beam models, provided the basic formulations for more refined models such as those by Oplinger [32]. More recently, Tsai et al. and others [33-36] published extensive work on the application of three dimensional (3D) linear elastic and 2D geometrically linear and nonlinear finite element models to analyze single-lap joints with or without a spew fillet. Because of the eccentric loading path of the single lap joint in which large deflections of the adherends and the overlap are generated, the 2D geometrically nonlinear finite element analysis has been found to be a very convenient computational method for approximating the overlap stress and strain distributions. Based on studies by Tsai et al., the maximum tensile peel stresses and strains within

the adhesive bond occur near the adhesive-adherend interface at the corner ends of the joint overlap. The peak peel stresses and strains lie between the centerline and the adhesive-adherend interface. The thicker the adhesive bond layer, the higher the magnitude of the peel stresses and strains, and thus the larger the bending deformation. The magnitude of shear and longitudinal stresses are lower than the peel stresses and are distributed symmetrically along the overlap. The shear stresses reach maximum values at both joint ends. Longitudinal stresses, on the other hand, increase towards the joint ends but drop sharply at the ends itself.

Volkersen's analysis [29] introduced the concept of differential shear illustrated in Figures 1.6 and 1.7. It was initially assumed that the the adhesive deforms only in shear and the adherends deform only in tension, which is shown in Figure 1.6. The tensile stress in the upper adherend is maximum at A (see Fig. 1.6) and decreases to zero at B (free surface), so the strain must also progressively reduce from A to B. The reduction of the strain in the adherends along the overlap and the continuity of the adhesive/adherend interface cause a non-uniform shear strain (and stress) distribution in the adhesive layer. The shear stress is maximum at the ends of the overlap and is much lower in the middle.

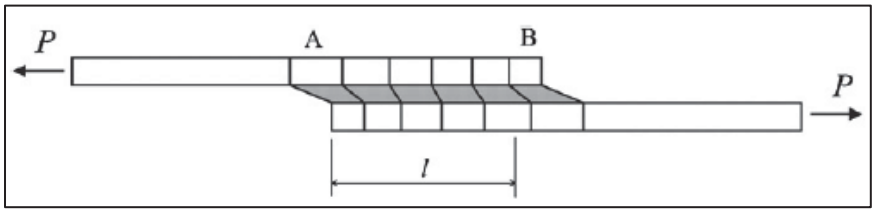

Figure 1.6: Deformations in a loaded single-lap joint with elastic adherends in Volkersen's model [29]

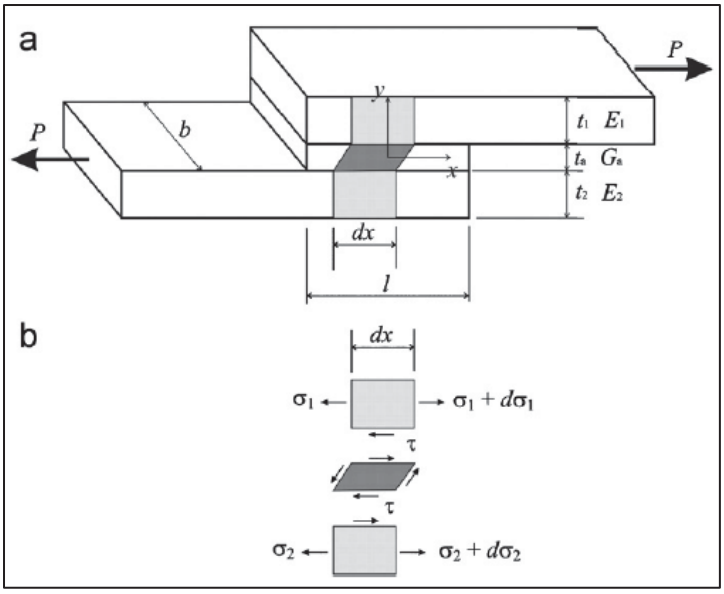

Figure 1.7: Single-lap joint analyzed by Volkersen – (a) Geometry and (b) elemental diagram

Goland and Reissner [30] proposed that the eccentric load path of a single-lap joint causes a bending moment (M), and a transverse shear force (V) to be applied to the joint ends in addition to the applied tensile load P per unit width, as shown in Figure 1.8. Because of this bending moment, the joint rotates, altering the direction of the load line with the tendency of the applied tensile forces to come into line. As the joint rotates, the bending moment decreases, giving rise to a nonlinear geometric problem where the effects of large deflections of the adherends must be accounted for [31].

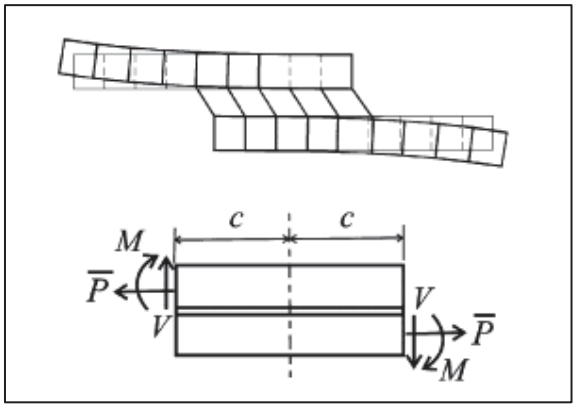

Figure 1.8: Goland and Reissner's model [30]

Oplinger [32] presented a more detailed analysis which departed from the analysis of Goland and Reissner for large adherend-to-adhesive layer thickness ratios; however, his results for large adherend-to-adhesive layer thickness ratios were relatively similar. He not only considered the effects of large deflections (both outside and inside the overlap) but also the individual deformation of the upper and lower adherends in the overlap.

Srinivas [22] did an extensive parametric study of the effect of the transverse and shear deformations in the adherends, and investigated methods of reducing the maximum shear and peel stresses in the adhesive. He showed that neglecting the transverse and shear deformation in the adherends gave a good estimate of the maximum adhesive peel and shear stresses for long overlaps or flexible bonds in both longitudinal and thickness directions. This model however has the disadvantage of needing a numerical solution and ignoring important features such as the variation of the adhesive stresses through the thickness and the stress-free end condition.

Most of the analytical models for adhesively bonded joints are two-dimensional. In these analyses, it is assumed that the adhesive joints are in a state of plane strain in the plane perpendicular to the width direction, neglecting the stresses across the width direction caused by Poisson's ratio strains in the adherends and the anticlastic bending of the adherends. If the joint bending is not severe and the adhesive is brittle, Volkersen'*s* analysis is sufficient. However, if there is yielding of the adhesive and/or the adherends and substantial peeling is present, a more complex model is necessary.

1.1.6 Strength Improvement of Adhesive Joints

Various adhesive joint designs have been developed to improve their strength since it is the basic requirement for selecting them to assemble materials/components. The strength of any joint depends upon the type of applied load and stress distribution within the joint, which in turn depends on the joint geometry and the mechanical properties of adhesive and adherend. From the design requirements point of view, the joint should be designed to minimize stress concentrations to avoid failures and thus to enhance strength. Some stresses, such as peel and cleavage, should be minimized and others like shear and compressive stresses be maximized.

The single-lap joint is the most common joint used mainly due to its simplicity and efficiency. However, one of the problems associated with this joint is the fact that the stress

distribution (shear and peel) is concentrated at the ends of the overlap. Researchers have adopted various techniques to improve the efficiency of the single-lap joints. These include altering the adherend geometry [12–14], adhesive geometry [15, 16] and spew geometry [17-20].

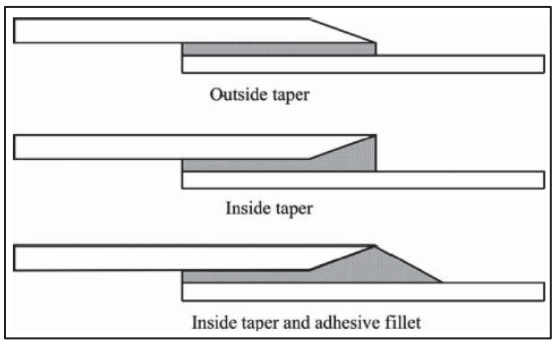

Figure 1.9: Adherend shaping to decrease the peel stresses in the composite joints

Adherend shaping is sometimes used to decrease the peel stresses in the composite joints [10]. Figure 1.9 shows different joints where the upper adherend end has been shaped. These joints will produce stresses that are lower than the standard joints with square ends. Zeng and Sun [21] proposed a novel 'wavy' lap joint configuration (Figure 1.10). In this joint, the through thickness stresses at the edges of the overlap are compressive, which provided a significant improvement in joint strength, especially in fatigue loading.

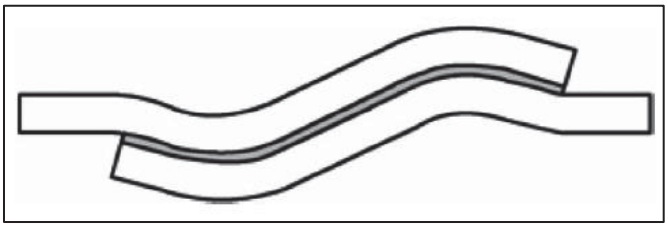

Figure 1.10: 'Wavy' lap joint configuration proposed by Zeng and Sun [21]

Lang and Mallick [16] introduced a new bonding technique called recessing by removing portions of the adhesive layer from the overlap. Their study indicated that average strength of the adhesive bond increases with recessing. This positively contributes towards weight and cost reduction. However, the small effective lap length due to recessing may adversely affect the fatigue failure.

Spew shape and size (the spew is an excess of adhesive squeezed out of the lap region during joint manufacturing) are another two parameters studied to reduce stress concentration [17-20]. The peak stress at the overlap ends is dependent on the size and shape of the spew. It is shown that shaping the spew can provide smoother transition in joint geometry, significantly reducing the stress concentration [17].

One technique currently being intensively investigated to improve the strength of an adhesive joint is the use of more than one adhesive along the overlap i.e. mixed adhesive bonded joint (an adhesive bond line with variable modulus to relieve the high-stress concentrations at the end regions of the overlap) [22–26]. Figure 1.11 shows an example of a mixed adhesive joint having a flexible and ductile adhesive placed at the ends of the overlap and a rigid and brittle adhesive placed at the center of the overlap.

Another technique which could potentially affect the strength of an adhesive joint is varying the adherend material properties in the overlap region. Ganesh et al. [27] have shown that composite materials with continuously varying material properties can be fabricated by modifying conventional braiding technology of fiber placement. They showed that spatial grading of adherend elastic modulus of an adhesively bonded single-lap joint reduced the peak elastic shear stresses and caused more uniformly distributed stresses in the adhesive layer [28].

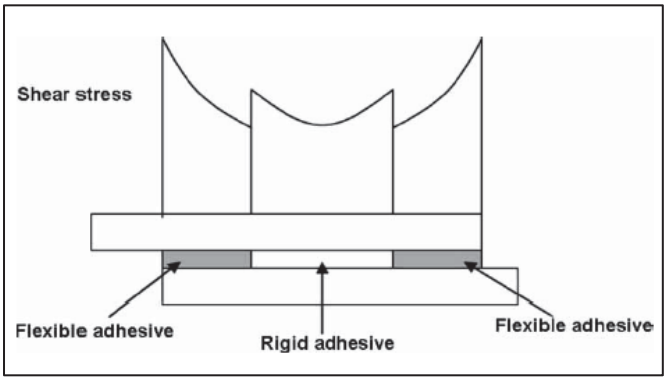

Figure 1.11: Mixed-adhesive bonded joint

1.2 Motivation for the Thesis

To design a cost effective and structurally sound solution for vehicle body structures consisting of highly dissimilar materials, such as steel and magnesium or steel and a fiber-reinforced composite,

adhesive joining is considered the best alternative among various joining techniques available today. In many structural applications, adhesive joining may be a better option compared to mechanical fastening or conventional welding methods. However, it has its several limitations. The key among them is the presence of high peel and shear stresses that limit the strength of adhesive joints. The strengthening methods discussed in Section 1.1.6 are not commonly practiced; instead mechanical fastening is combined with adhesive joining to not only improve the strength, but also to increase the margin of safety and resistance to fatigue failure [37, 38]. The mechanical fasteners, such as bolts and rivets located in the lap area of the adhesive joint share the load applied on the structure. Cracks generated in the adhesive or at the adhesive-substrate interfaces are either stopped or slowed down from progressing along the lap length, thus avoiding a rapid failure. The combination of adhesive joining and mechanical fastening, also called hybrid joining, is used extensively in the aerospace industry and is expected to become more common in the automotive industry.

In order to create a hybrid joining, a hole must be either drilled or punched in the substrates and the adhesive layer through which the mechanical fastener will be inserted in the joint area. The presence of a hole generates an area of stress concentration which will increase the stresses around the hole. The effect of stress concentration will be diminished by the use of clamping force to tighten the fastener onto the substrates. The effect of the stress concentration due to a hole on the stresses in the adhesive layer and its mitigation by the clamping force have not been studied in the past. This study considers this topic by determining the stresses in the adhesive of a single lap adhesive joint with a hole with and without a clamping pressure, and then comparing them with stresses in a similar joint without a hole.

1.3 Objectives of the Thesis

The objectives of the thesis are as follows.

- To determine the stresses in a single-lap adhesive joint with different substrate thickness ratios and without any hole,
- To study the effect of a hole in the lap area on the stresses in the adhesive layer of a single-lap adhesive joint, and

- To study the effect of clamping pressure, which represents the transverse compressive load induced by the clamping torque, on the stresses in the adhesive layer of a single lap adhesive joint.

The substrate material selected in this study is magnesium (Mg). Magnesium is a promising material for automotive use, primarily because of its lower density, which is 36% lower than that of aluminum and 78% lower than that of steel. Mg alloys are already being used in a variety of automotive applications, such as instrument panels, steering wheels and brackets. Now it is being considered for several structural applications, including the front end of a vehicle [3].

1.4 Distribution of Thesis Chapters

A linear elastic three-dimensional finite element stress analysis was performed using a commercial finite element software. Stress distributions in the length, thickness and width directions of the adhesive layer were determined in Chapter 2. The effects of substrate thickness and lateral pressure on the maximum stresses were also examined in Chapter 2. The effects of hole size and hole location in the lap area were considered in Chapter 3. The addition of clamping pressure around the hole was also investigated in Chapter 3.

References

1. He X., Recent development in finite element analysis of clinched joints, Int J Adv Manuf Technol, 2010; 48:607.

2. He X., Pearson I, Young K. and J Mater, Self-pierce riveting for sheet materials, Process Technol, 2008; 199 (1-3):27.

3. Symietz, D., Structural adhesive bonding: The most innovative joining technique for modern lightweight design, safety and modular concepts, SAE Technical Paper Series, Switzerland, Vol. 01. 1747, 2005.

4. Kim KS, Yi YM, Cho GR and Kim CG, Failure prediction and strength improvement of uni-directional composite single lap bonded joints, Composite structures, 2008; 82:513-520.

5. Speth DR, Yang Y and Ritter GW, Qualification of adhesives for marine composite-to-steel applications, Int J Adhes Adhes, 2010; 30 (2):55.

6. Marshall SJ, Bayne SC, Baier R, Tomsia AP and Marshall GW, A review of adhesion science, Dental Mater, 2010; 26 (2):e11.

7. Landrock, A.H., Adhesives Technology Handbook, Park Ridge, NJ:Noyes Publications, 1985.

8. Bikerman,J.J., Cause of poor adhesion, Industrial and Engineering Chemistry, 1967; 59 (40-44).

9. Adams, R.D. and Wake, W.C., Structural adhesive joints in engineering, 1984; 15 (Elsevier, NewYork).

10. M D Banea and LFM da Silva, Adhesively bonded joints in composite materials: An overview, Journal of Material Design and Applications, 2009; 223:1.

11. Wang W., Adhesive joining of magnesium alloys, Master's Thesis, University of Michigan-Dearborn, 2009; 2-8.

12. Kim, J.-S., Kim C.G., and Hong C.S., Practical design of tapered composite structures using the manufacturing cost concept, Compos. Struct., 2001; 51 (3): 227-235.

13. Da Silva, L.F.M. and Adams R.D., Techniques to reduce the peel stresses in adhesive joints with composites, Int. J. Adhesion Adhes., 2007; 27 (3): 227-235.

14. Kaye, R.H. and Heller, M., Through thickness shape optimization of bonded repairs and lap joints, Int. J. Adhesion Adhes., 2002; 22 (1).

15. Mazumdar, S. K. and Mallick, P. K., Static and fatigue behavior of adhesive joints in SMC-SMC composites, Polym. Compos., 1998, 19(2), 139–146.

16. Lang, T. and Mallick, P. K., The effect of recessing on the stresses in adhesively bonded single-lap joints, Int. J. Adhesion Adhes., 1999, 19(4), 257–271.

17. Lang, T. and Mallick, P. K., Effect of spew geometry on stresses in single lap adhesive joints, Int. J. Adhesion Adhes., 1998, 18(3), 167–177.

18. Wang,C. H., Heller, M., and Rose, L. R.F., Substrate stress concentrations in bonded lap joints, J. Strain Anal. Eng. Des., 1998, 33(5), 331–346.

19. Rispler, A. R., Tong, L., Steven, G. P., and Wisnom, M. R., Shape optimisation of adhesive fillets, Int. J. Adhesion Adhes., 2000, 20(3), 221–231.

20. Belingardi, G., Goglio, L., and Tarditi, A. Investigating the effect of spew and chamfer size on the stresses in metal/plastics adhesive joints, Int. J. Adhesion Adhes., 2002, 22(4), 273–282.

21. Zeng,Q. and Sun,C.T., Novel design of bonded lap joint, AIAA J., 2001, 39, 1991–1996.

22. Srinivas, S. Analysis of bonded joints. NASA TN D-7855, 1975.

23. Patrick, R. L. (Ed.), Treatise on adhesion and adhesives – structural adhesives with emphasis on aerospace applications, 1976, vol. 4 (Marcel Dekker, Inc., New York).

24. Fitton, M. D. and Broughton, J. G., Variable modulus adhesives: an approach to optimized joint performance, Int. J. Adhesion Adhes., 2005, 25(4), 329–336.

25. da Silva, L. F. M. and Adams, R. D., Joint strength predictions for adhesive joints to be used over a wide temperature range, Int. J. Adhesion Adhes., 2007, 27(5), 362–379.

26. da Silva, L. F. M. and Adams, R. D., Adhesive joints at high and low temperatures using similar and dissimilar adherends and dual adhesives, Int. J. Adhesion Adhes., 2007, 27(3), 216–226.

27. Ganesh, V. K., Ramakrishna, S., and Leck, H. J., Fiber reinforced composite based functionally gradient materials, Adv. Compos. Letters, 1998, 7, 111–115.

28. Ganesh, V. K. and Choo, T. S., Modulus graded composite adherends for single-lap bonded joints, J. Compos. Mater., 2002, 36(14), 1757–1767.

29. Volkersen O., Die nietkraftverteilung in zugbeanspructen nietverbindungen mit konstanten laschenquerschnitten, Luftfarhrtforschung 1938; 15:41-7.

30. Goland M and Reissner E., The stresses in cemented joints, J Appl. Mech. 1944, 11: A17-27.

31. Hart-Smith LJ., Adhesive-bonded single-lap joints, CR-112235. NASA Langley Research Center, 1973.

32. Oplinger, D.W., Effects of adherend deflections in single-lap joints, Int J Solids Struct 1994; 31: 2565-87.

33. Tsai MY and Morton J., Three-dimensional deformations in a single-lap joint, J Strain Anal 1994; 29:137-45.

34. Sawa T, Suzuki Y, Watanabe S and Horiuchi M., An elasto-plastic finite element analysis of single-lap adhesive joints subjected to tensile shear loads, Trans. of the Japan Society of Mechanical Engineers, Part A, 1993; 59:1881-7.

35. Tsai MY and Morton J., The effect of a spew fillet on adhesive stress distributions in laminated composite single-lap joints, Composite Structures 1995; 32:123-31.

36. Tsai MY, Morton J and Matthews J., Experimental and numerical studies of a laminated composite single-lap adhesive joint, J Composite Mater 1995; 29:1154-275.

37. Fu, M. and Mallick, P.K., Fatigue of hybrid (adhesive/bolted) joints in SRIM, International J. Adhesion and Adhesives, 2001; 21:145-159.

38. Kelly, G., Load transfer in hybrid (bonded/bolted) composite single-lap joints, Composite Structures. 2005; 69: 35-43.

39. Bhambure, S.A., Stress analysis of adhesive joints with magnesium alloys, Master's Thesis, Automotive Systems Engineering, University of Michigan-Dearborn, 2011.

CHAPTER 2

3D-Stress Analysis of Mg-Mg Adhesive Joints without a Hole

2.1 Introduction

This chapter will investigate the stress distributions and maximum stresses in the adhesive layer in a single lap adhesive joint between two magnesium substrates without a hole. Three-dimensional finite element analysis was performed to determine the stress distributions in the length, width and thickness directions of the adhesive layer due to a tensile load applied on the substrates. The finite element model developed in this chapter is focused on studying the stresses without emphasizing on the failure load of the joint (in line with the objective of our study). The following sections of this chapter will explain the finite element model and present results for stress analysis of the adhesive lap joint.

Many researchers have performed stress analysis of single-lap adhesive joints in the past. Their work is briefly cited in the Literature Review section in Chapter 1. The first stress analysis of single lap joints was published in 1938, which was based on the assumption that the adhesive joints experience only shear deformation [1]. Since then, there have been numerous publications, some of which have given analytical solutions, while others have used numerical methods, such as finite element analysis (*FEA*). However, a vast majority of these publications are two-dimensional in nature [1-4] and investigated the stresses in the length and thickness directions of the joint. Stresses in the width direction of the joint were neglected, even though they can be a significant contributor to predicting the mechanical behavior of the joint and its failure mode. Recently, several publications have appeared in which *FEA* was used to determine stresses in all three directions [5-7].

In this chapter, a baseline finite element model is established to determine stresses in all three directions in a Mg-Mg single lap adhesive joint without a hole. The next chapter extends the study by considering the presence of a hole. In addition to stresses in the adhesive layer, two

additional studies are included in this chapter. In one of these studies, the effect of difference in substrate thickness on the maximum stresses is investigated. In the second study, the effect of the application of lateral pressure in the overlap area in mitigating the detrimental peel stresses is considered. The loads acting on the substrates in a single lap joint are not collinear, which gives rise to the bending effect and ultimately peel stresses (σ_{zz}) in the adhesive layer. Peel stresses often cause failure in the adhesive or at the adhesive-substrate interface.

2.2 Finite Element Model

2.2.1 Specimen Dimensions and Material Properties

The selected specimen dimensions and axis location used for the single lap joints are shown schematically in Figure 2.1. The length and width dimensions of both substrates are 100 mm and 25 mm, respectively. Both substrates have a uniform thickness of 2 mm. The length of the overlap is 12.5 mm and the adhesive thickness is assumed to be 0.25 mm [7]. The location of the origin and the co-ordinate axis directions are also defined in Figure 2.1. The adhesive layer has been assumed to have square ends. In practice, unless the adhesive ends are cleaned after applying the adhesive, there will be a small spew, which is created by the squeezed-out adhesive at each end. Several investigators have observed in the past that the presence of spew reduces the maximum stresses in the adhesive layer [2-4]. However, this study considers that no spew is present at the adhesive ends, i.e. the specimen was subjected to a treatment to remove the spew prior to applying the load.

The elastic properties of the substrate material, namely magnesium alloys, and the adhesive material are listed in Table 2.1. The adhesive is an unfilled epoxy, which is a common adhesive material in the automotive and aerospace industries. The adhesive properties listed in Table 2.1 are typical of those that are obtained after curing the adhesive.

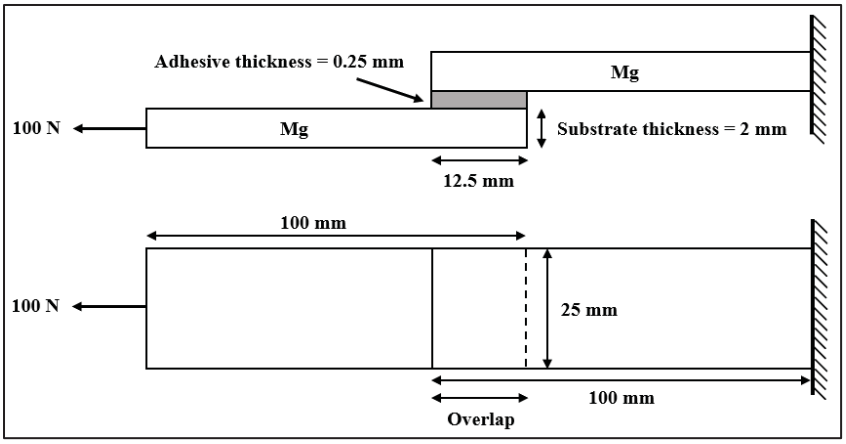

Figure 2.1 Specimen dimensions

Table 2.1: Material properties [7]

Adhesive/Adherend	Density (g/mm^3)	Modulus of Elasticity (GPa)	Poisson's Ratio	Yield Strength (MPa)
Magnesium	1.738 x e-3	45	0.35	285
Adhesive	1.01 x e-3	1.4	0.45	190

The finite element model was developed using Catia V5 and Hypermesh software. A three-dimensional linear elastic finite element stress analysis of the lap joint was conducted using Optistruct, a commercially available finite element solver from Altair. Post processing was done using Hypermesh and Microsoft Excel (primarily for graphical visuals). The different steps involved for the analysis and the respective software used in the current study are described in Table 2.2.

Table 2.2: Steps and corresponding software utilized in stress analysis

Steps	Software
Modeling	Catia V5R20, Altair Hypermesh 13.0
Meshing and Boundary Conditions	Altair Hypermesh 13.0
Solving	Optistruct 13.0
Results and Post Processing	Altair Hypermesh 13.0, Microsoft Excel

2.2.2 Defining Meshing, Contacts and Boundary Conditions

A 3D fine mesh was created in the overlap region and over a distance of 12.5 mm on each side of the overlap. A relatively coarse mesh was used in the rest of the specimen that are outside the area of interest in this study. The two different mesh patterns were selected to reduce the time for simulation and to improve the accuracy of obtained results in the adhesive joint area. An overview of the mesh pattern is shown in Figure 2.2. The upper part of the figure shows the top view of the specimen and lower part of the figure shows the front view.

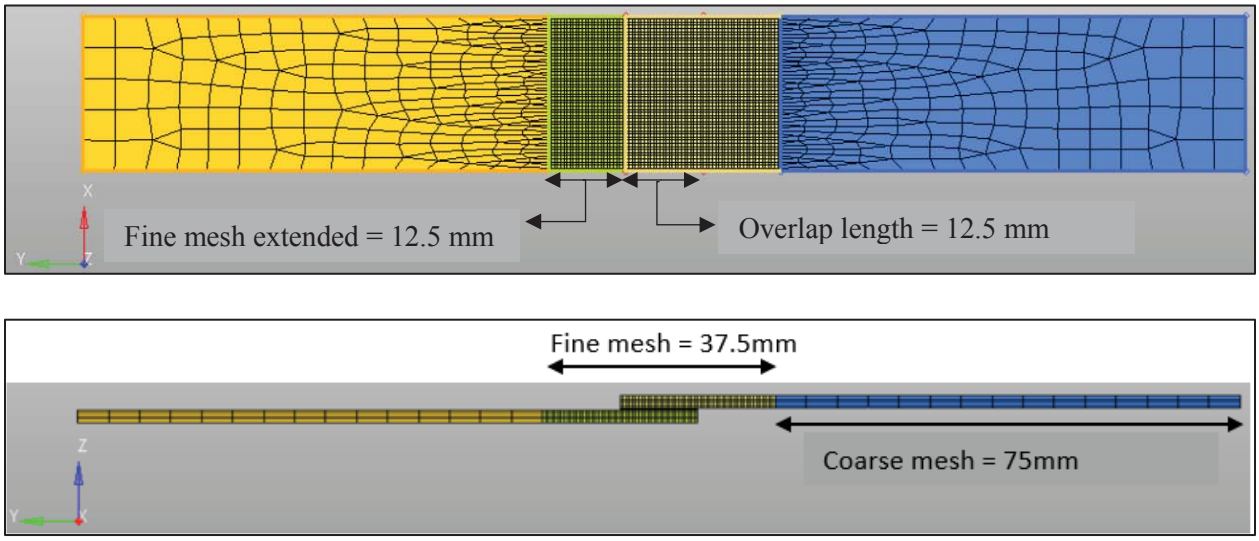

Figure 2.2 Mesh pattern for single lap joint in Hypermesh

Figure 2.3 shows the nodal structure of the 8-noded solid brick elements used for the adhesive and substrates. The adhesive thickness was divided into six layers of elements with dimensions of 0.5 mm (length) x 0.5 mm (width) x 0.0416 mm (thickness). The substrate thickness was divided into four layers so that the element thickness in the substrates was 0.5 mm. Figure 2.4 shows a diagrammatic representation of various layers of the adhesive and substrates. The dimensions of a single element of the substrate in the overlap zone and 12.5 mm on each side of the overlap are 0.5 mm x 0.5 mm x 0.5 mm. These dimensions are in the fine mesh region of the lap joint; they change substantially in the coarse region (as shown in Figure 2.2). The substrate and the adhesive share common nodes at the interface and a “stick” type contact condition was enforced at the substrate-adhesive interfaces.

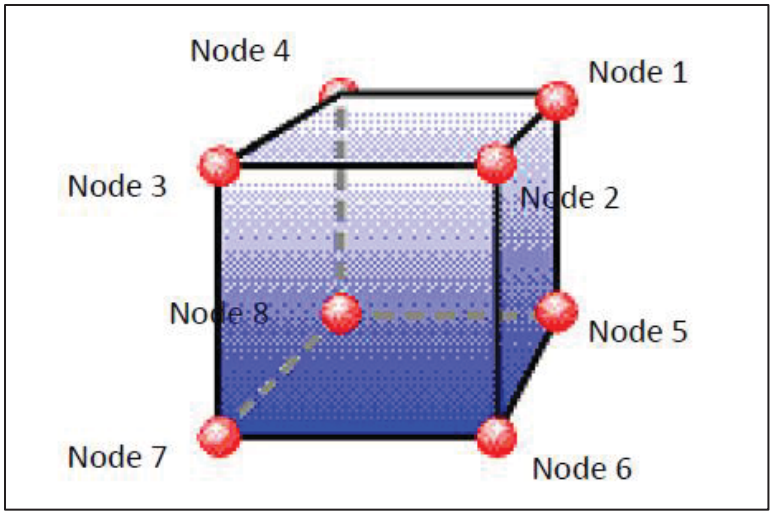

Figure 2.3 Eight nodded 3D solid brick element

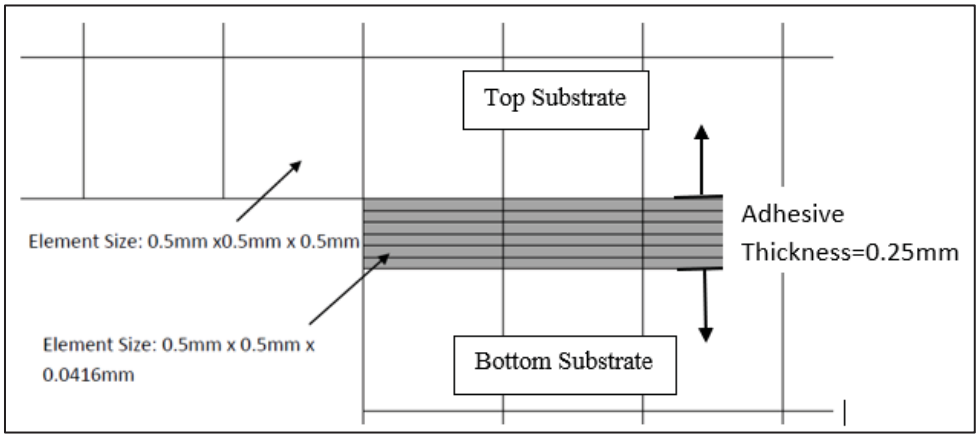

Figure 2.4: Element dimensions in the adhesive and substrate in the fine mesh area

For the analysis, the top substrate of the single lap adhesive joint was fixed at one end and the bottom substrate was loaded at the other end with an axial force F as shown in Figure 2.5. The loading end is free to translate along the Y direction and free to rotate about the X direction. A constant tensile force F of 100 N was applied at the loading end, which was small enough to cause very small bending deformation at the joint and also keep the substrates and the adhesive in the elastic condition. The average longitudinal tensile stress in each substrate due to 100 N load is 100 N/ (25 mm) (2 mm) = 2 MPa and the average shear stress in the adhesive layer due to 100 N load is 100 N/(25 mm) (12.5 mm) = 0.32 MPa. Both these stresses are much smaller than the yield

strengths of the substrate and adhesive materials. The axial force was distributed equally among all nodes on the loading end (Figure 2.6). Model verification was done by calculating the reaction forces in all three directions at the fixed end and checking that they are in equilibrium with the applied loading condition.

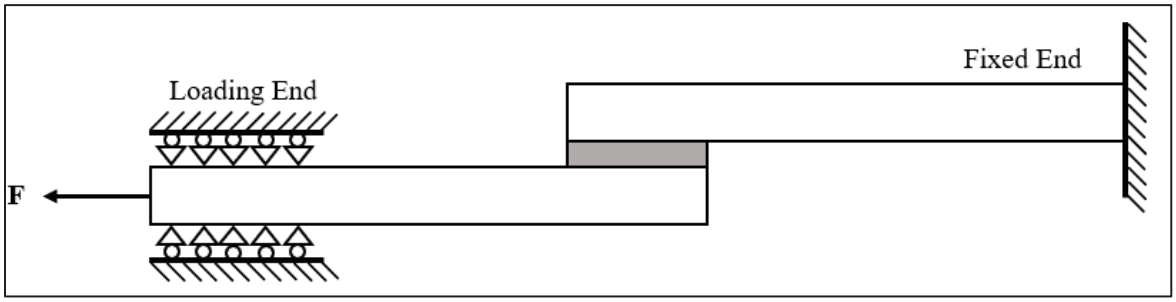

Figure 2.5: Boundary conditions at the fixed and loading ends

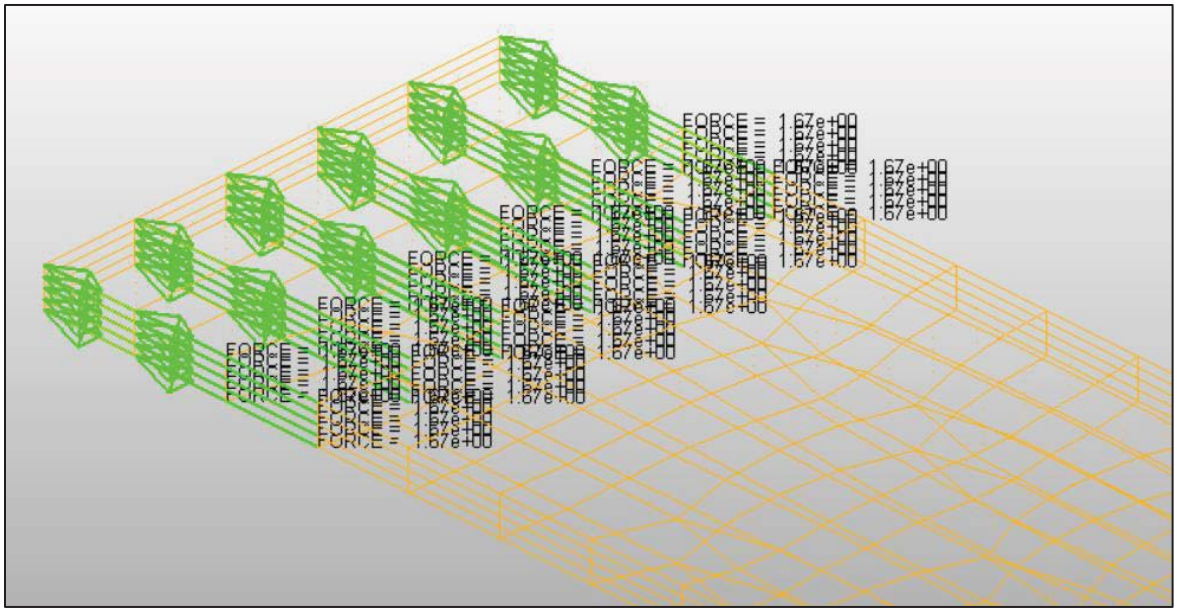

Figure 2.6: Equal distribution of load along the nodes of the loading end

MAT1 material card was used to define both the substrates and the adhesive. This bulk data entry card is used to define the properties for isotropic materials in Optistruct. It can be referenced by any of the structural elements, and can also be referenced by any property card. The element properties were defined by PSOLID, which defines the properties of solid elements in

Optistruct bulk data format. PSOLID element is referenced by CHEXA – six-sided solid element with eight grid points, as shown in Figure 2.3.

2.2.3 Stress Notations

When discussing stresses at "a point," it is important to visualize a three-dimensional stress element, aligned with an orthogonal right-handed coordinate system. Figure 2.7 shows one of the many eight-noded stress elements in the adhesive. The X, Y and Z axes in the figure represent width, length and thickness directions of the adhesive, respectively. Each face of the stress element has three stresses acting on it: a normal stress acting normal to the face, and two shear stresses acting parallel to the face in the other two directions as shown in Figure 2.7. Since for equilibrium, $\tau_{xy} = \tau_{yx}$, $\tau_{xz} = \tau_{zx}$ and $\tau_{yz} = \tau_{zy}$, there are six unknown stresses acting on each stress element. In the case of an adhesive joint, σ_{zz} (peel stress) and τ_{yz} (shear stress) are the most significant stresses and will be studied in detail in this chapter. In general, these two stresses dominate the failure in single lap adhesive joints. The longitudinal stress σ_{yy} acts parallel to the adhesive layer. The third normal stress σ_{xx} acts in the width direction of the adhesive layer and is generated due to the plane strain condition that exists in the joint area. Shear stresses, τ_{xy} and τ_{xz}, are generally relatively small. The magnitudes and distributions of all six stress components are determined here.

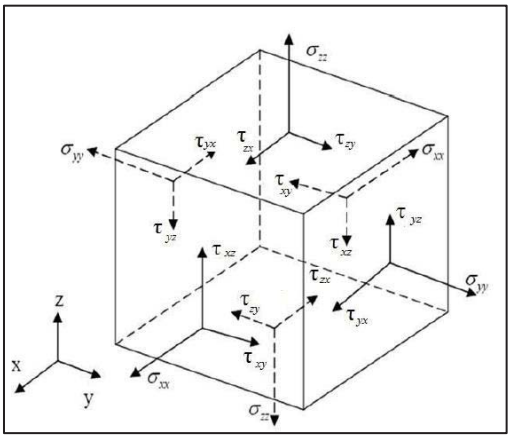

Figure 2.7: Stresses acting on an eight noded, three-dimensional stress element in the adhesive layer (Note: x, y and z are the width, longitudinal and thickness directions, respectively)

2.3 Adhesive Joint with 2 mm Thick Substrates

2.3.1 Stress Distributions in Adhesive Width Direction

Three reference planes were selected to represent the complex stress distribution in the adhesive layer. These three planes are denoted as reaction side (R), mid-length (M) and loading side (L), as shown in Figure 2.8. Stresses are recorded at the top interface (1), mid-thickness (2) and the bottom interface (3) (Figure 2.8). A constant tensile load of 100 N was applied, which was small enough to cause very small bending deformation at the joint and keep the substrates and the adhesive in the elastic condition. The average longitudinal tensile stress in each substrate due to 100 N load is 100 N/ (25 mm) (2 mm) = 2 MPa and the average shear stress in the adhesive layer due to 100 N load is 100 N/(25 mm) (12.5 mm) = 0.32 MPa.

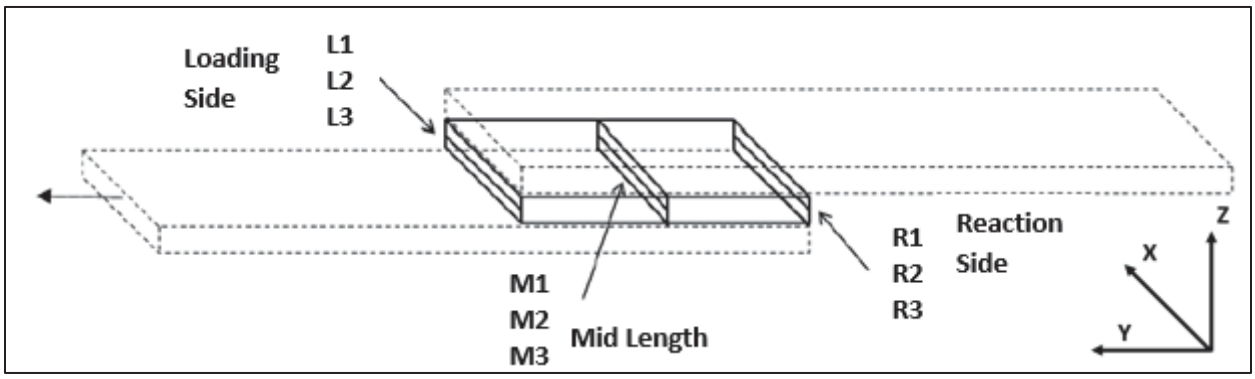

Figure 2.8: Reference planes selected along the thickness and length directions of the bond-line to analyze the stress distributions along the width direction [7]

(a) Reaction and Loading Ends (Figs. 2.9 – 2.10):

Figures 2.9 – 2.11 show the stress distributions along the 'top interface', 'mid-thickness' and 'bottom interface' in the adhesive width direction (x-axis) at the reaction side (R), mid-length (M) and loading side (L) as defined in Figure 2.8. Following observations can be made from these figures.

Stresses σ_{xx}, σ_{yy}, σ_{zz} and τ_{yz} increase rapidly from zero or near-zero values at the front and back edges to their highest values at the mid-width. All four stress components have their maximum values at the mid-width. τ_{xz} and τ_{xy} have their highest values at or close to the front and back edges, but they have zero values at the mid-width. The distributions of σ_{xx}, σ_{yy}, σ_{zz} and τ_{yz}

are symmetric about the mid-width, whereas the distributions of τ_{xy} and τ_{xz} are anti-symmetric about the mid-width. The presence of σ_{yy}, σ_{zz} and τ_{yz} in adhesive joints is well known and can be determined using a two-dimensional analysis. The three-dimensional analysis shows that the width-direction normal stress (σ_{xx}) can have a significant value along much of the width; however, shear stresses τ_{xz} and τ_{xy} are relatively small. The width-direction normal stress σ_{xx} arises due to the plane strain condition that exists in the adhesive layer due to its width being 100 times larger than its thickness.

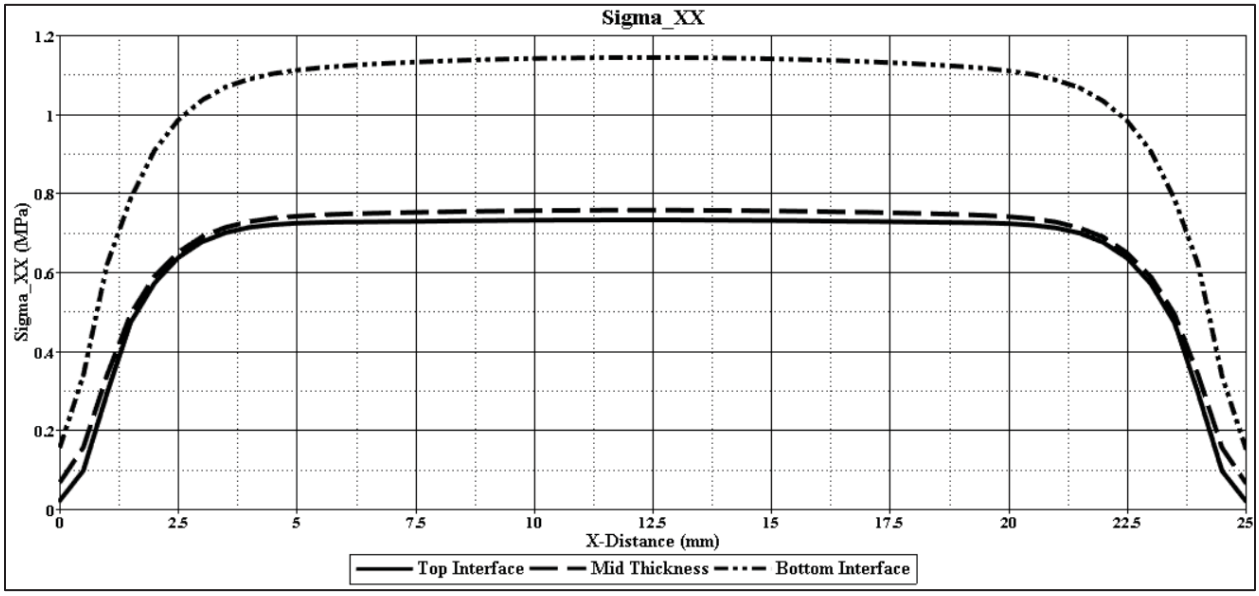

(a): σ_{xx} at the loading side

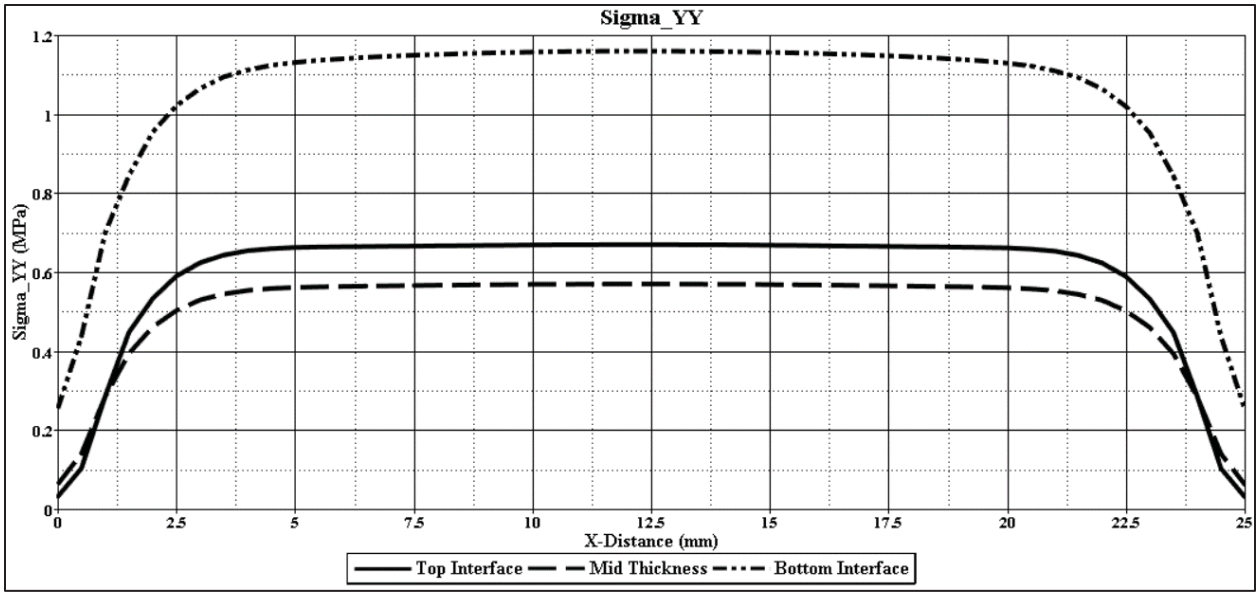

(b): σ_{yy} at the loading side

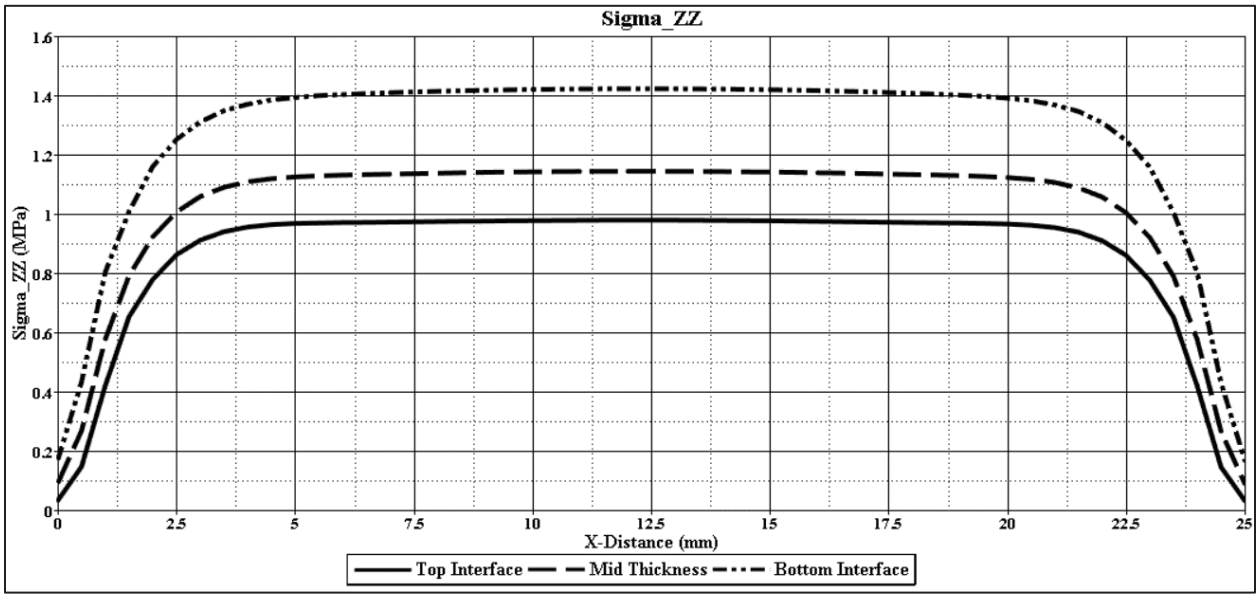

(c): σ_{zz} at the loading side

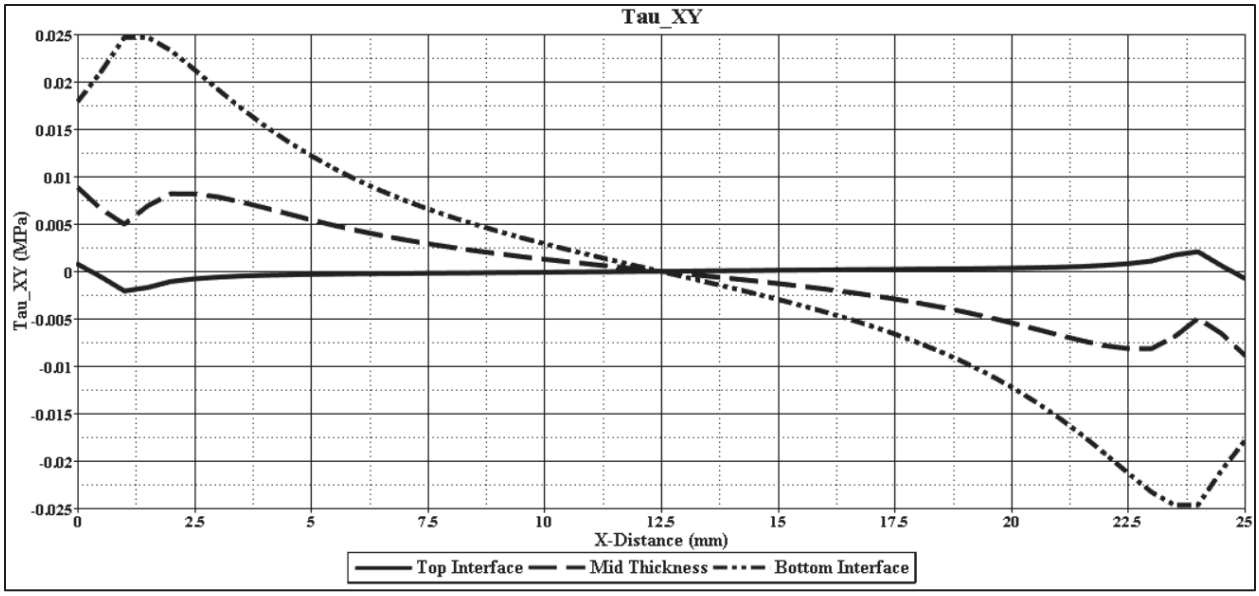

(d): τ_{xy} at the loading side

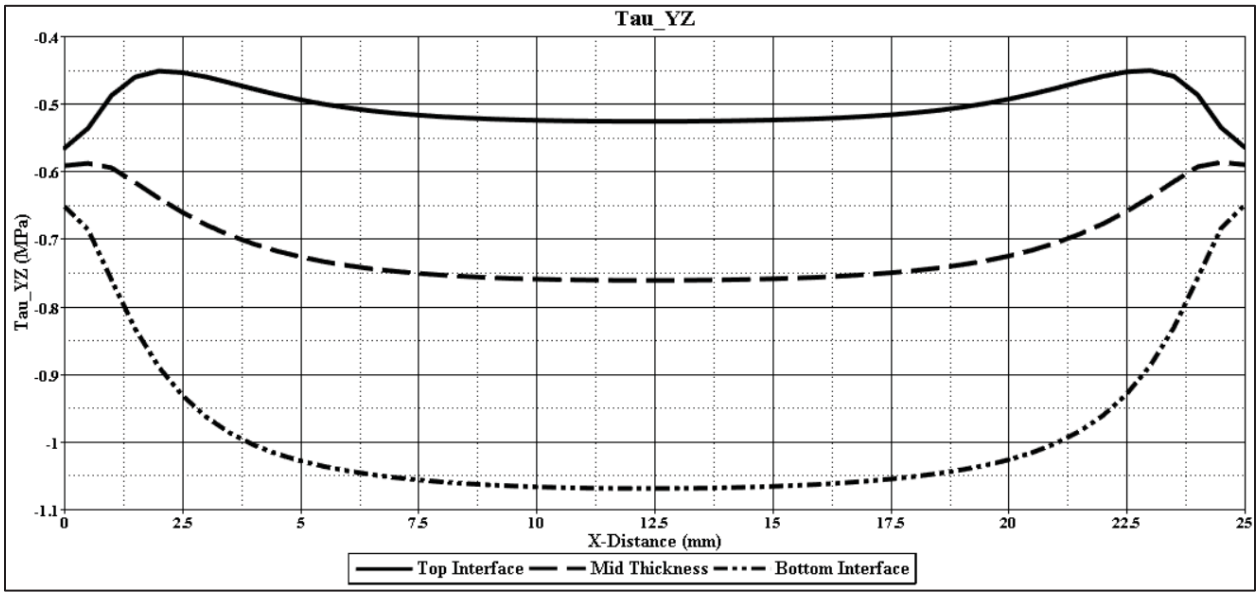

(e): τ_{yz} at the loading side

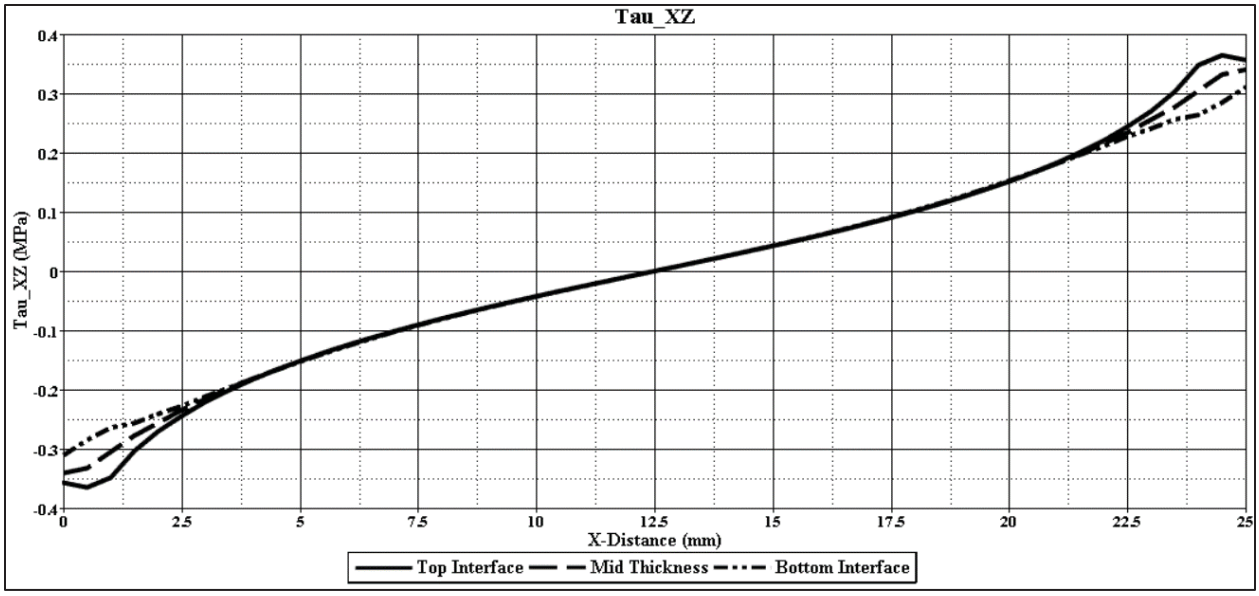

(f): τ_{xz} at the loading side

Figures 2.9: σ_{xx}, σ_{yy}, σ_{zz}, τ_{xy}, τ_{yz} and τ_{xz} distributions along the adhesive width direction at the loading side (L1, L2 and L3) for a tensile load of 100N

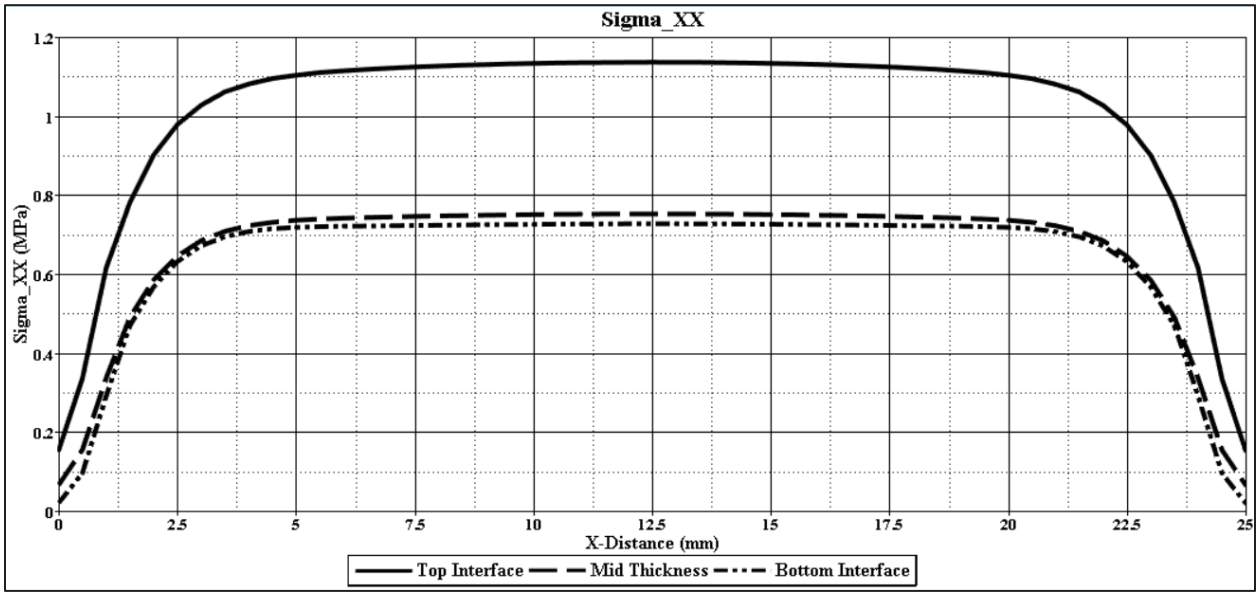

(a): σ_{xx} at the reaction side

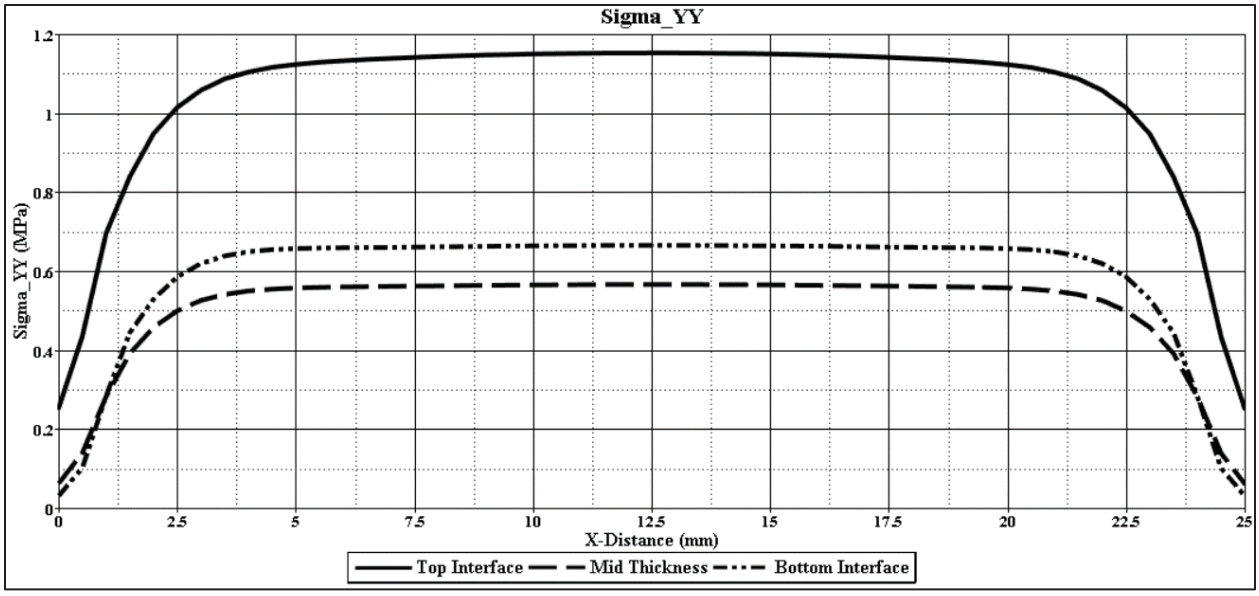

(b): σ_{yy} at the reaction side

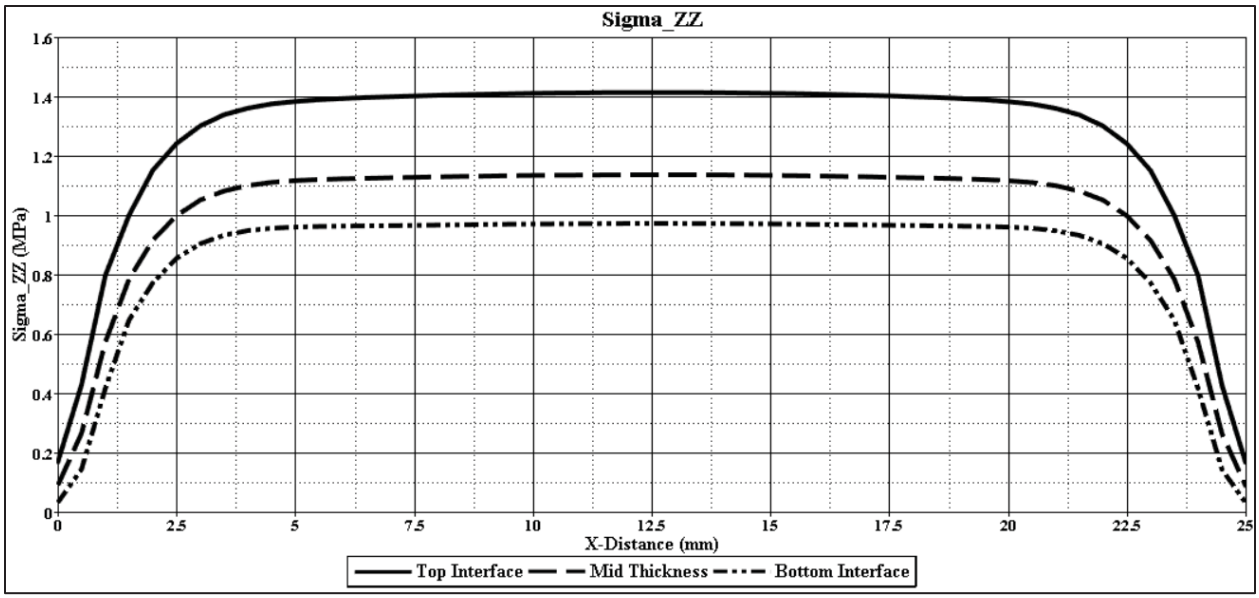

(c): σ_{zz} at the reaction side

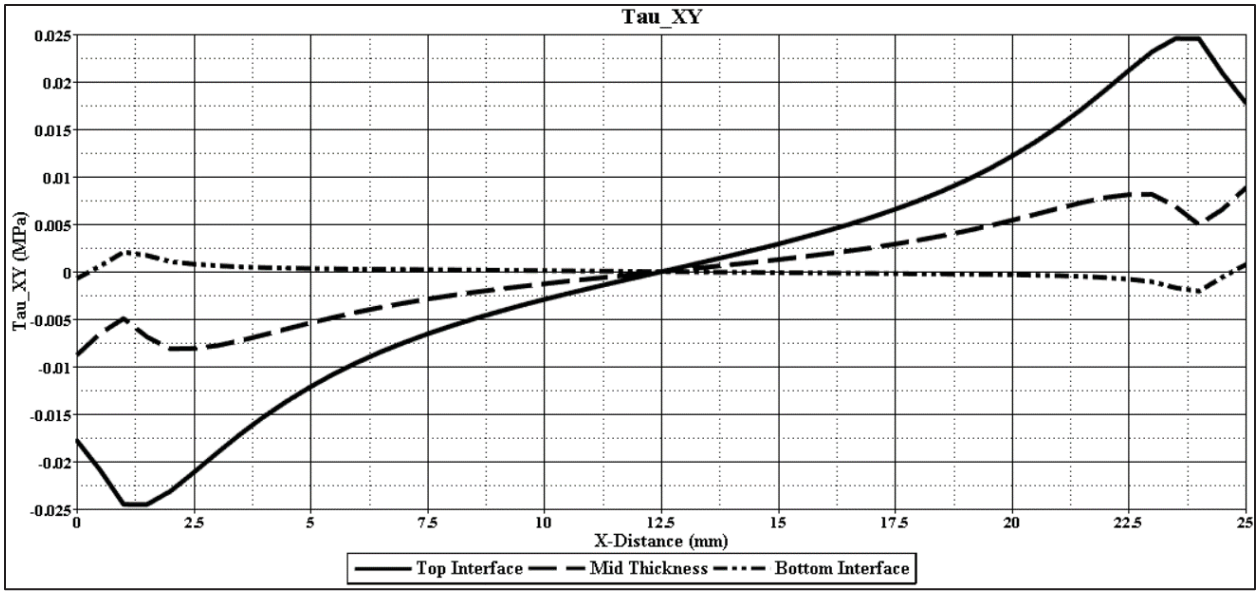

(d): τ_{xy} at the reaction side

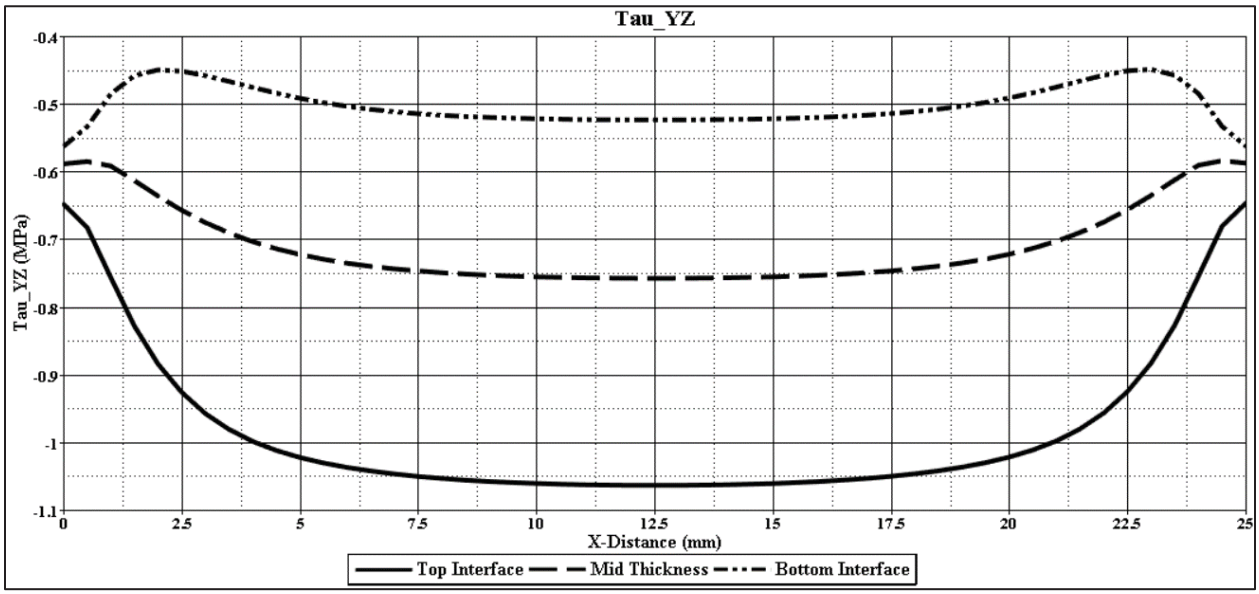

(e): τ_{yz} at the reaction side

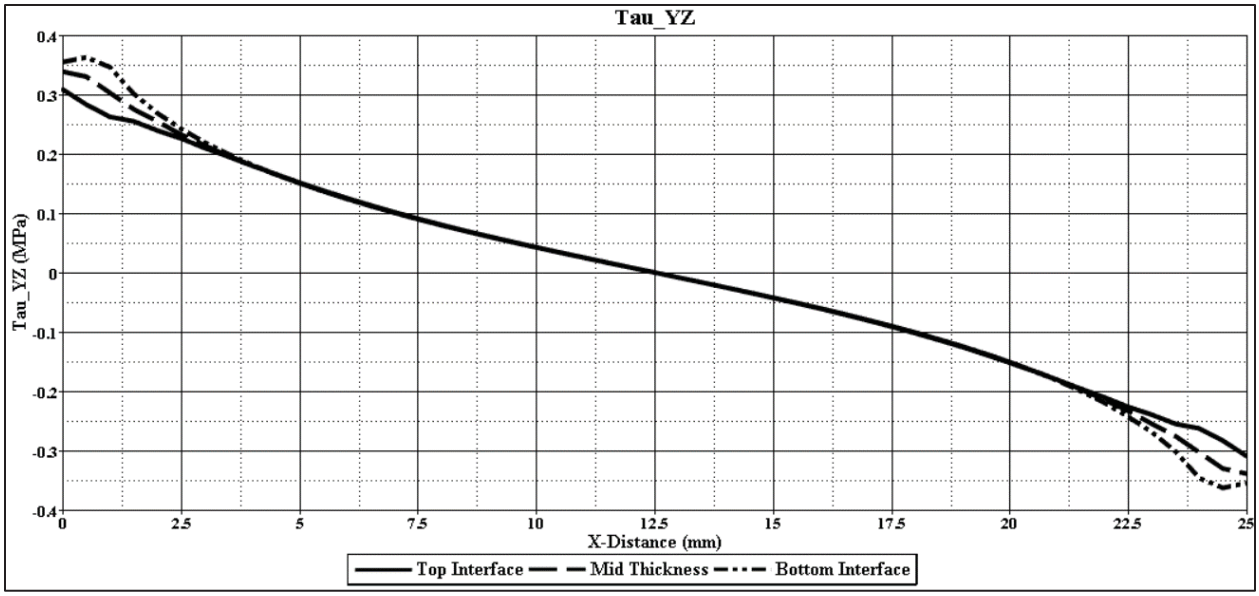

(f): τ_{xz} at the reaction side

Figure 2.10: σ_{xx}, σ_{yy}, σ_{zz}, τ_{xy}, τ_{yz} and τ_{xz} distributions along the adhesive width direction at the reaction side (R1, R2 and R3) for a tensile load of 100N

(b) Mid-length (Fig. 2.11):

Compared to the reaction and loading sides, all six stress components are relatively small at the mid-length of the adhesive layer. Like the reaction and loading sides, the longitudinal normal stress σ_{yy} at the mid-length is also positive, i.e., tensile in nature; however, unlike the reaction and loading sides, the peel stress σ_{zz} and width-direction normal stress σ_{xx} are negative i.e., compressive in nature.

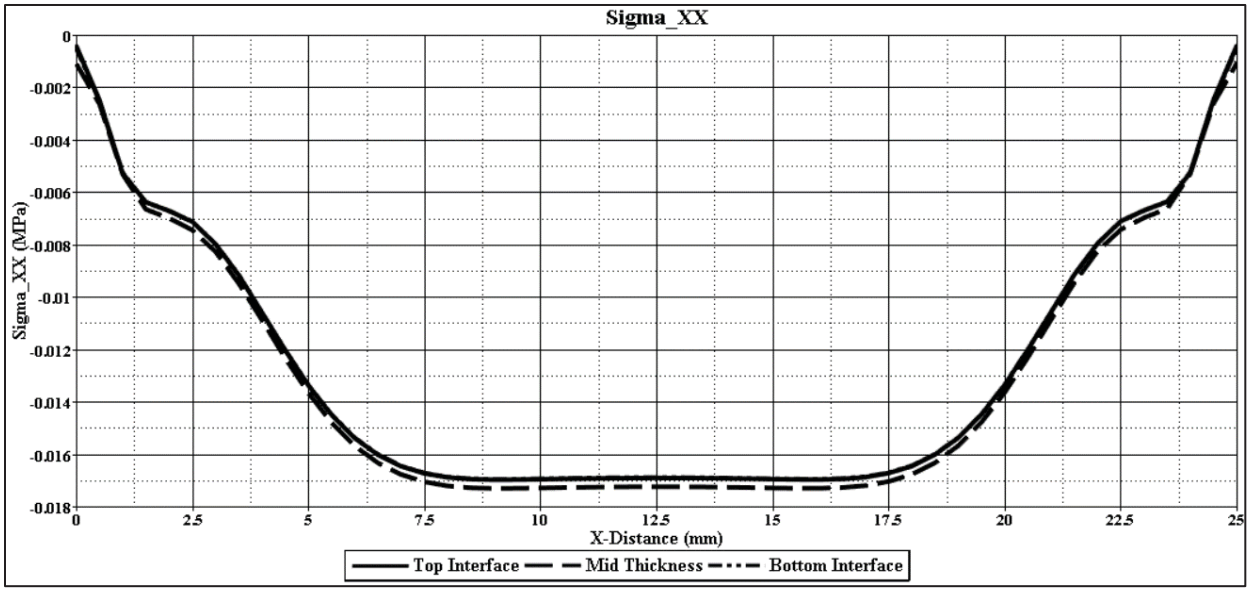

(a): σ_{xx} at the middle-length

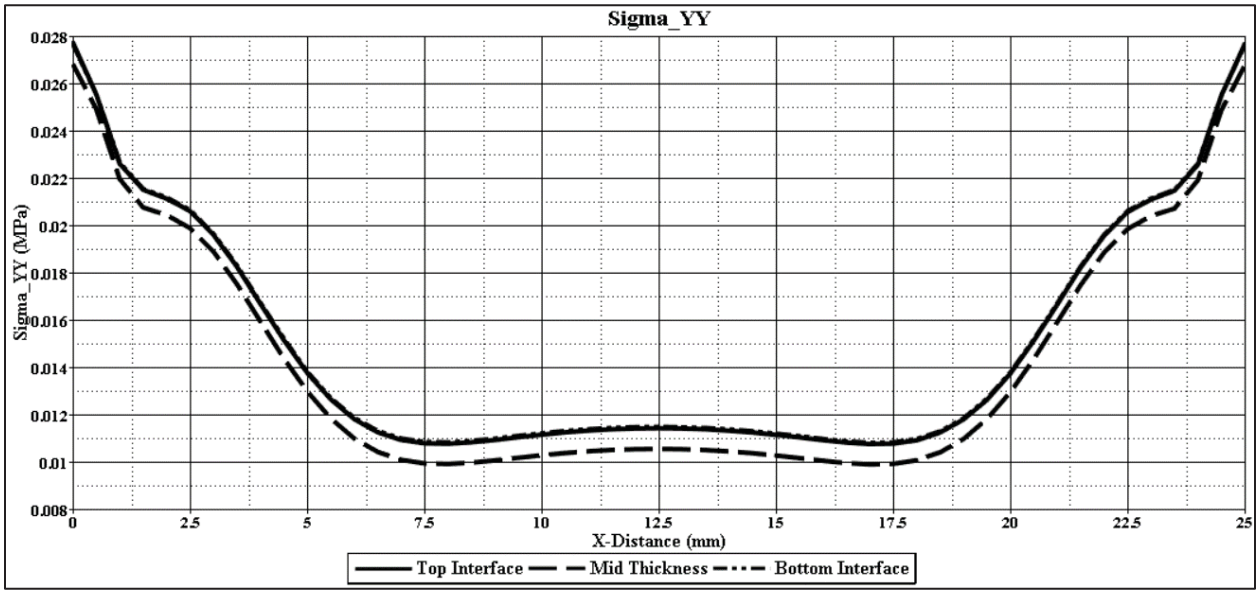

(b): σ_{yy} at the middle-length

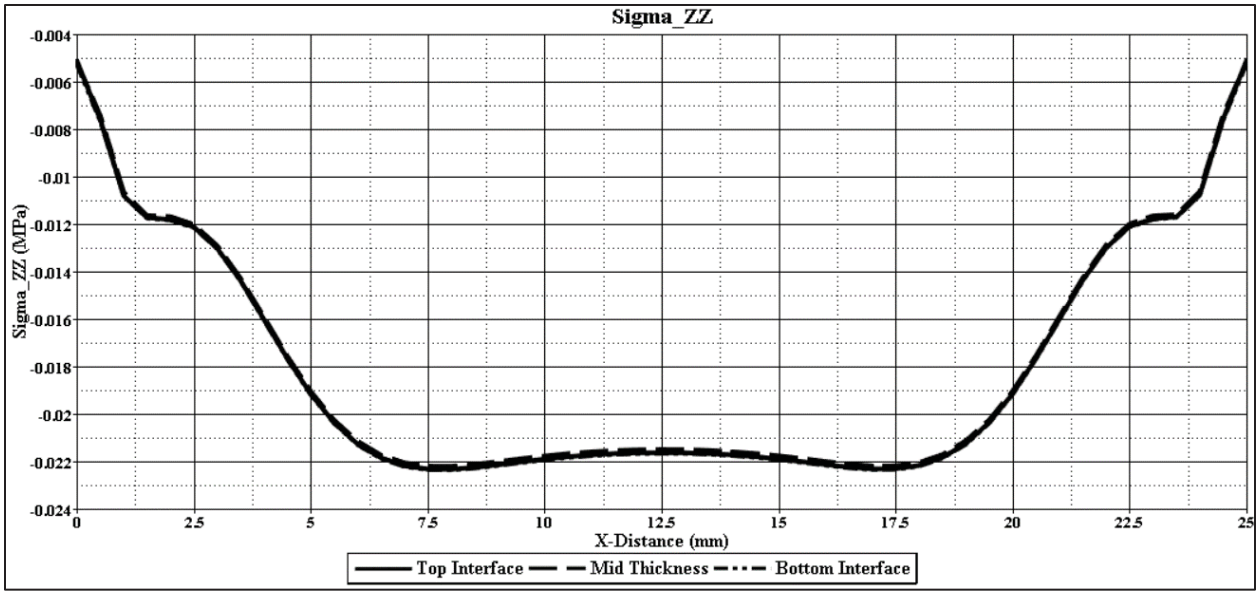

(c): σ_{zz} at the middle-length

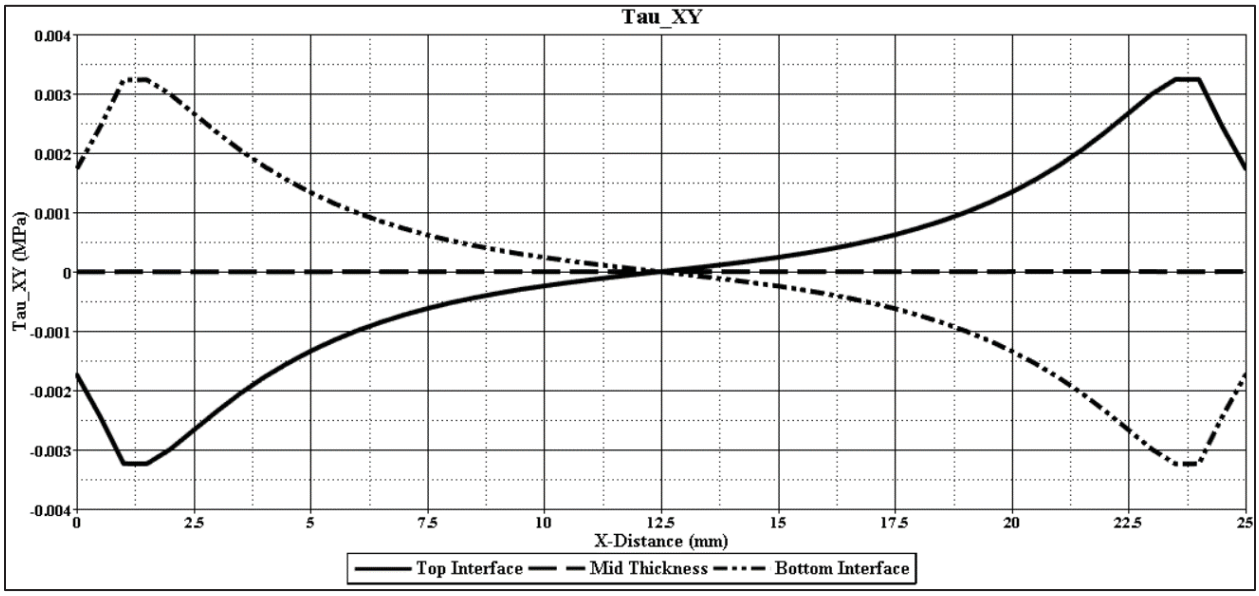

(d): τ_{xy} at the middle-length

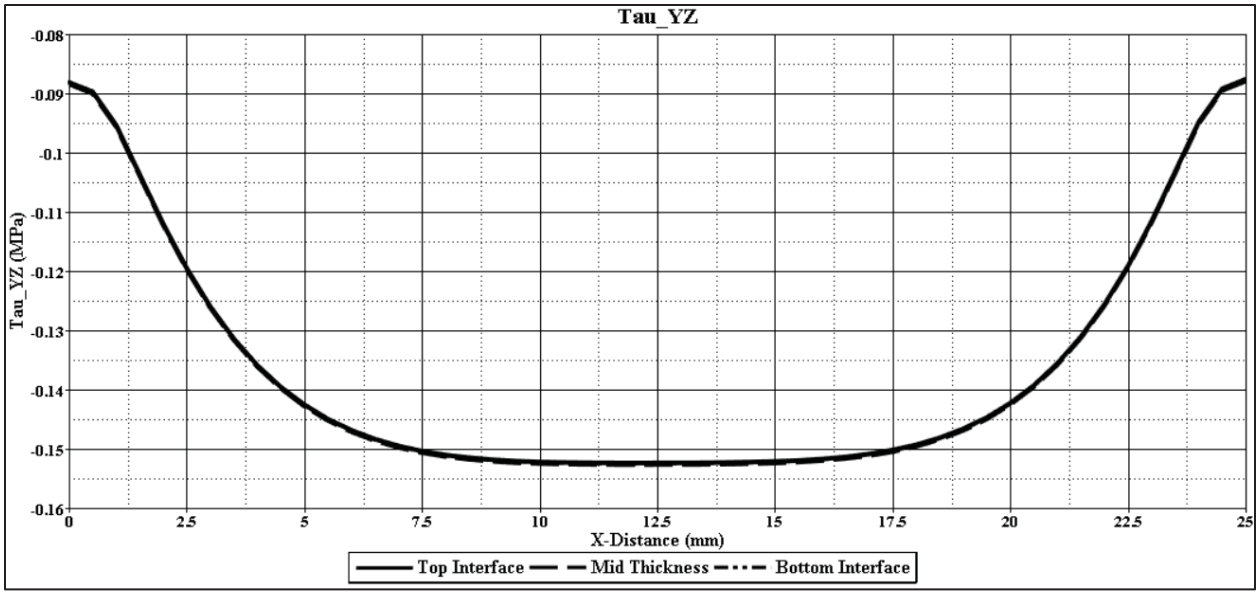

(e): τ_{yz} at the middle-length

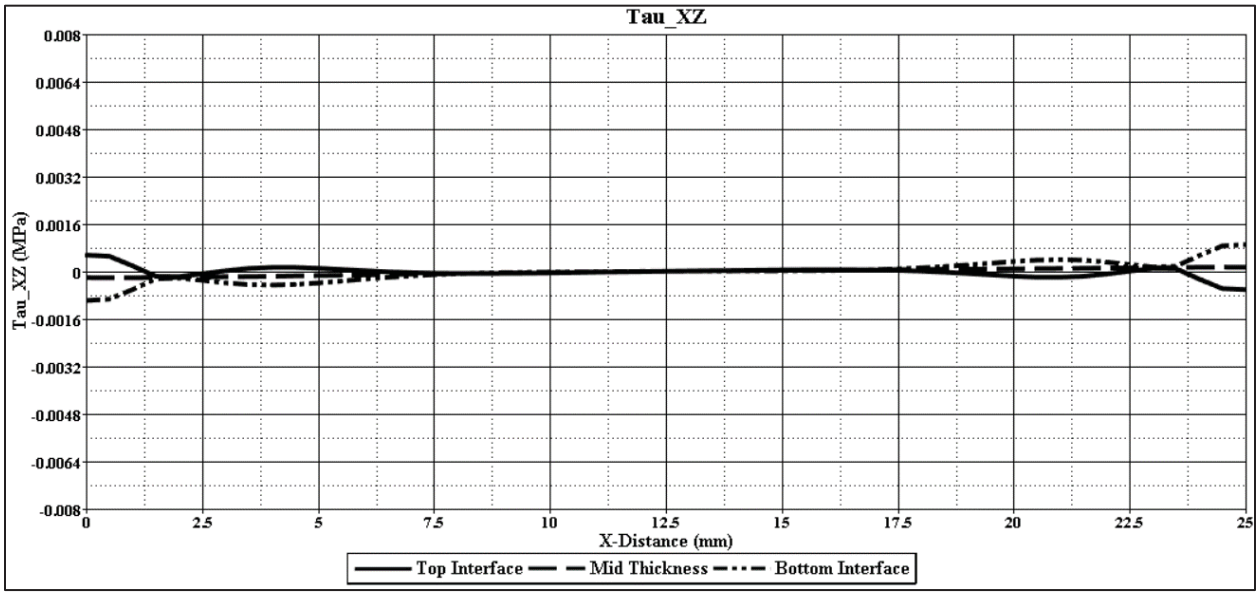

(f): τ_{xz} at the middle-length

Figure 2.11: σ_{xx}, σ_{yy}, σ_{zz}, τ_{xy}, τ_{yz} and τ_{xz} distributions along the adhesive width direction at the mid-length (M1, M2 and M3) for a tensile load of 100N

2.3.2 Stress Distributions in the Adhesive Length Direction

Figure 2.12 shows the distributions of all six stress components along the adhesive length (y-direction) at the top interface, mid-thickness plane and bottom interface at the mid-width of a magnesium-magnesium single lap joint at a load of 100 N. The peel stress σ_{zz} is tensile near the lap ends; from the stress plots, it can be observed that σ_{zz} increases over a distance of approximately 1.6 mm at both reaction and loading sides. In the middle portion of the overlap, the peel stress σ_{zz} is slightly compressive. However, the distribution of σ_{zz} is not symmetric about the mid-length, particularly at the top interface, where σ_{zz} is higher at the reaction side compared to its value at the loading side. The longitudinal and width-direction normal stresses, σ_{yy} and σ_{xx}, increase sharply near the loading ends of the bottom interface. The distribution and magnitude of the width-direction normal stress σ_{xx} are similar to those of the peel stress σ_{zz}. The highest value of the in-plane shear stress τ_{yz} occurs at the reaction side of the top interface. The distribution of the in-plane shear stress τ_{yz} is symmetric about the mid-length at the mid-thickness plane of the adhesive layer, but it is non-symmetric at both top and bottom interfaces. Finally, the magnitudes of the other two shear stresses, τ_{xz} and τ_{xy} , are very small in the length direction. The highest value of τ_{xz} occurs at both sides of the overlap and the highest value of τ_{xy} occurs at the loading side of the bottom interface.

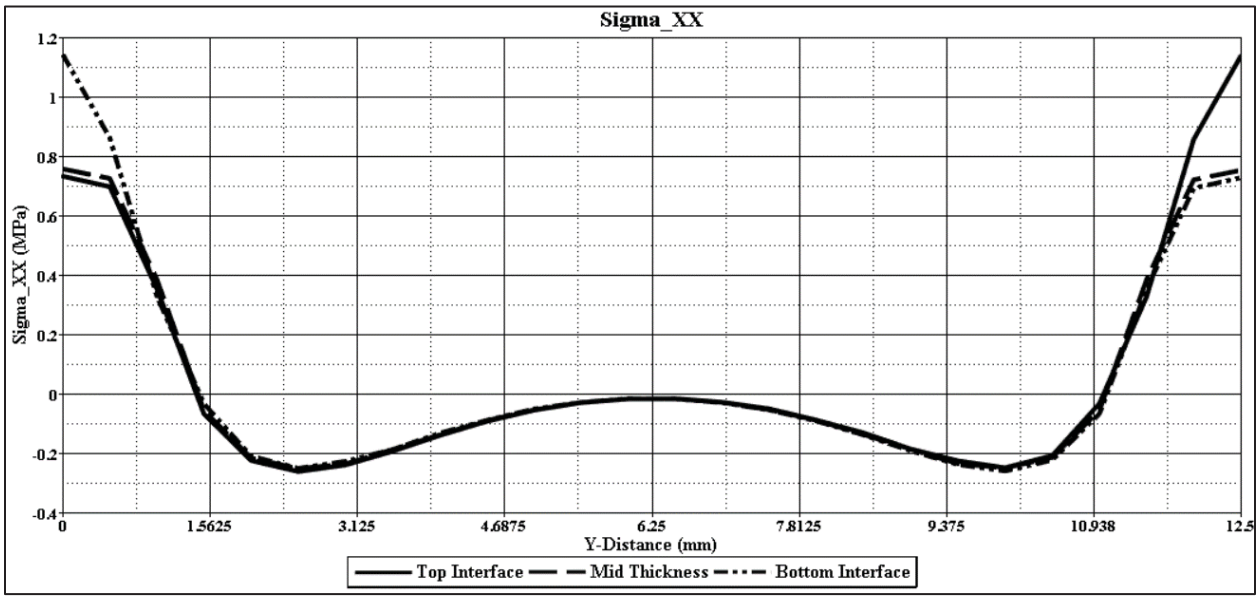

(a): Width-direction normal stress (σ_{xx}) at mid-width

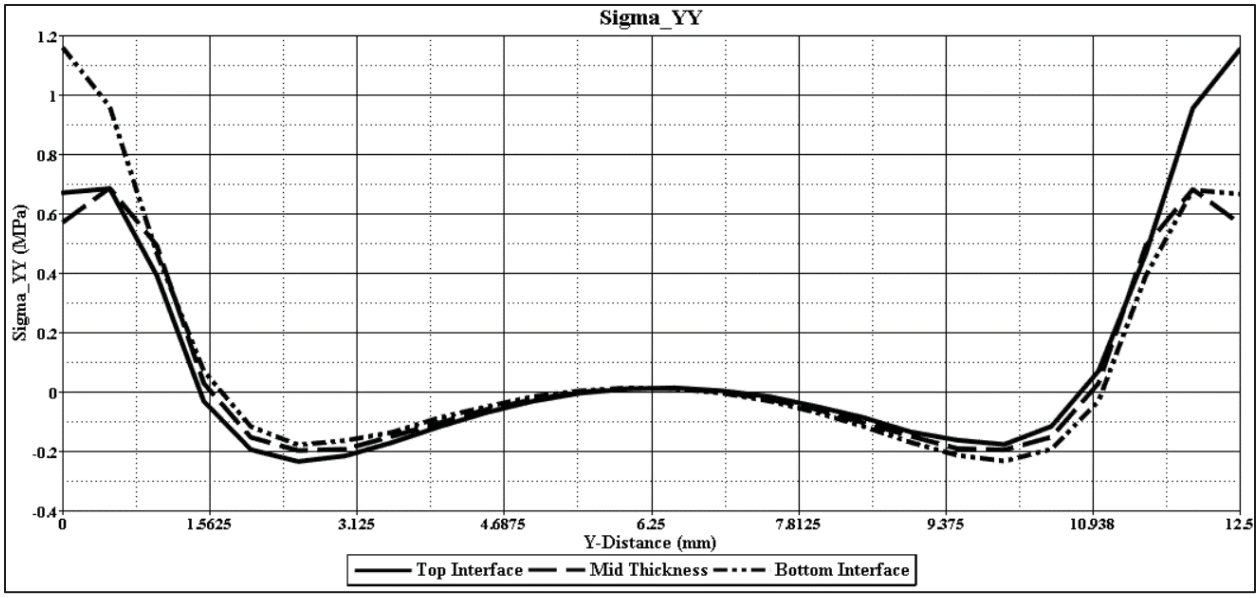

(b): Longitudinal stress (σ_{yy}) at mid-width

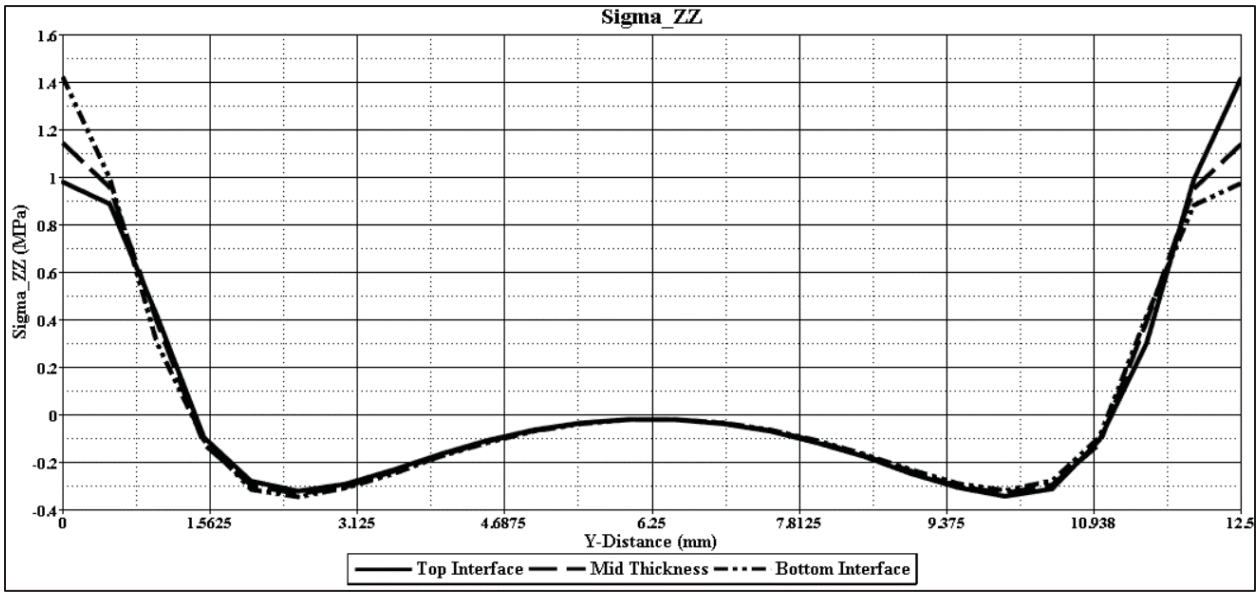

(c): Peel stress (σ_{zz}) at mid-width

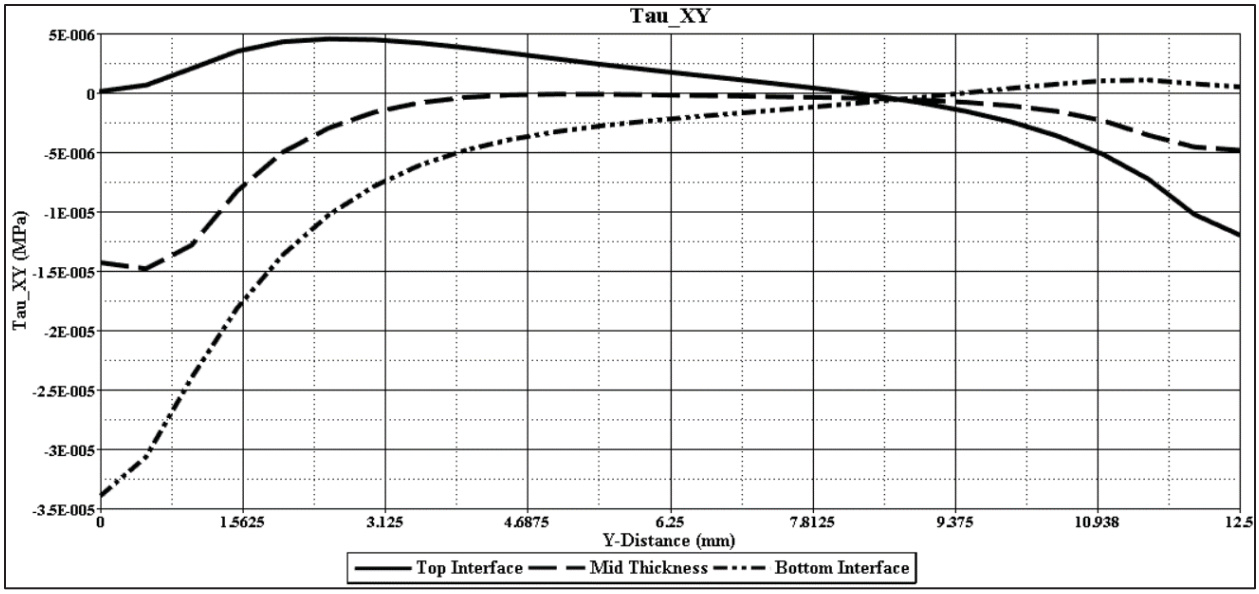

(d): XY-shear stress (τ_{xy}) at mid-width

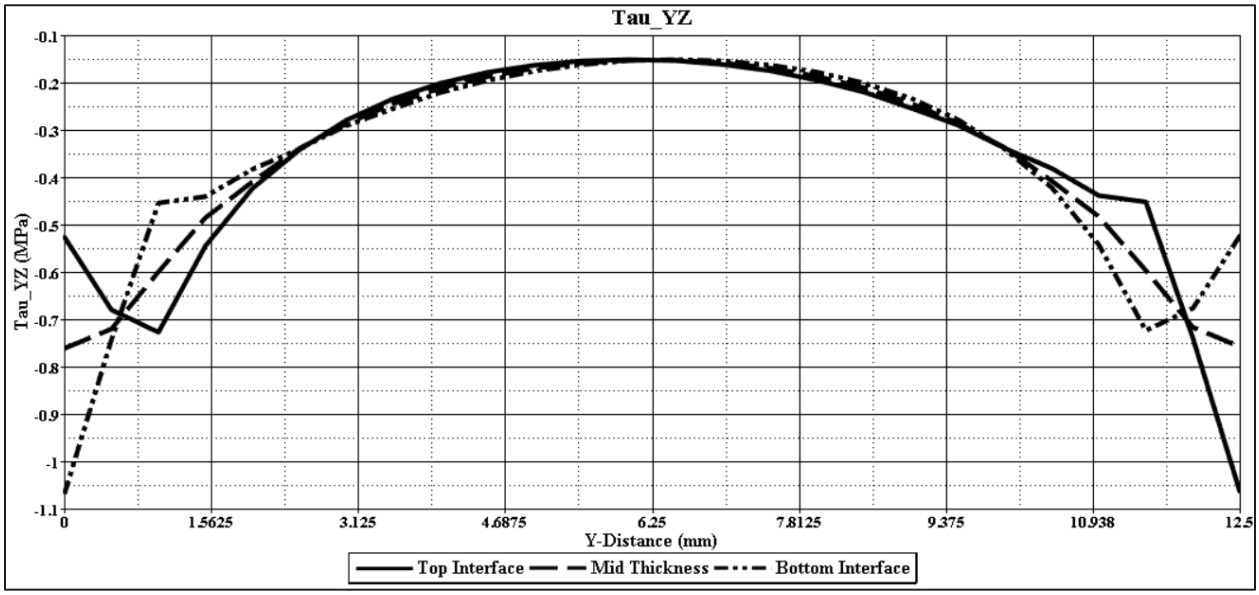

(e): In-plane shear stress (τ_{yz}) at mid-width

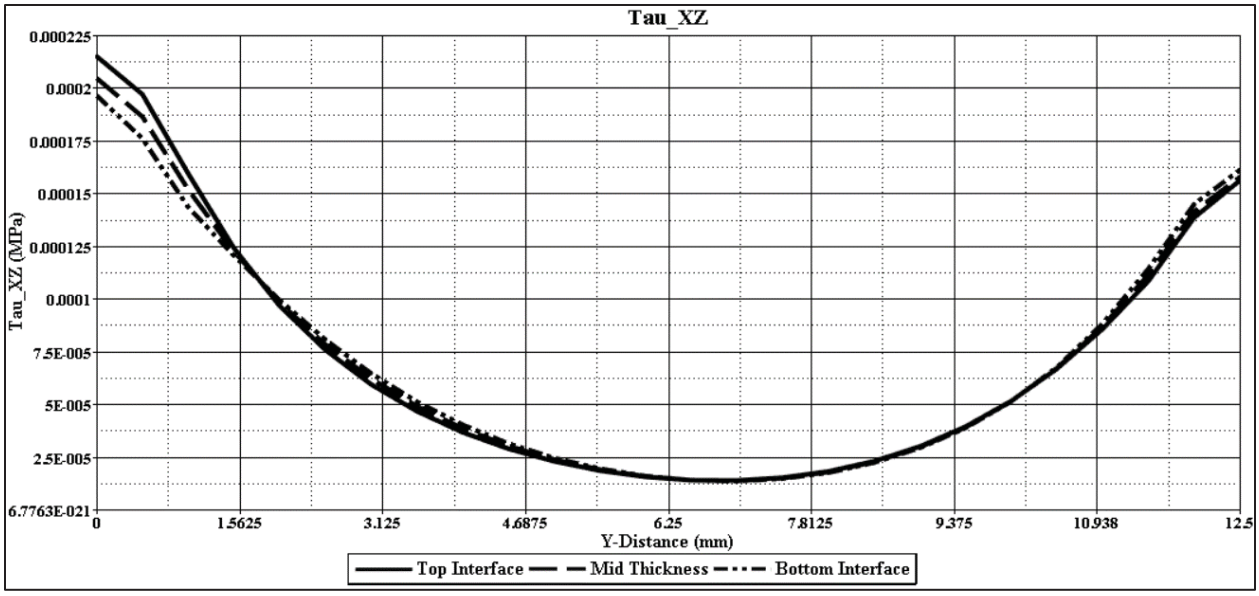

(f): XZ-shear stress (τ_{XZ}) at mid-width

Figure 2.12: Stress distributions in the length direction at top interface, mid-thickness and bottom interface at a tensile load of 100 N

2.3.3 Stress Distributions in the Adhesive Thickness Direction

In Figure 2.13, the stress distributions are shown at the mid-width and at three different distances in the length direction (Y-direction). At Y = 0 and 12.5 mm, all three normal stresses are tensile in nature and their maximum values occur at approximately near the overlap end of the top interface or the bottom interface. Likewise, the in-plane shear stress, τ_{yz} has its maximum value at Y = 0 and 12.5 mm and at either the top or the bottom interface.

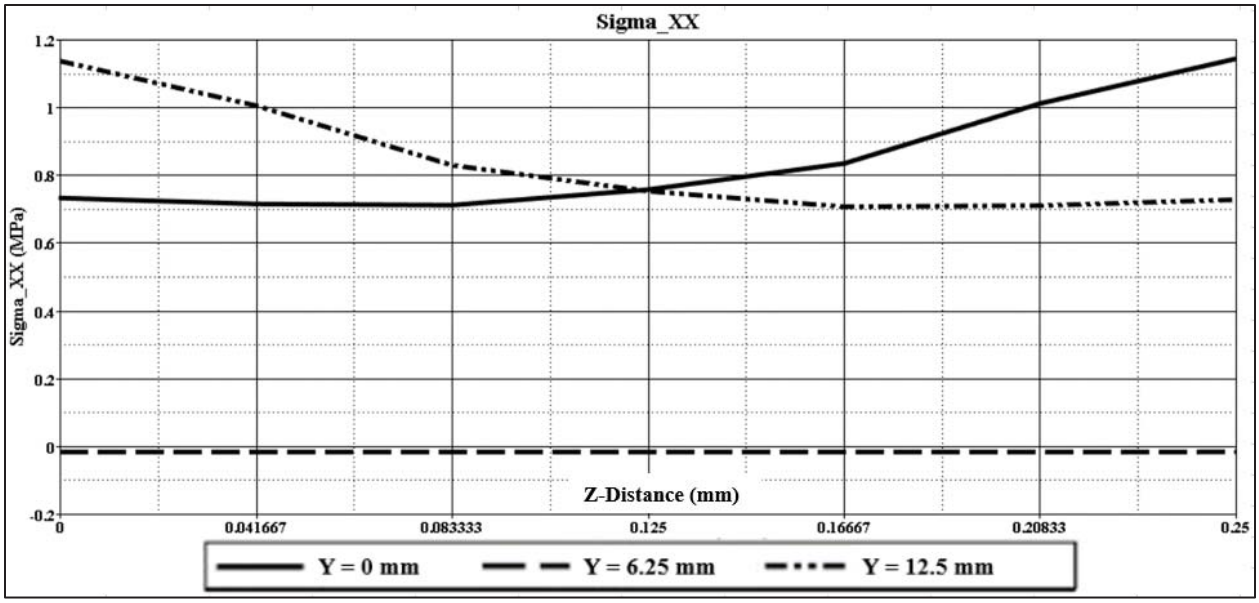

(a): Width-direction normal stress (σ_{xx}) at mid-width

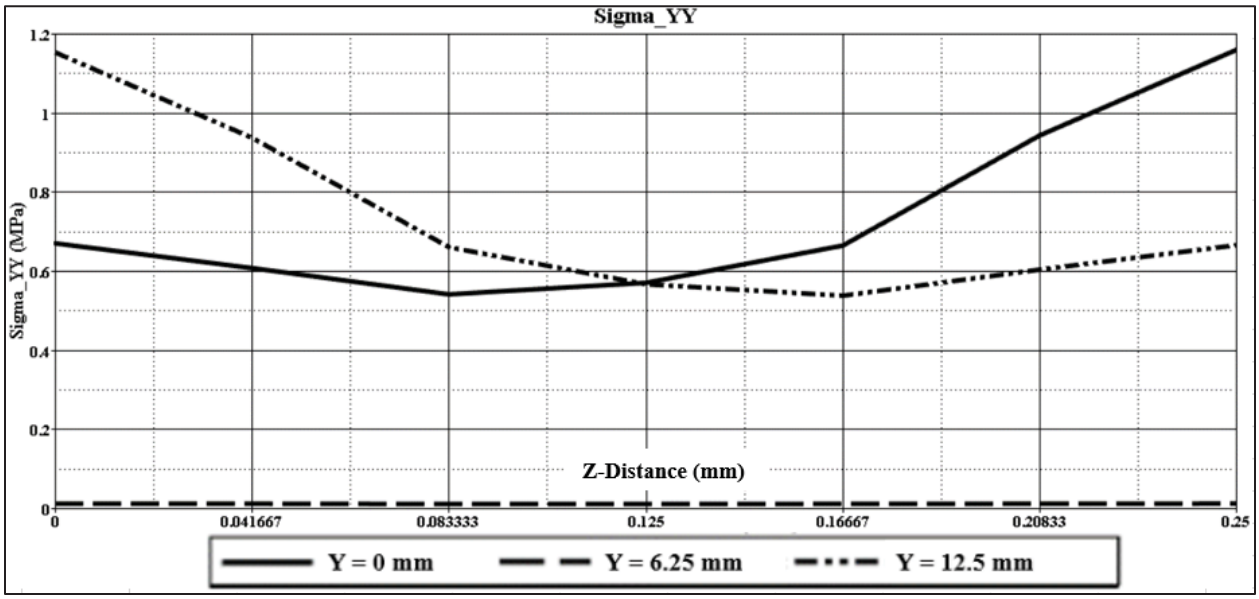

(b): Longitudinal stress (σ_{yy}) at mid-width

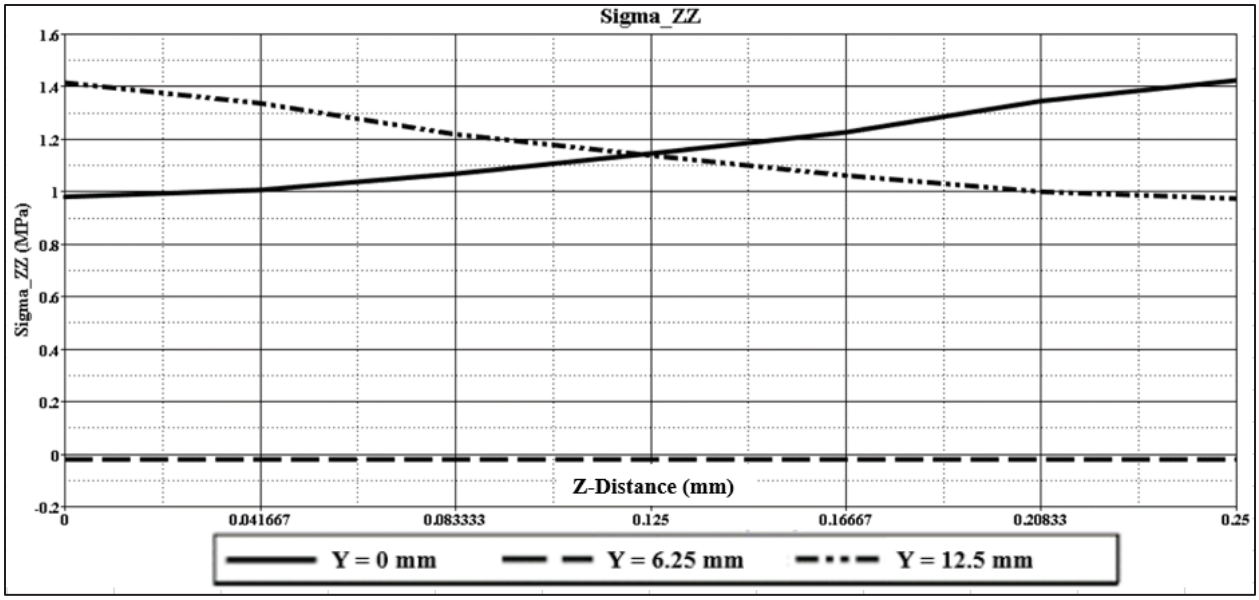

(c): Peel stress (σ_{zz}) at mid-width

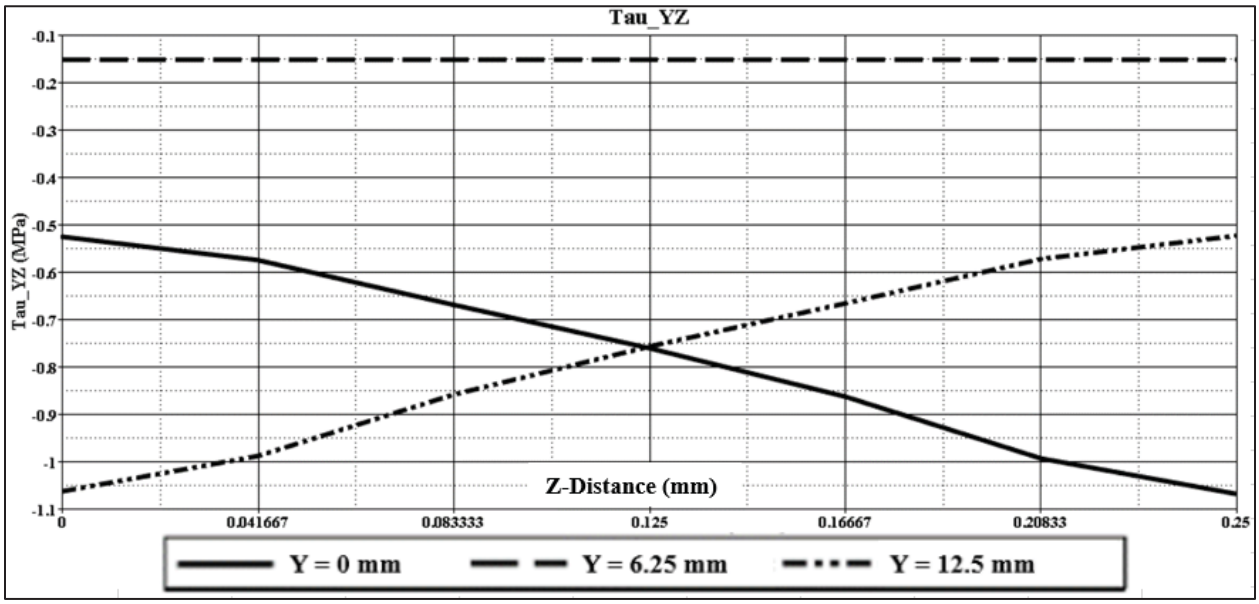

(d): In-plane shear stress (τ_{yz}) vs. Adhesive thickness at mid-width

Figure 2.13 – Variations of stress components (σ_{yy}, σ_{xx}, σ_{zz} and τ_{yz}) in the adhesive thickness direction at a tensile load of 100 N. Variations are shown at the mid-width (X = 12.5 mm) and at the reaction end (Y = 0 mm), mid-length (Y = 6.25 mm) and at the loading end (Y = 12.5mm)

2.3.4 Maximum Stresses in the Adhesive Layer

Table 2.3 compares the maximum stress values for Mg-Mg joint at a 100 N axial tensile load. The following observations can be made from this table.

(a) All three normal stresses and the in-plane shear stress (τ_{yz}) exhibit either maximum values at either the top interface or the bottom interface. The other two shear stresses (τ_{xy} and τ_{xz}) are very small.

(b) The width-direction normal stress σ_{xx} is of the same order of magnitude as the longitudinal stress σ_{yy} and peel stress σ_{zz}. Therefore, it can be concluded that the stress condition in the adhesive layer is truly three-dimensional and a two-dimensional stress analysis may not be adequate in predicting the behavior of an adhesive joint.

(c) Depending on the interface, the highest values occur at either the reaction end or the loading end. At the reaction end, the maximum stress values are at the top interface and at the loading end, the maximum stress values are at the bottom interface.

(d) The maximum normal stresses are tensile in nature. Out of the three normal stresses, the peel stress σ_{zz} has the highest value.

(e) Out of the three shear stresses, the in-plane shear stress τ_{yz} has the highest value and it occurs at the overlap ends.

Table 2.3 – Maximum stress values at 100 N Load

Location	σ_{xx} (MPa)	σ_{yy} (MPa)	σ_{zz} (MPa)	τ_{xy} (MPa)	τ_{yz} (MPa)	τ_{xz} (MPa)
R1 (Top Interface)	1.136	1.153	1.414	0.025	-1.064	0.309
R2 (Mid-Thickness)	0.752	0.566	1.137	0.009	-0.758	0.339
R3 (Bottom Interface)	0.727	0.665	0.972	0.002	-0.563	0.355
M1 (Top Interface)	-0.017	0.028	-0.022	0.003	-1.152	0.001
M2 (Mid-Thickness)	-0.017	0.027	-0.022	0	-0.153	0
M3 (Bottom Interface)	-0.017	0.028	-0.022	0.003	-0.152	0.001
L1 (Top Interface)	0.733	0.67	0.979	0.002	-0.566	0.356
L2 (Mid-Thickness)	0.757	0.57	1.144	0.009	-0.761	0.34
L3 (Bottom Interface)	1.144	1.159	1.423	0.025	-1.069	0.31

2.4 Effect of Substrate Thickness Difference on Maximum Stresses and Joint Deformation

To study the effect of the substrate thickness difference on the stress distribution in the adhesive layers, the bottom substrate thickness was varied from 1.6 mm to 4.4 mm in steps of 0.4 mm while maintaining the top substrate thickness at 2 mm. The difference in the bottom and top substrate thicknesses creates a difference in their bending stiffness values as shown by the following equation.

$$\frac{k_2}{k_1} = \frac{E_2 . h_2^3}{E_1 . h_1^3} \tag{1}$$

where, k, E and h represent bending stiffness, modulus of the substrate material and substrate thickness, respectively, and the subscripts 1 and 2 represent top and bottom substrate, respectively. Since in this study, the material for both substrates is the same, the bending stiffness ratio becomes

$$\frac{k_2}{k_1} = \left(\frac{h_2}{h_1} \right)^3 \tag{2}$$

Thus, as the bottom substrate thickness h_2 is increased with respect to the top substrate thickness h_1, the bending stiffness of the bottom substrate k_2 becomes increasingly higher than that of the top substrate and the joint starts to exhibit lower bending deformation compared to the top substrate. This can be observed in Figure 2.14, which compares the bending deformations of the single lap specimens in which the top substrate thickness is 2 mm and the bottom substrate thickness is increased from 1.6 mm to 4.4 mm in steps of 0.4 mm. Thus, the ratio of the bottom substrate thickness and top substrate thickness was varied from 0.8 to 2.2. For the bottom substrate thickness of 1.6 and 2 mm, the bottom substrate bends upward and there was significant joint rotation. As the bottom substrate thickness becomes higher than 2 mm, its bending deformation decreases. In the deformation plot for Mg-Mg specimens (Figure 2.14), it can be observed that the joint had undergone rotation, but there was very little displacement of the center of the joint. The joint rotation decreased and the displacement on the reaction side substrate increased as loading side substrate material thickness was changed from 2 mm to 4.4 mm.

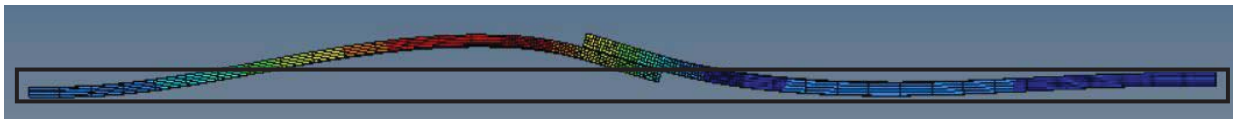

(a) Bottom substrate thickness = 1.6 mm, Top substrate thickness = 2 mm

(b) Bottom substrate thickness = 2 mm, Top substrate thickness = 2 mm

(c) Bottom substrate thickness = 2.4 mm, Top substrate thickness = 2 mm

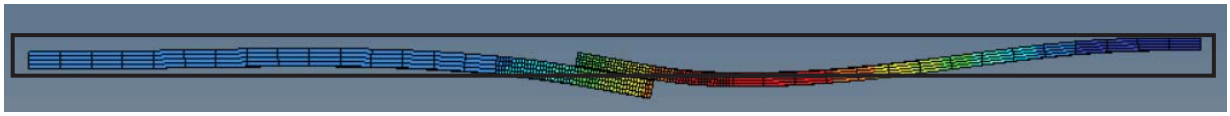

(d) Bottom substrate thickness = 2.8 mm, Top substrate thickness = 2 mm

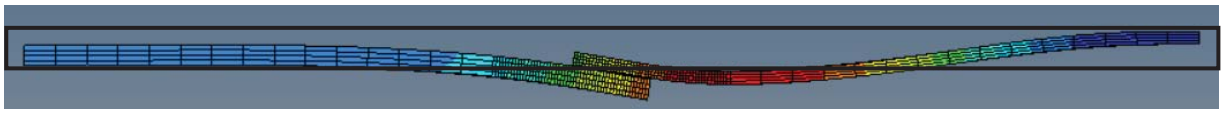

(e) Bottom substrate thickness = 3.2 mm, Top substrate thickness = 2 mm

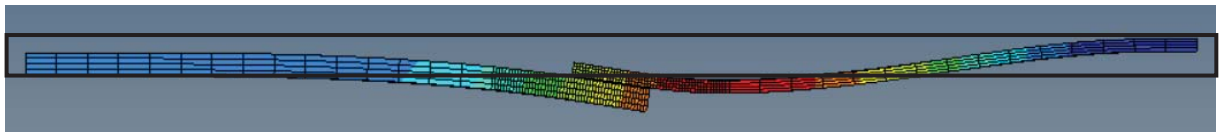

(f) Bottom substrate thickness = 3.6 mm, Top substrate thickness = 2 mm

(g) Bottom substrate thickness = 4 mm, Top substrate thickness = 2 mm

(h) Bottom substrate thickness = 4.4 mm, Top substrate thickness = 2 mm

Figure 2.14: Comparison of the joint deformation with increasing bottom substrate thickness

Figures 2.15 – 2.18 show the variations of σ_{yy}, σ_{zz} and τ_{yz} in the adhesive length direction at the mid-width of the overlap area and at the top interface, mid-thickness and bottom interface of the adhesive layer. On the loading side, σ_{yy} and σ_{zz} decrease as the bottom substrate thickness is increased form 1.6 mm to 4.4 mm. The reverse occurs on the reaction side. Both normal stresses have their maximum values on the reaction side for bottom substrate thicknesses of 1.6 and 2 mm. As the bottom substrate thickness becomes higher than 2 mm, their maximum values occur on the reaction side.

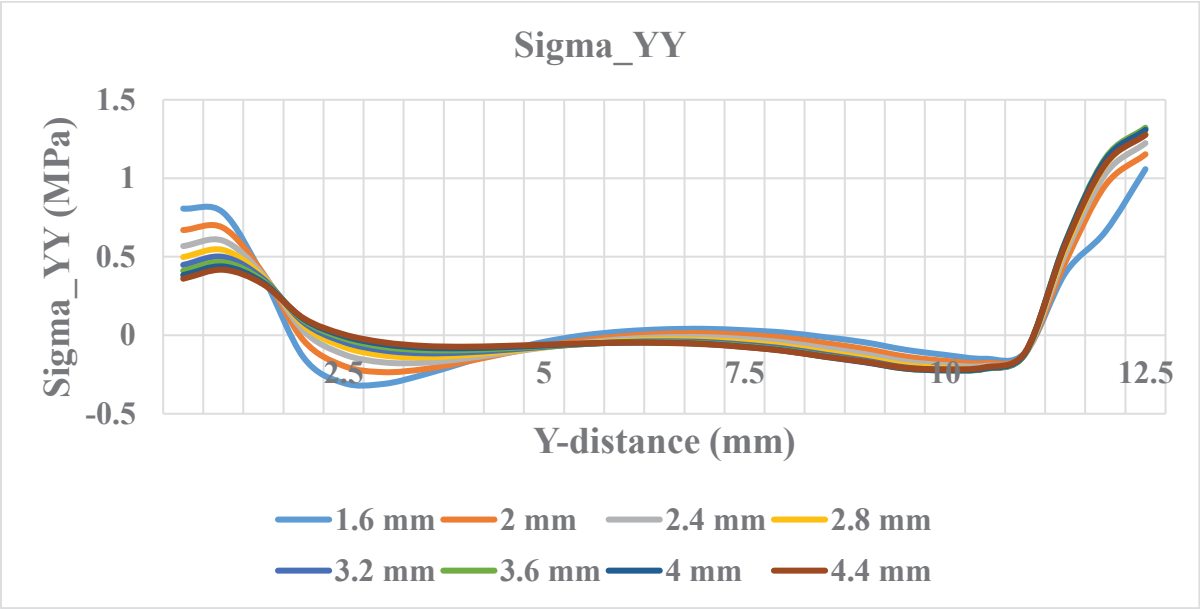

(a) Longitudinal stress (σ_{yy})

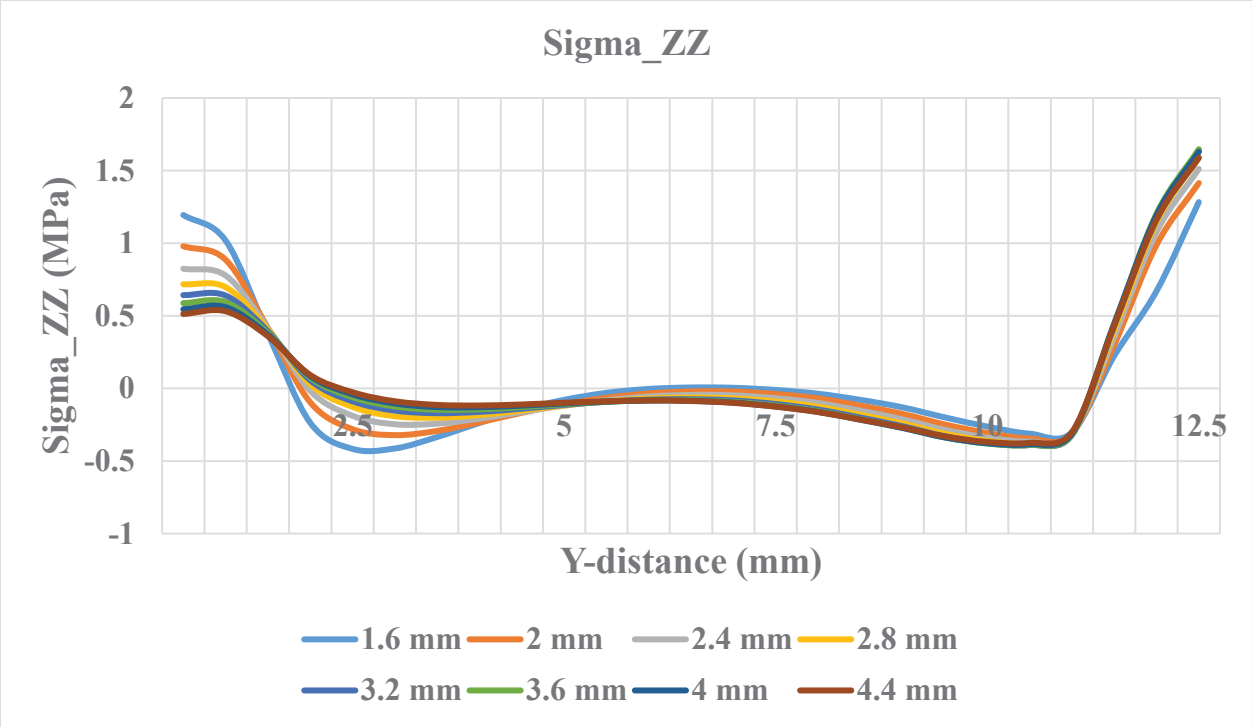

(b) Peel stress (σ_{zz})

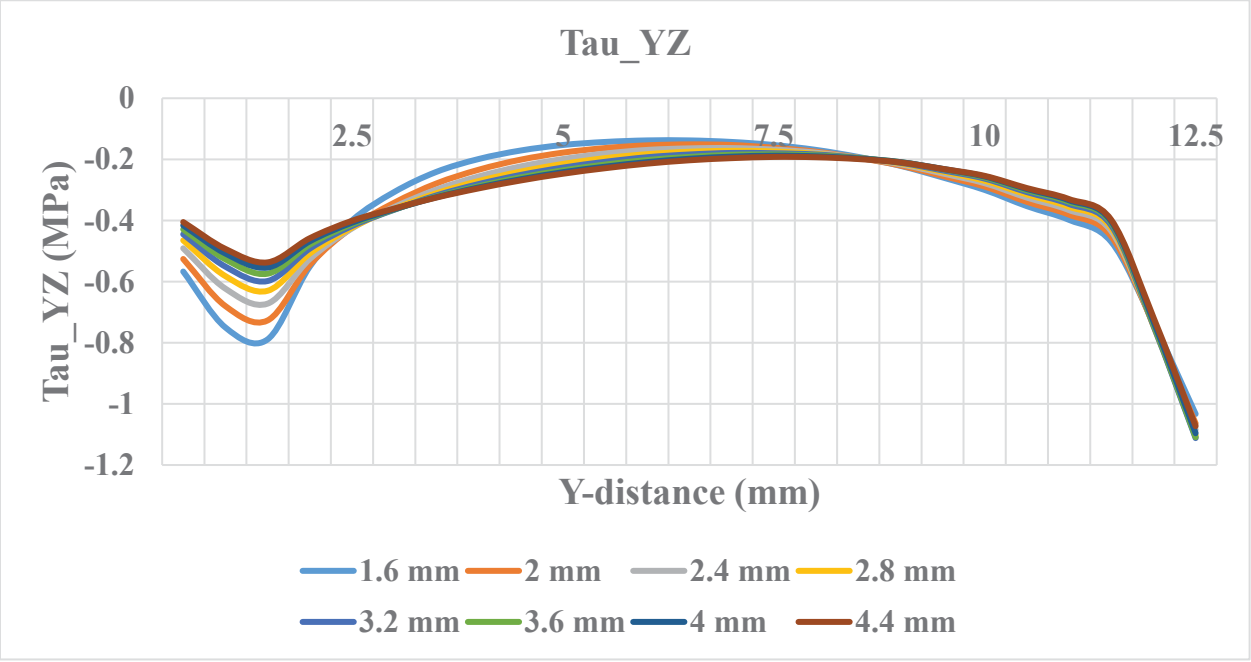

(c) In-plane shear stress (τ_{yz})

Figure 2.15: Stress distributions in the length direction at the top interface for different bottom substrate thickness

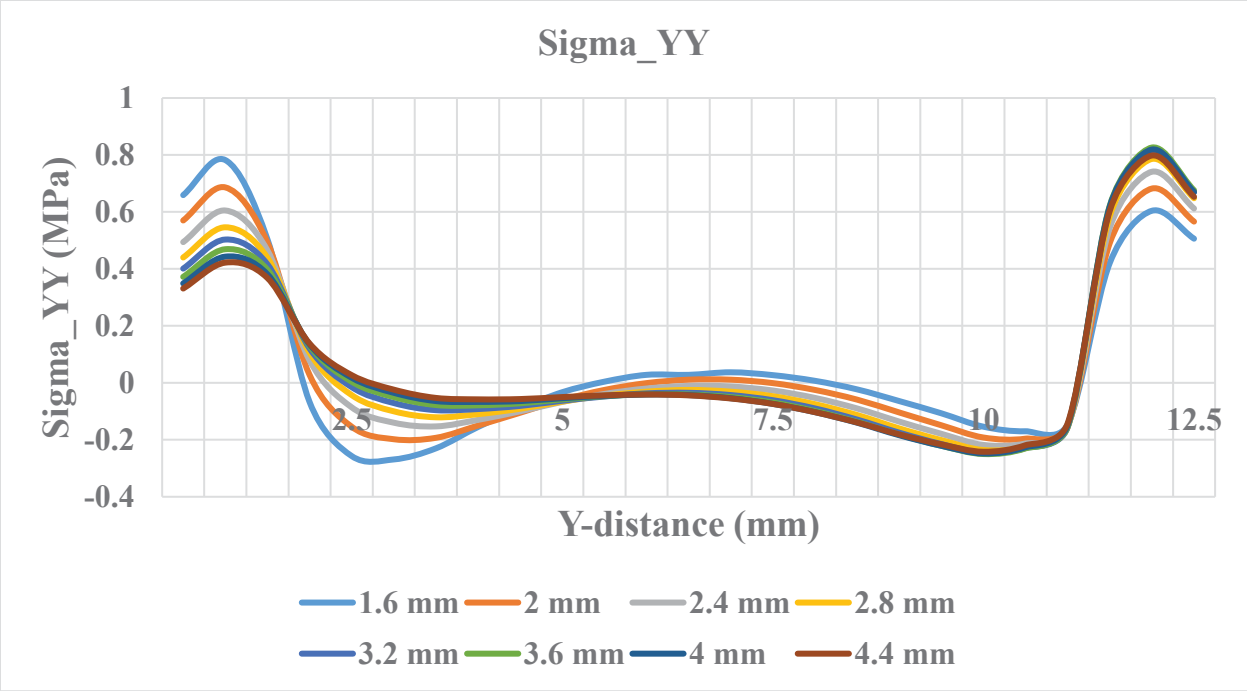

(a) Longitudinal stress (σ_{yy})

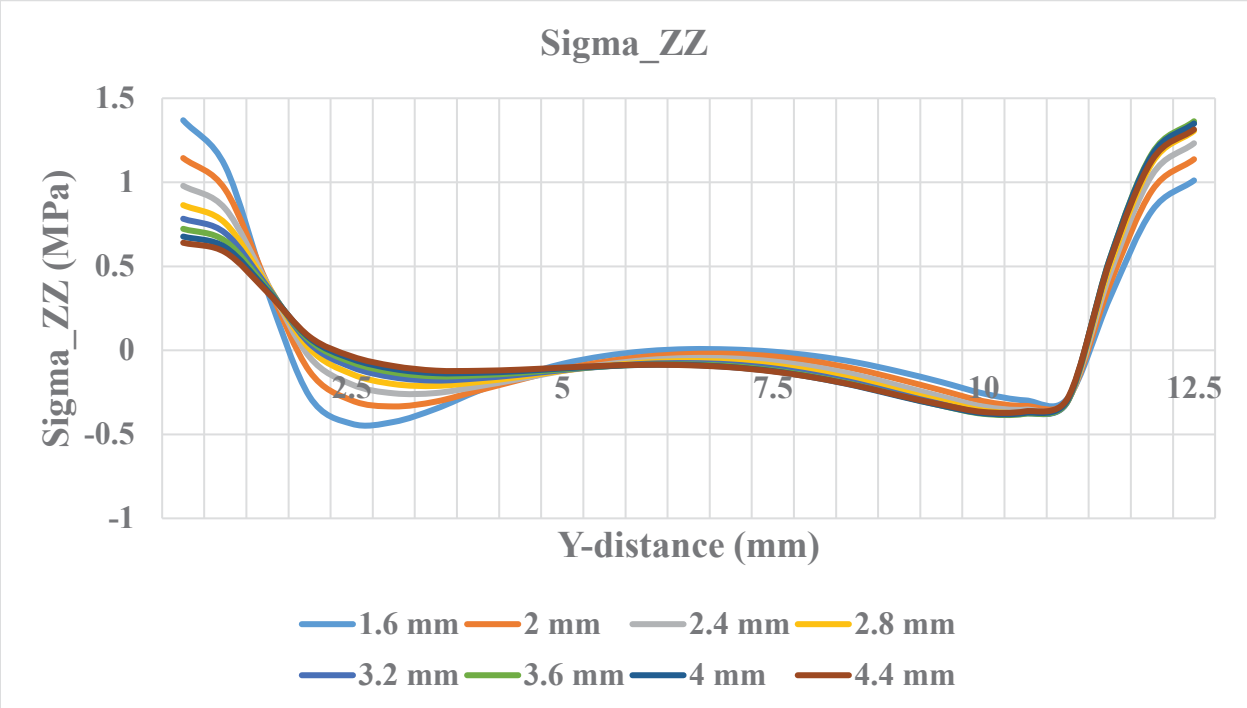

(b) Peel stress (σ_{zz})

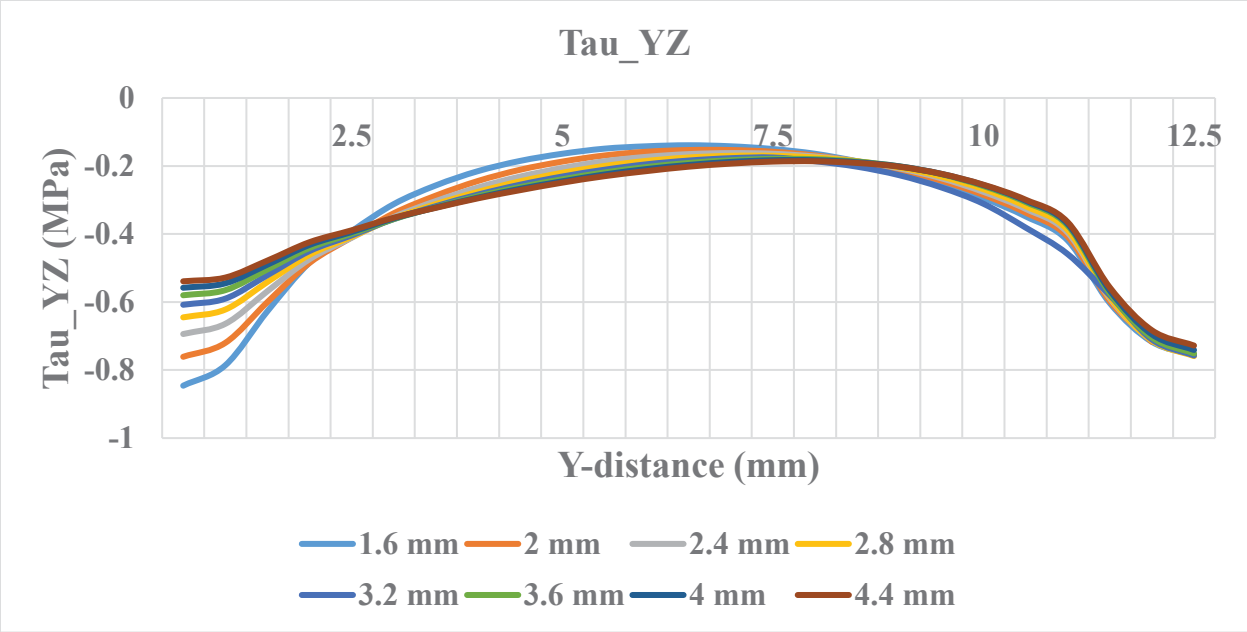

(c) In-plane shear stress (τ_{yz})

Figure 2.16: Stress distributions in the length direction at the mid-plane for different bottom substrate thickness

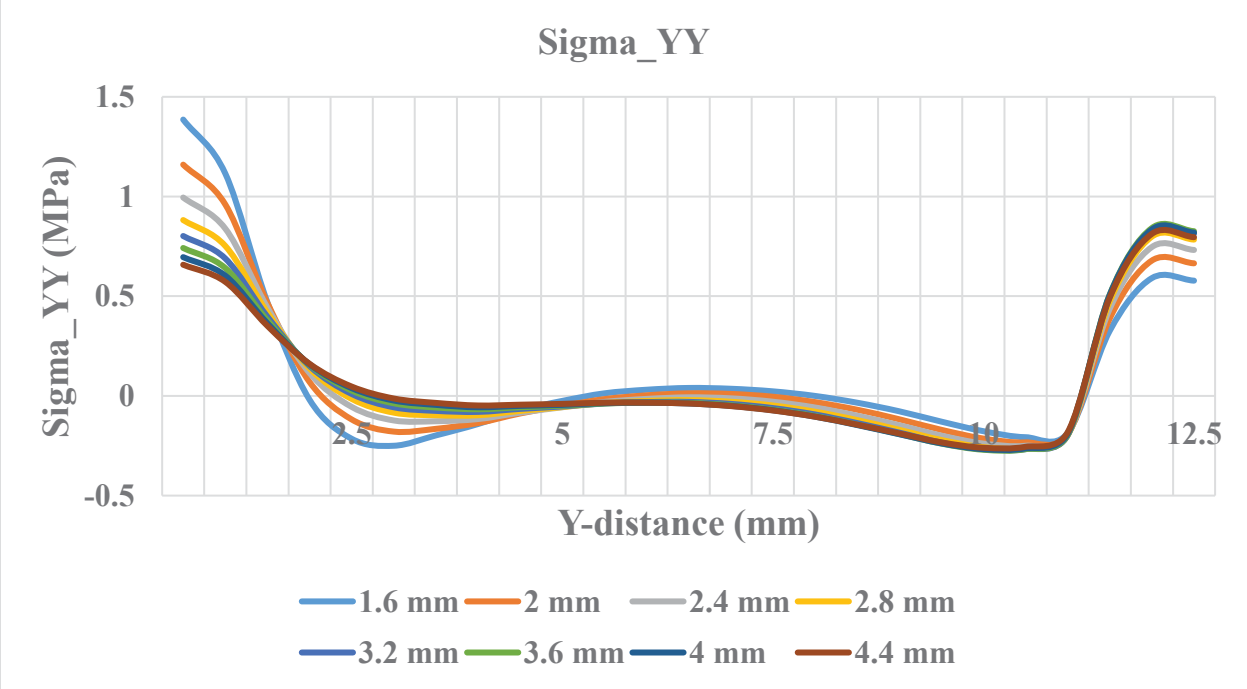

(a) Longitudinal stress (σ_{yy})

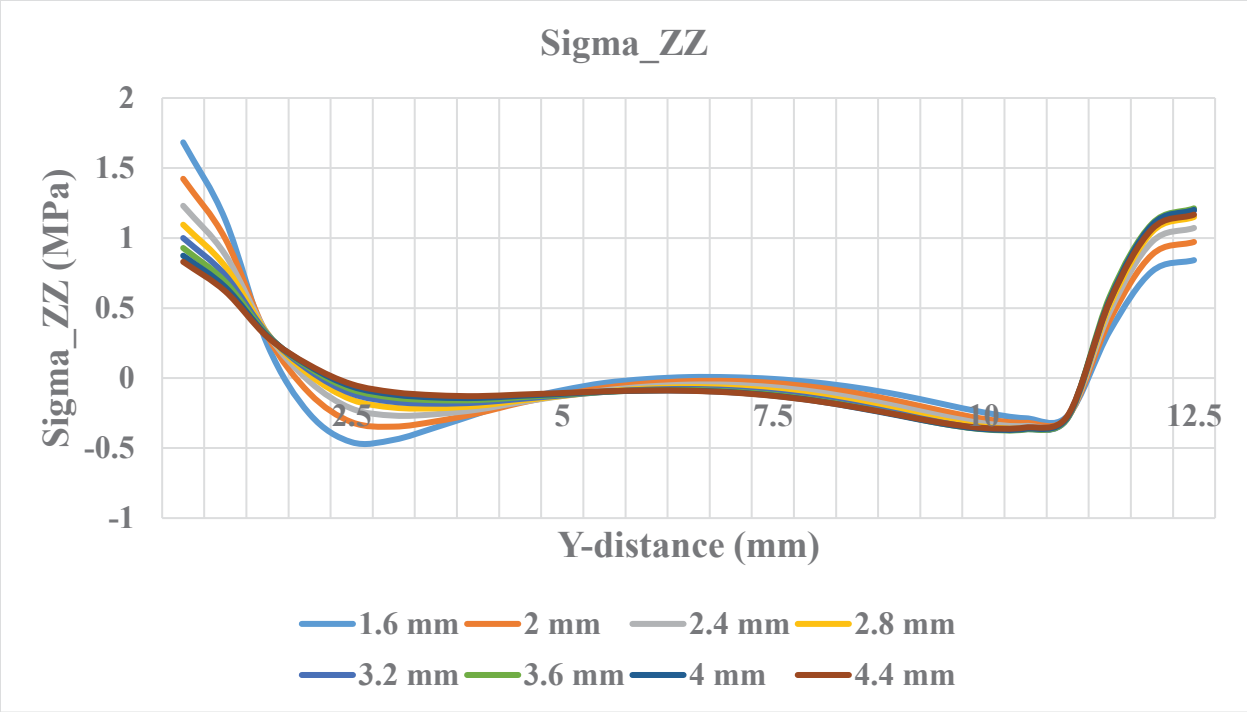

(b) Peel stress (σ_{zz})

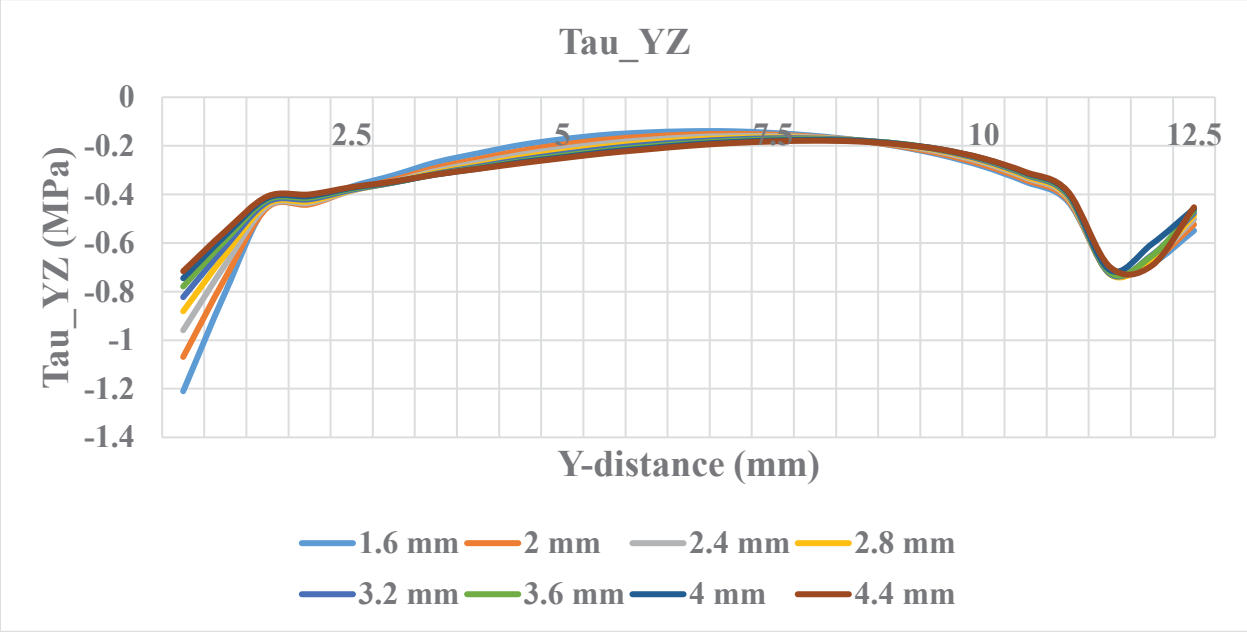

(c) In-plane shear stress (τ_{yz})

Figure 2.17: Stress distributions in the length direction at the bottom interface for different bottom substrate thickness

Figures 2.18 and 2.19 compare the peel stress σ_{zz} and in-plane shear stress τ_{yz} values for Mg-Mg joints at a 100-N load for different bottom substrate thicknesses. The following observations can be made from these figures.

(a) The peel stress (σ_{zz}) in the width-direction has the highest value for 1.6 mm thick bottom substrate thickness, which is lower than the top substrate thickness. It has the lowest value for 2 mm thick bottom substrate thickness which is the same as the top substrate thickness. At higher bottom substrate thicknesses, the peel stress first increases and then starts to decrease.

(b) The variation of the maximum shear stress with increasing bottom substrate thickness is similar to that observed for the maximum peel stress. The highest maximum shear stress occurs with 1.8 mm bottom substrate thickness and the lowest occurs with 2 mm bottom substrate thickness.

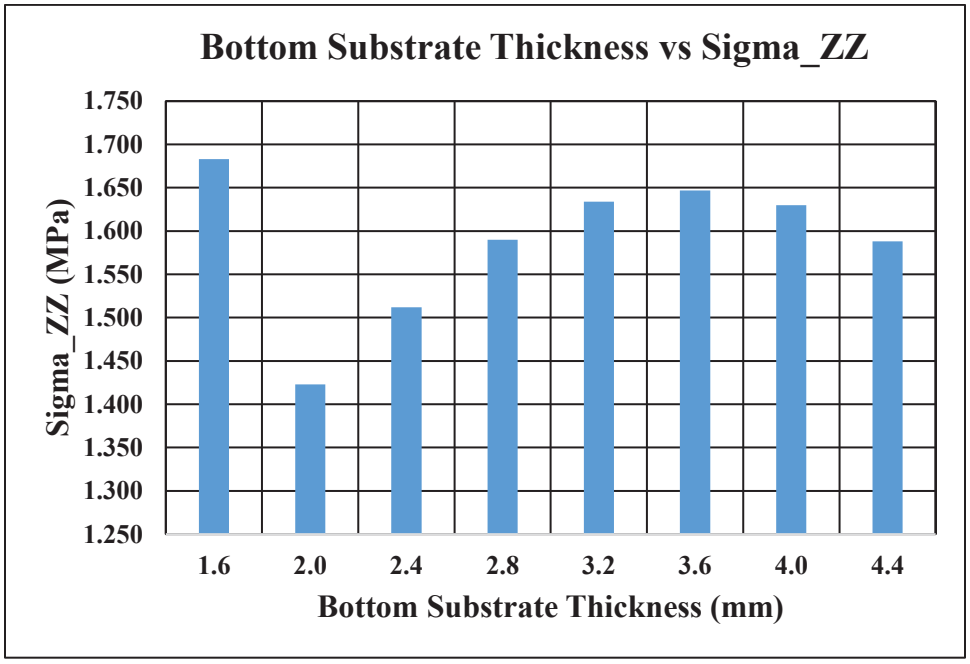

Figure 2.18: Maximum peel stress (σ_{zz}) vs. bottom substrate thickness

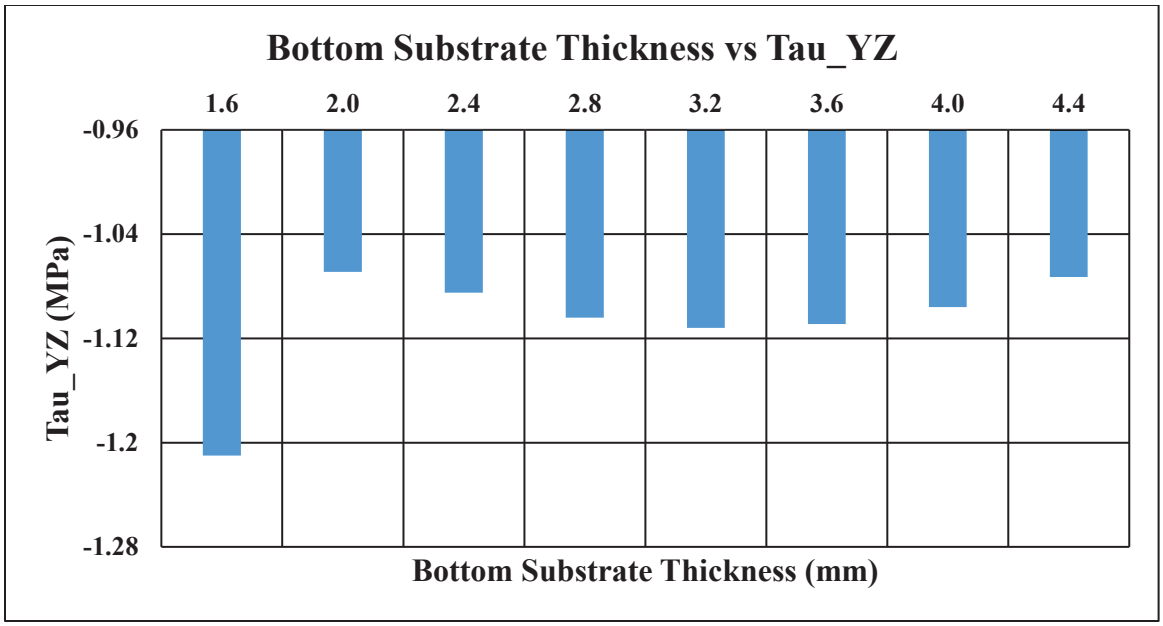

Figure 2.19: Maximum shear stress (τ_{yz}) vs. bottom substrate thickness

2.5 Single lap adhesive joint with lateral pressure applied in the overlap area

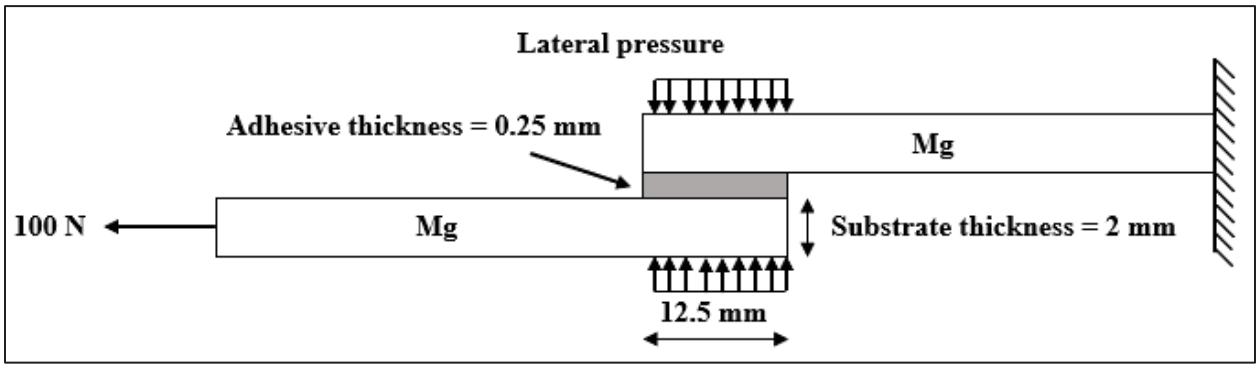

Figure 2.20: Single lap adhesive joint with lateral pressure applied in the overlap area

The study in this section investigates the effect of applying lateral pressure in the overlap area of the top and bottom substrates (Figure 2.10) on the stress distribution and maximum stresses in the adhesive layer. The area over which the lateral pressure was applied uniformly is 12.5 mm x 25 mm = 312.5 mm^2. The applied lateral pressure is 1, 2, 5 and 10 MPa.

Figure 2.21 shows the stress distributions along the length direction at the mid-width of the adhesive layer with a 2 MPa lateral pressure. The stress distributions are shown on top and bottom

interfaces as well as at the mid-thickness. As can be observed in Figure 2.21, all three normal stresses σ_{xx} , σ_{yy} and σ_{zz} are compressive. Their minimum values occur at the ends of the overlap and their maximum values occur within 2 mm from each end. In-plane shear stresses (τ_{yz}) are maximum near the overlap ends and nearly zero at the mid-length of the adhesive layer.

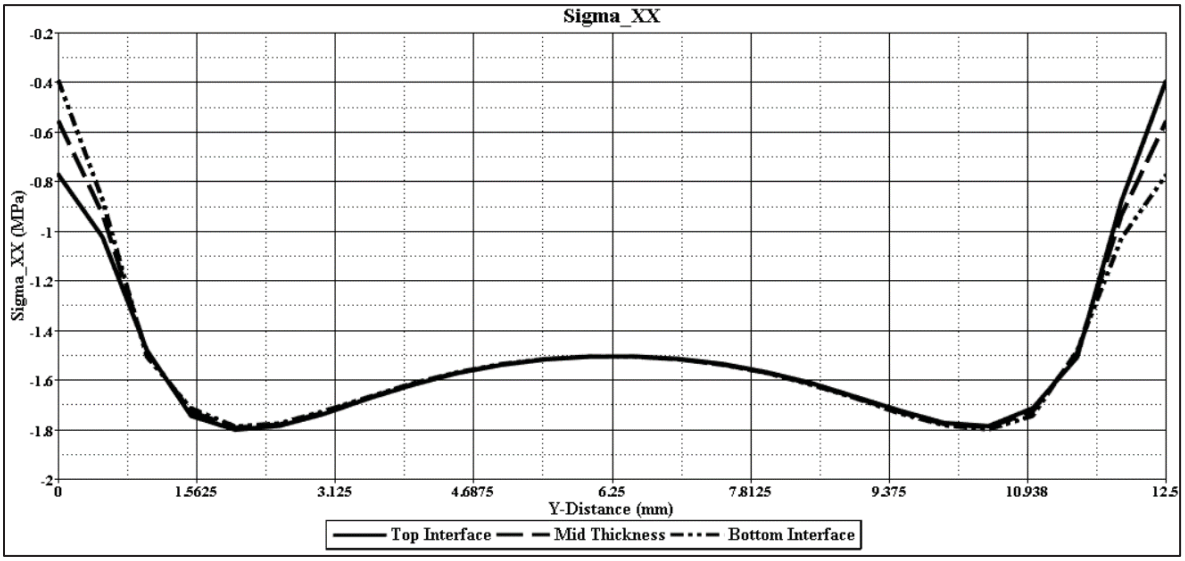

(a) Width-direction stress (σ_{xx})

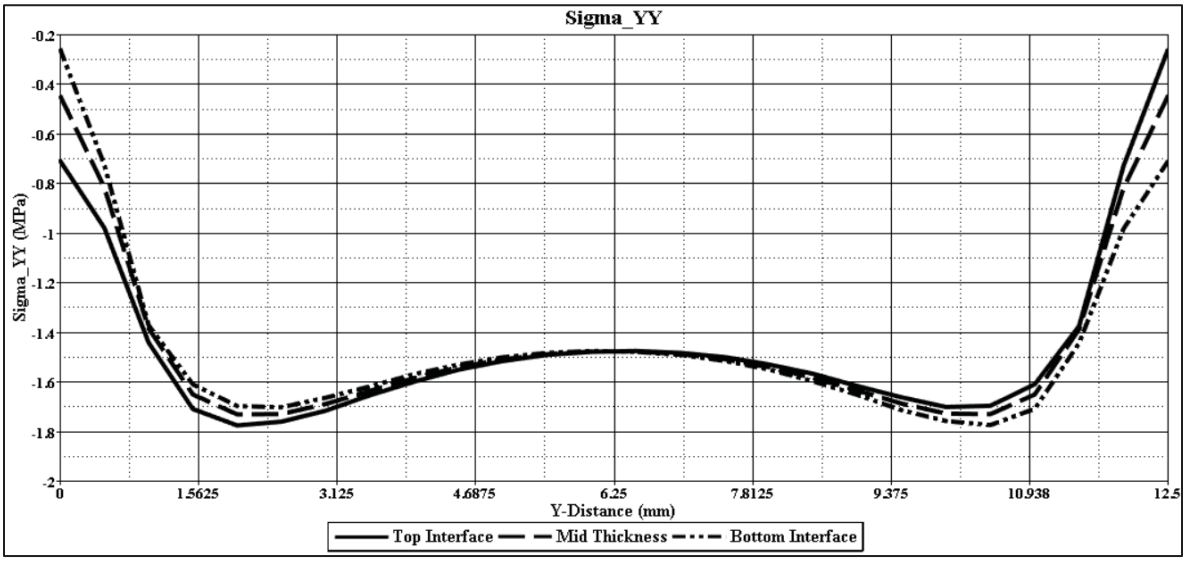

(b) Longitudinal stress (σ_{yy})

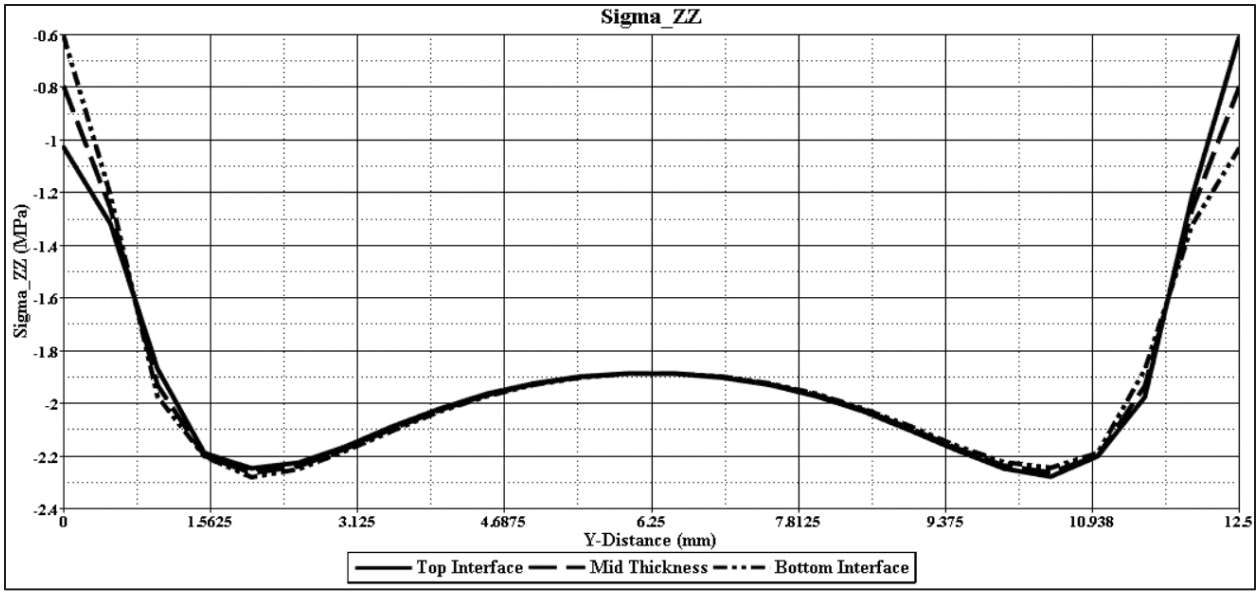

(c) Peel stress (σ_{zz})

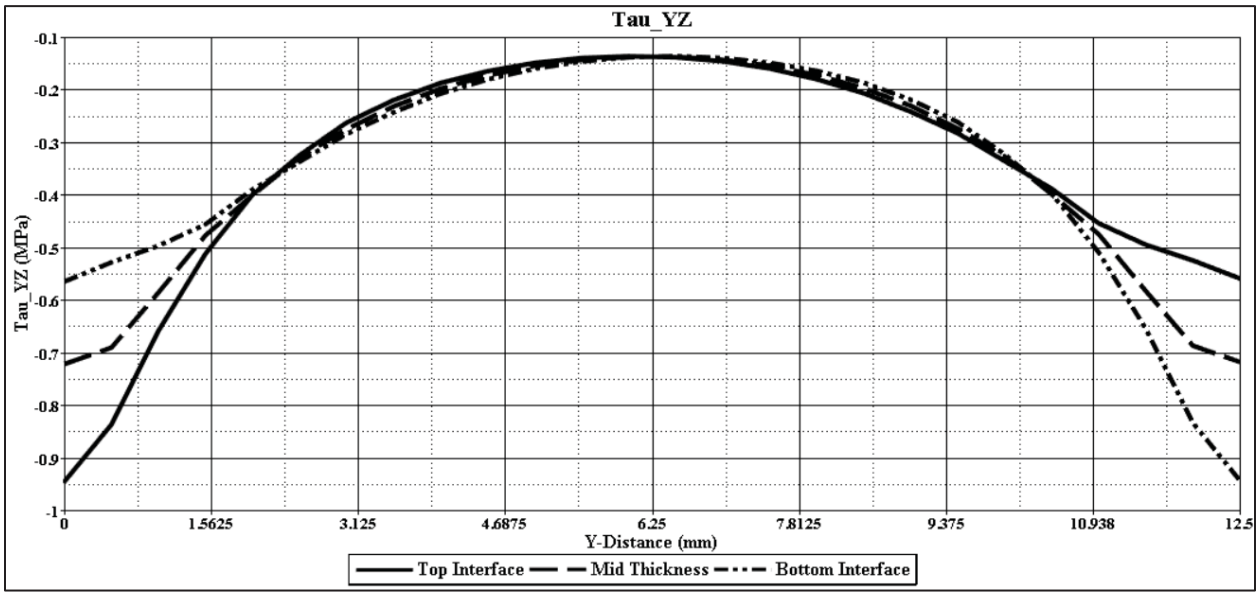

(d) Shear stress (τ_{yz})

Figure 2.21: Stress distributions in the adhesive layer of a single lap adhesive joint with a lateral pressure of 2 MPa applied in the overlap area

Table 2.4 lists the peel and in-plane shear stresses at the two overlap ends (y = 0 and 12.5 mm). Both these stresses increase in magnitude as the applied pressure is increased. The peel stress is compressive in nature, whereas without the lateral pressure, the peel stress is tensile. This

is beneficial since the lateral pressure reduces the peel stress at the overlap ends and changes it to compressive. However, the magnitude of in-plane shear stress at the overlap end increases with increasing clamping pressure.

Table 2.4 Effect of lateral pressure applied in the overlap area(1) on peel and in-plane shear stresses

Lateral Pressure (MPa)	Peel Stress (σ_{zz}) (MPa)			Inplane Shear Stress (τ_{yz}) (MPa)		
	Y = 0	Y = 6.25 mm	Y = 12.5 mm	Y = 0	Y = 6.25 mm	Y = 12.5 mm
0	0.979	-0.022	1.423	-0.565	-0.153	-1.069
1	-1.028	-1.160	-0.902	-0.806	-0.146	-0.813
2	-2.197	-2.314	-1.980	-1.053	-0.142	-0.559
5	-5.771	-5.771	-5.424	-1.849	-0.196	0.609
10	-11.747	-11.531	-11.318	-3.208	-0.304	1.972

(1) Overlap area = 12.5 mm x 25 mm =312.5 mm^2.

2.6 Conclusions

A three-dimensional stress analysis of a single lap adhesive joint between two magnesium substrates was performed using a finite element software. It was observed that in addition to the longitudinal and peel stresses, there is a significant width-direction normal stress at the top and bottom interfaces. Thus, the stress state in the adhesive layer is tri-axial in nature, which a two-dimensional stress analysis will not exhibit. All three normal stresses have their highest values at the overlap ends where the in-plane shear stress also has its highest value.

The difference in substrate thickness is shown to cause significant difference in bending deformation and joint rotation. As the ratio of the bottom and top substrate thicknesses is increased, both bending deformation and joint rotation decreased. The peel stress and in-plane

shear stress values have their lowest values when the two substrate thicknesses are equal and therefore, their bending stiffness values are also equal.

Finally, it is shown that application of lateral pressure can cause significant reduction in the maximum peel stress. With increasing values of the lateral pressure, the peel stress at the lap ends becomes increasingly compressive, which can be beneficial in terms of preventing joint failure due to tensile peel stress which ordinarily exist without the lateral pressure. However, there is also an increase in in-plane shear stress with increasing lateral pressure. This can contribute to shear failure at the joint.

References

1. Adams, R.D., Comyn, J. and Wake, W.C., Structural Adhesive Joints in Engineering, Chapman and Hall, London, 1997.

2. Crocombe, A.D. and Adams, R.D., Influence of the spew fillet and other parameters on the stress distribution in the single lap joint, Journal of Adhesion, Vol.13, p. 141-155, 1981.

3. Lang, T.P and Mallick, P. K., Effect of spew geometry on stresses in single-lap adhesive joints, International Journal of Adhesion and Adhesives, Volume 18, p. 167-177, 1998.

4. Belingardi, G., Gogilo, L. and Tarditi, A., Investigating the effect of spew and chamfer size on the stresses in metal/plastics adhesive joints, International Journal of Adhesion and Adhesives, Volume 22, p. 273-282, 2002.

5. Gonçalves, J.P.M., de Moura, M.F.S.F and de Castro, P.M.S.T., A three-dimensional finite element model for stress analysis of adhesive joints, International Journal of Adhesion and Adhesives, Volume 22, p. 357-365, 2002.

6. Li, G., Lee-Sullivan, P. and Thring, R.W., Nonlinear finite element analysis of stress and strain distributions across the adhesive thickness in composite single-lap joints, Composite Structures, Volume 46, p. 395-403, 1999.

7. Bhambure, S.A., Stress analysis of adhesive joints with magnesium alloys, Master's Thesis, Automotive Systems Engineering, University of Michigan-Dearborn, 2011.

CHAPTER 3

Stress Analysis of an Adhesive Joint with a Hole

3.1 Introduction

Adhesive joints are gaining importance in many industries owing to a significant number of advantages over welding and traditional mechanical fastening techniques such as riveting and bolting. The advantages include the uniform stress distributions along the joint length, possibility of joining different substrate materials, better fatigue performance, improved damping characteristics and lower cost. Among the available bonding configurations, the single-lap joint is the most commonly used and studied joint in the literature due to its simplicity, although it experiences significant bending deformations due to the non-collinear load path. The load eccentricity is responsible for peak peel stresses at the overlap ends, which added to peak shear stresses, also at the overlap ends, due the differential shear deformation effects can negatively affect the joints effectiveness [1]. To improve the joint strength and durability, an adhesive joint is often combined with one or more mechanical fasteners, such as bolts, that are securely tightened in the overlap area of the substrates using a clamping pressure. In order to include a mechanical fastener, a hole is drilled through both substrates and the adhesive layer. The mechanical fastener, which may include a bolt, two washers and a nut, is tightened using a clamping torque, which creates clamping pressure in the thickness direction of the joint [2]. The clamping pressure depends on the clamping torque and the clamping area, which is typically the area of the washer used in a bolted joint.

In this chapter, the effect of the presence of a hole on the stress distribution in the adhesive layer in a single lap adhesive joint is investigated. The hole diameter and location are varied to determine their effects on the stress distributions and maximum stresses in the adhesive layer. The effect of clamping pressure distributed over a circular area around the hole, simulating an actual bolted joint with washers, is also studied.

3.2 Specimen, Material and Finite Element Model

The specimen dimensions and axis location used for the single lap joints are shown schematically in Figure 3.1. The length and width dimensions of both the substrates are 100 mm and 25 mm, respectively. Both substrates have a uniform thickness of 2 mm. The length of the overlap is 12.5 mm and the adhesive thickness is assumed to be 0.25 mm. The location of the origin and the co-ordinate axis directions are also defined in Figure 3.1. Also shown in the figure is a hole of 5 mm diameter located at the center of the adhesive joint. The other hole diameters considered in this chapter are 2, 3, 4 and 5 mm.

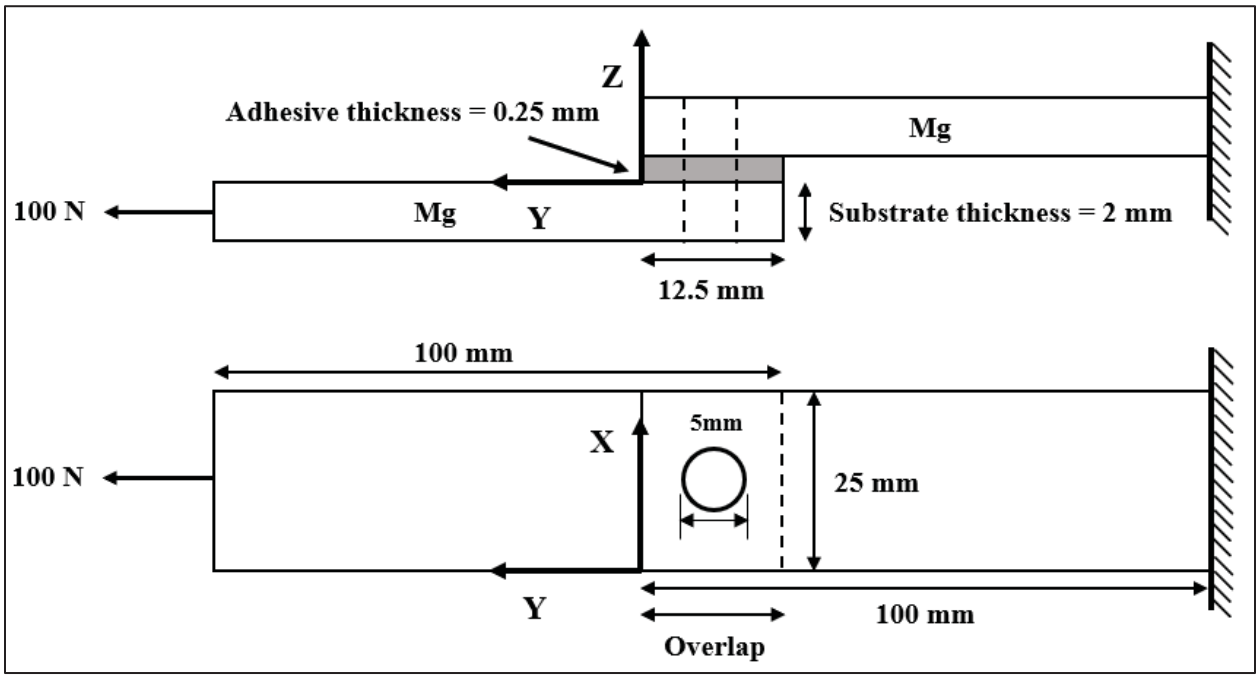

Figure 3.1 Specimen dimensions with a hole at the center of the overlap in a single-lap joint

The elastic properties of the substrate material, namely magnesium alloys, and the adhesive material are listed in Table 2.1 in Chapter 2. The adhesive is an unfilled epoxy, which is a common adhesive material in the automotive and aerospace industries. The boundary conditions are as described in Chapter 2. A 100 N load is applied in the Y-direction at the end of the bottom substrate.

A 3D fine mesh was used around the overlap region and a relatively coarse mesh was used towards the ends of the joint. This particular mesh pattern was selected to reduce the computation

time for simulation while maintaining the accuracy of results. The overview of the mesh pattern is shown in Figure 3.2. The details of the elements used in the finite element model are given in Chapter 2.

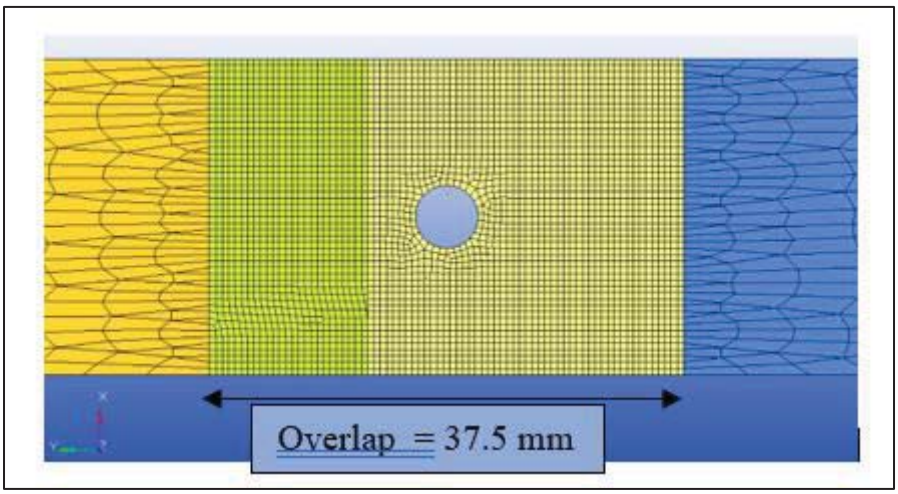

Figure 3.2 Mesh pattern used along the single lap joint

The following studies were conducted in this chapter.

(1) Effect of hole size by considering 2, 3, 4 and 5 mm holes (Figure 3.3a) located at the center of the overlap area,

(2) Effect of hole location by considering a 3 mm hole off-centered by 2.5 mm toward the reaction side (Figure 3.3b), and

(3) Effect of clamping pressure on the top and bottom substrates around a hole of 2, 3 and 5 mm at the center (Figure 3.3c). The clamping pressures are 1, 2, 5, and 10 MPa and are applied over an area of 16.5, 31.5 and 59 sq. mm, respectively, around each hole. The respective outer diameters of the washer are 5, 7 and 10 mm.

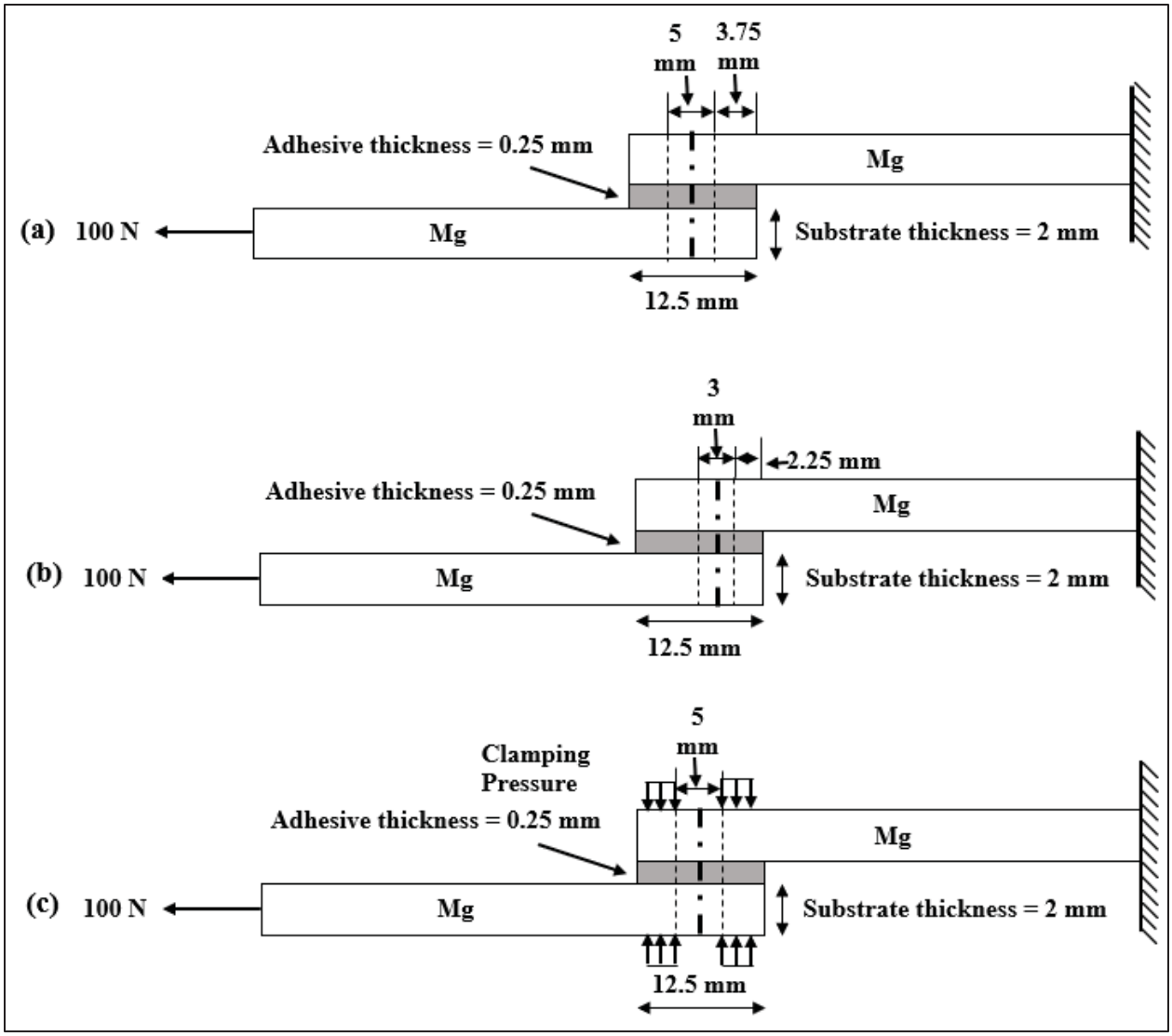

Figure 3.3 Adhesive joint with a hole (a) a centered hole, (b) an off-centered hole (offset by 2.5 mm towards reaction side), and (c) a centered hole with lateral clamping pressure

3.3 Effect of a 5 mm Central Hole on the Stress Distributions in the Adhesive

3.3.1 Stress Distributions in the Width Direction

Figures 3.5 – 3.7 show the stress distributions along the 'top interface', 'mid-thickness' and 'bottom interface' in the adhesive width direction (x-axis) at 'Section A-A' and 'Section B-B' of the adhesive layer as defined in Figure 3.4. Section A-A is located at the mid-length of the overlap and passes through the hole center, whereas Section B-B is located along the left overlap end on the reaction side of the adhesive joint. Since shear stresses τ_{xz} and τ_{xy} are relatively very small,

they are not shown. The significant stresses are the three normal stresses, namely width direction stress σ_{xx}, longitudinal stress σ_{yy} and peel stress σ_{zz}, and the in-plane shear stress τ_{yz}. They are plotted as a function of distance along AA and BB in Figures 3.5 and 3.6. For the purposes of comparison, stress distributions without a hole are also plotted in these figures.

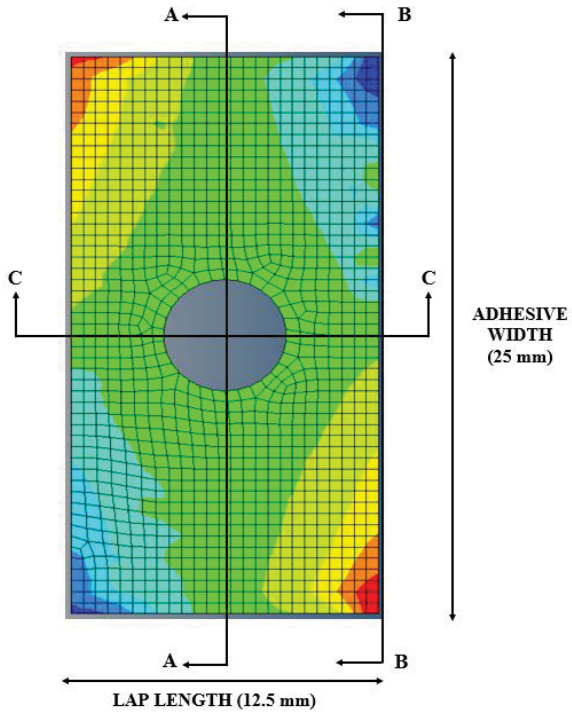

Figure 3.4: Sections considered for stress distribution plots. Sections AA and BB are in the width direction and Section CC is in the length direction of the adhesive

(a) Section A-A (Figure 3.5):

Due to the presence of the hole on Section AA, all four stress components reach their maximum values near the hole. The normal stress components σ_{xx}, σ_{yy} and σ_{zz} within 2.5 mm from the hole edge are tensile in nature. The magnitude of these stresses are much higher than those that exist at this section without the hole. The magnitude of the in-plane shear stresses τ_{yz} is also higher than that without the hole, but the difference is much smaller.

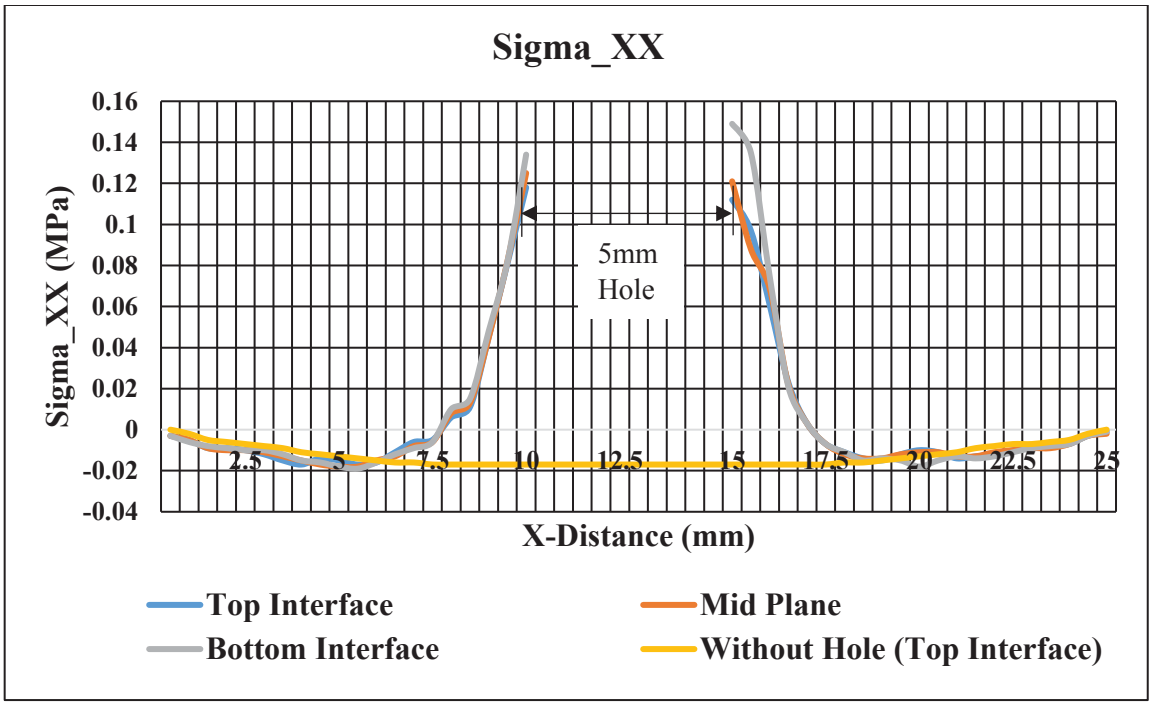

(a) Width-direction stress σ_{xx} along AA

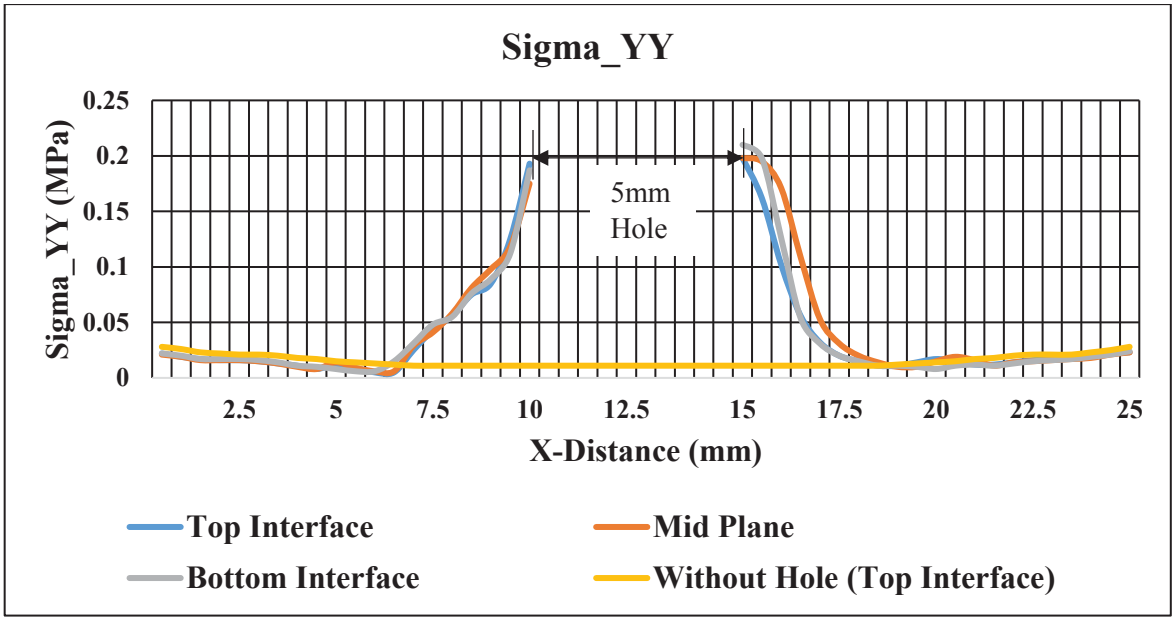

(b) Longitudinal stress σ_{yy} along AA

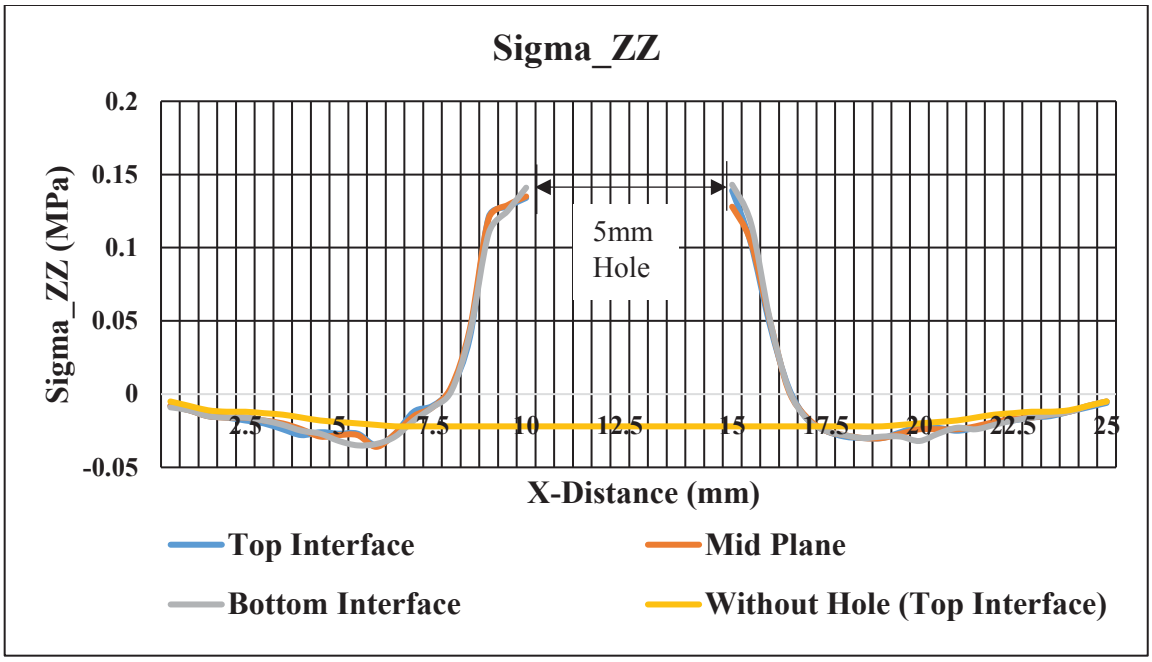

(c) Peel stress σ_{zz} along AA

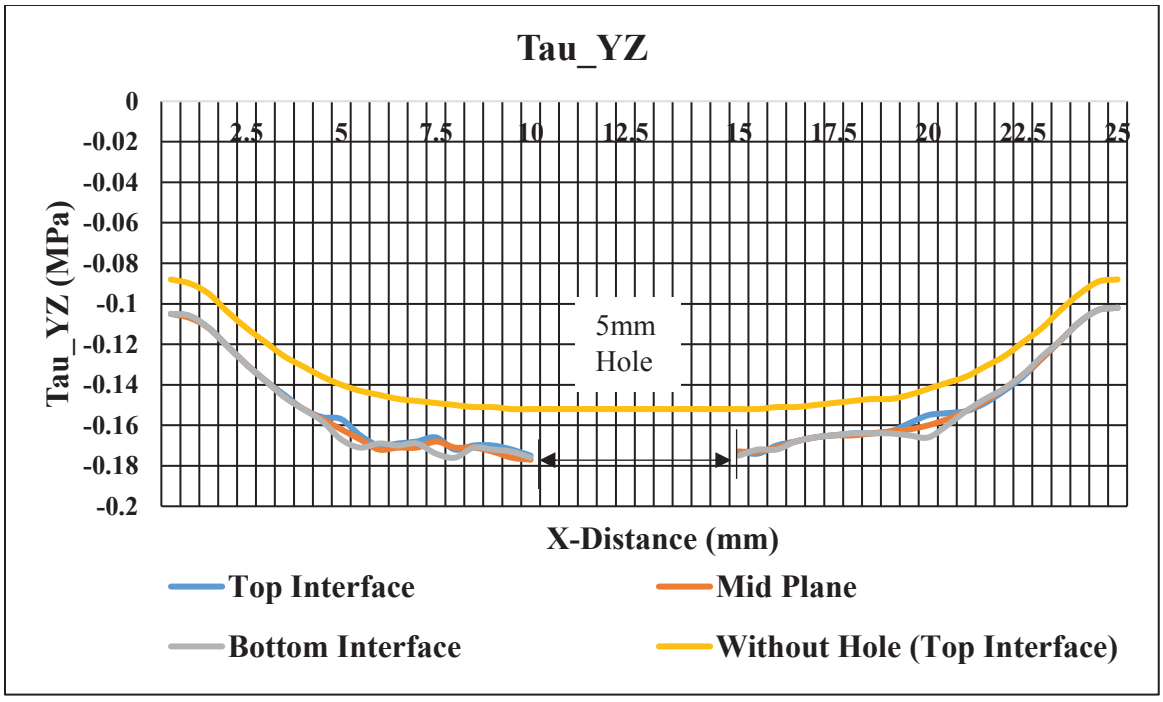

(d) Shear stress τ_{yz} along AA

Figure 3.5: σ_{xx}, σ_{yy}, σ_{zz} and τ_{yz} distributions in the adhesive width direction at 'Section A-A' for a tensile load of 100N

(b) Section B-B (Figures 3.6):

Figure 3.6 shows the stresses in the width direction along Section BB, which is the overlap end at the reaction side. It can be seen in this figure that σ_{xx}, σ_{yy}, σ_{zz} and τ_{yz} increase rapidly from zero or near-zero values at the edges to their highest values at the mid width. All four stress components have their maximum values at the center. Their values are equal to the values obtained without the hole, except that near the mid-width, there is a slight decrease in their values.

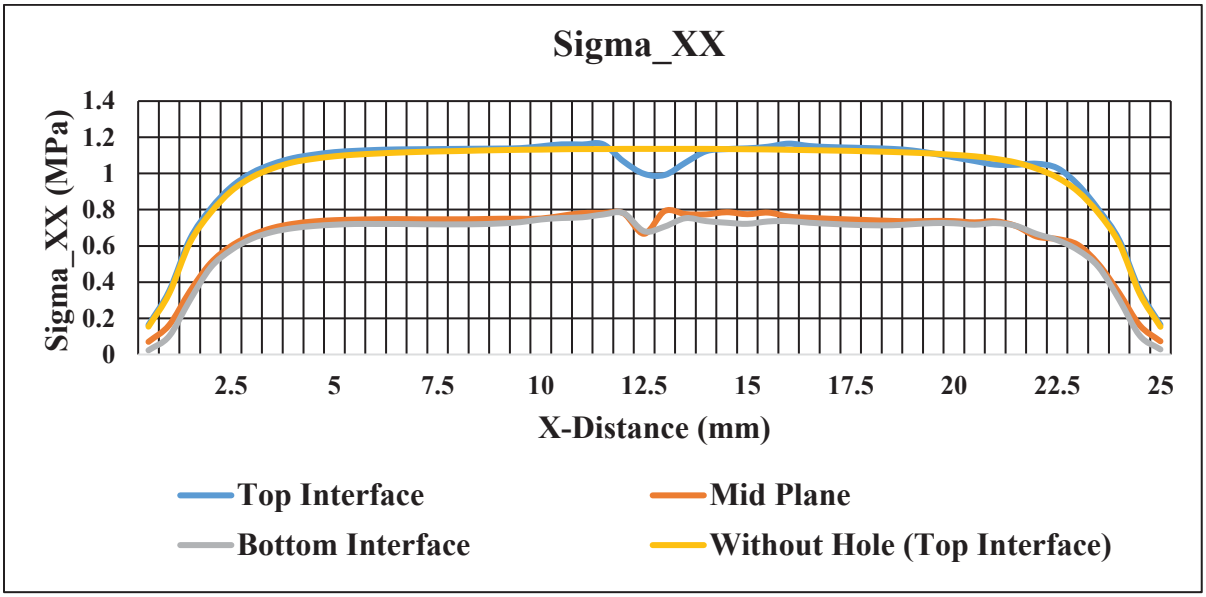

(a) Width-direction stress σ_{xx} along BB

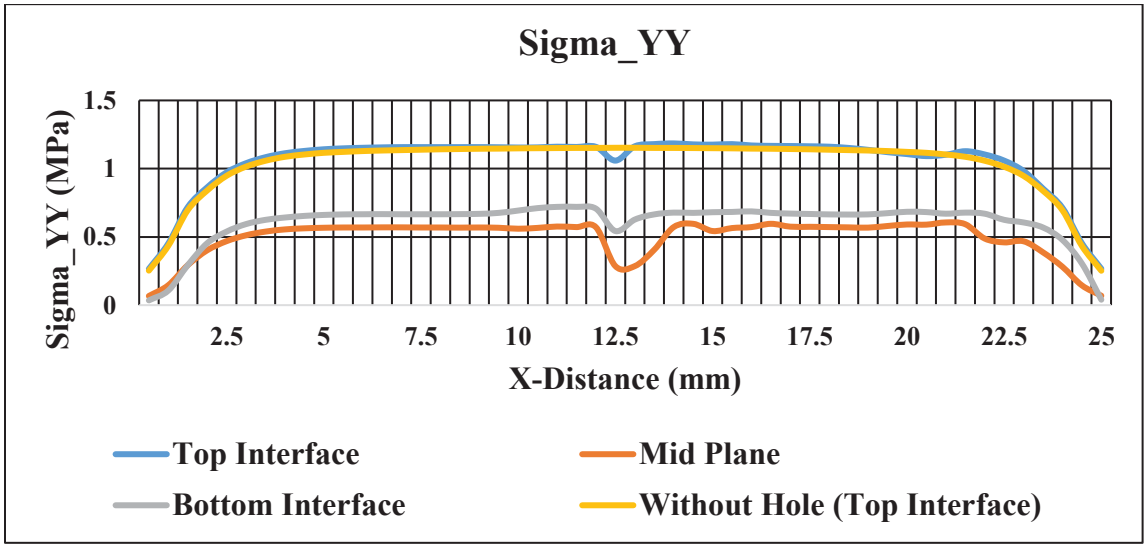

(b) Longitudinal stress σ_{yy} along BB

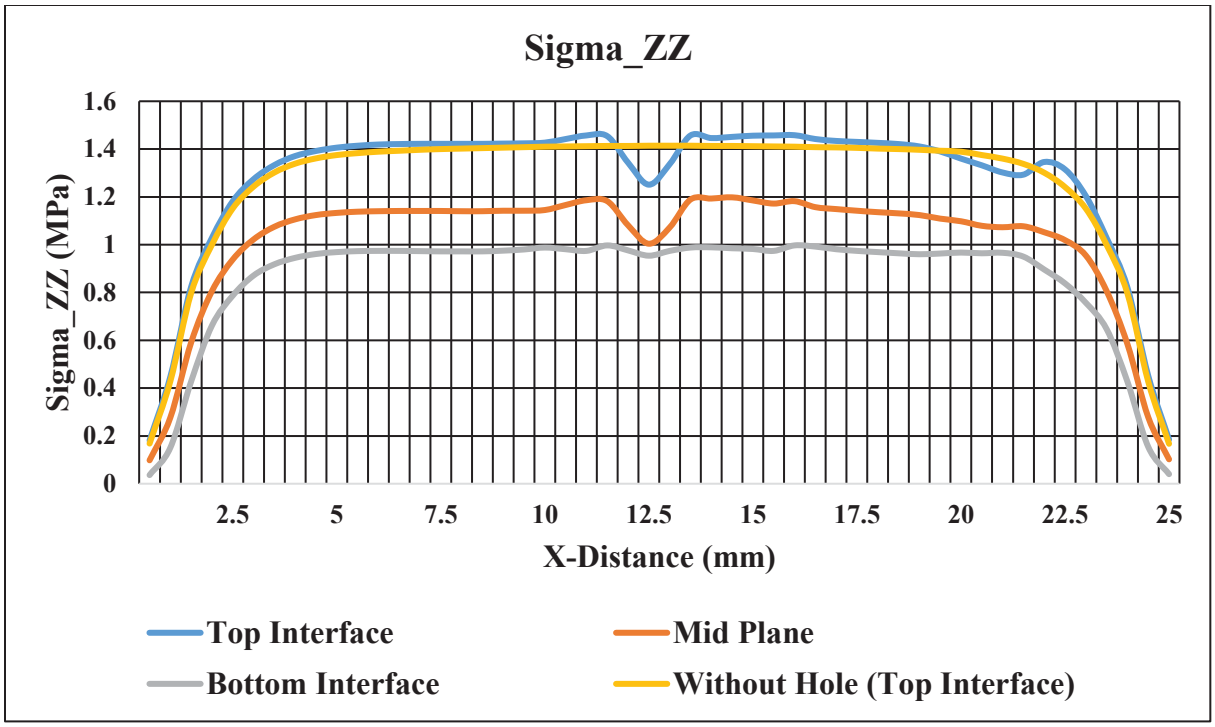

(c) Peel stress σ_{zz} along BB

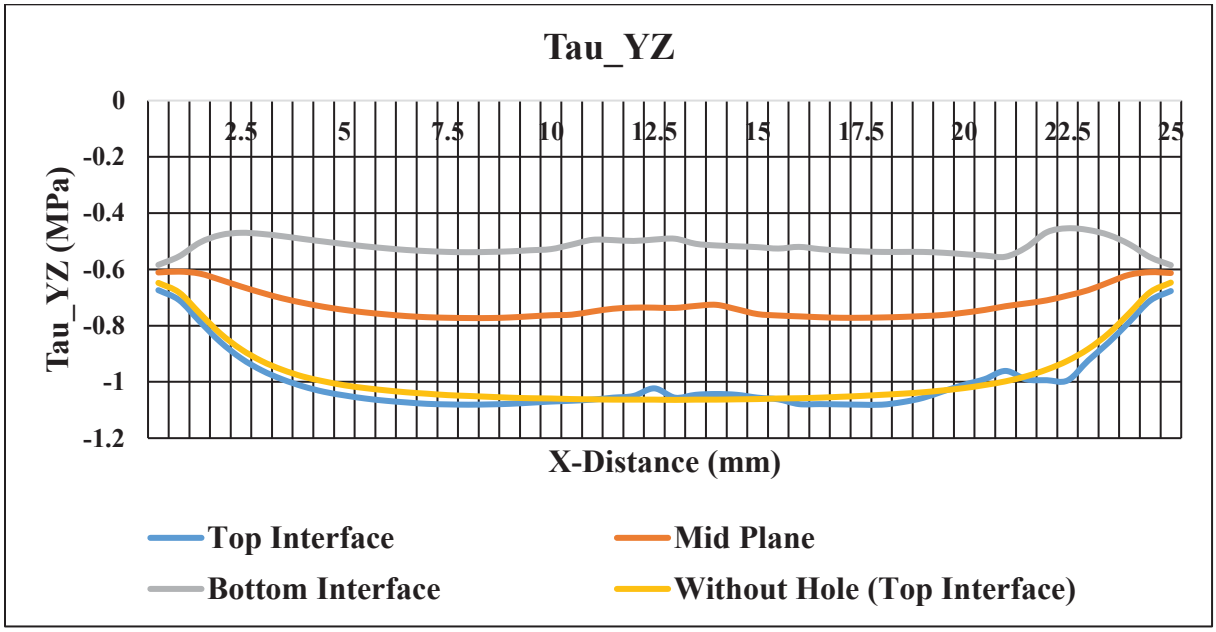

(d) Shear stress τ_{yz} along BB

Figure 3.6: σ_{xx}, σ_{yy}, σ_{zz} and τ_{yz} distributions in the adhesive width direction at the 'Section B-B' for a tensile load of 100N

3.3.2 Stress Distributions in the Length Direction

As shown in Figure 3.7, the stress distributions in the length direction are similar to those observed without a hole. This is expected since the 100-N load is acting along the Y-axis, which coincides with Section CC. There are only small differences in magnitudes in the stresses with a hole and without a hole.

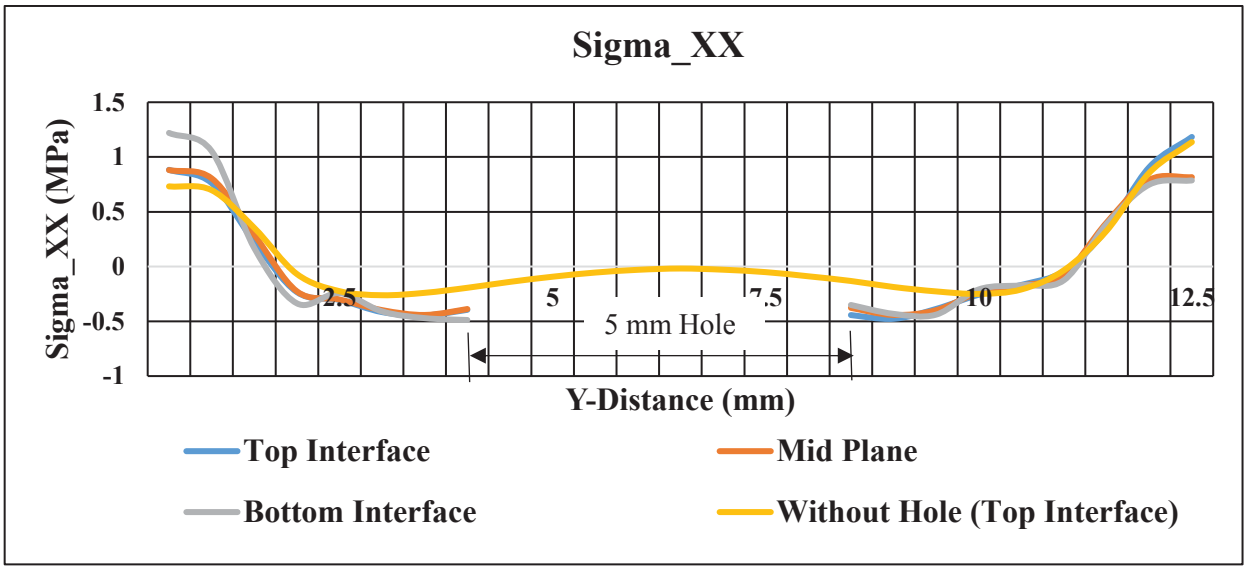

(a) Width-direction stress σ_{xx} along CC

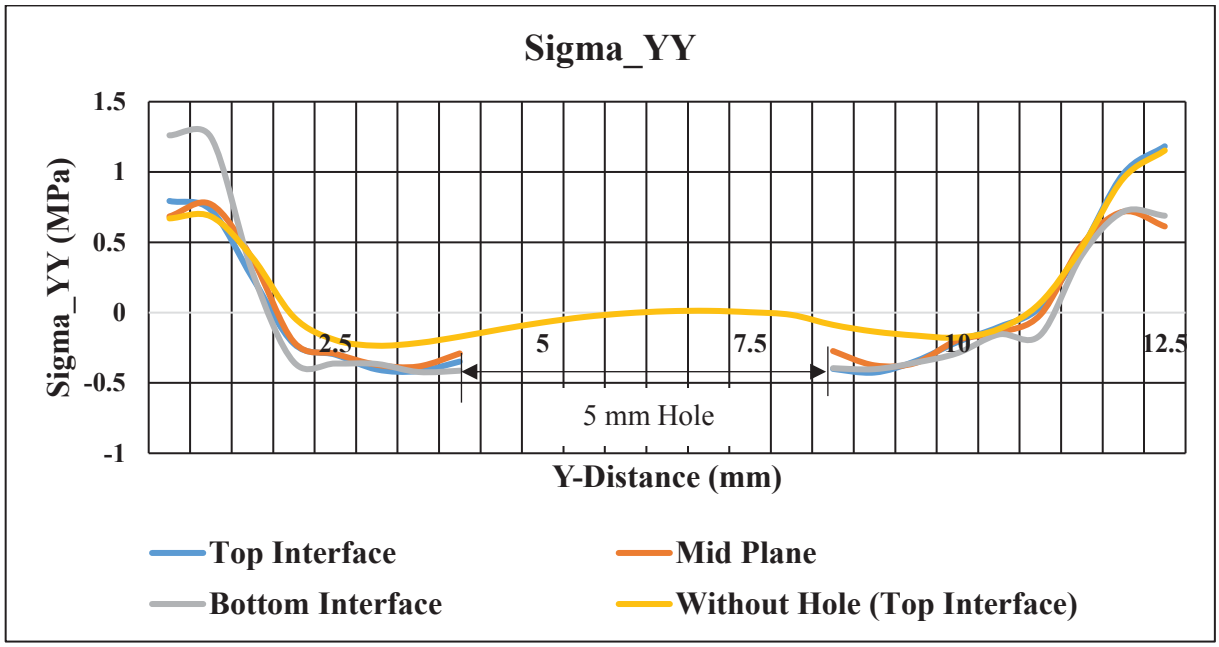

(b) Longitudinal stress σ_{yy} along CC

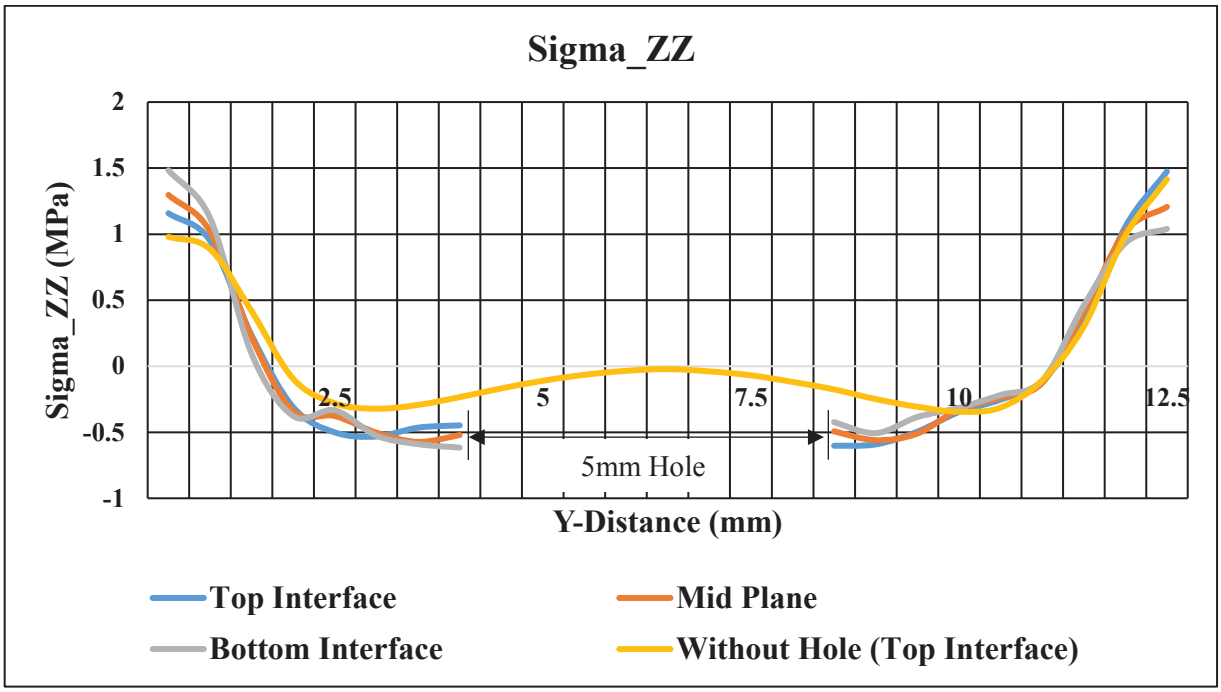

(c) Peel stress σ_{zz} along CC

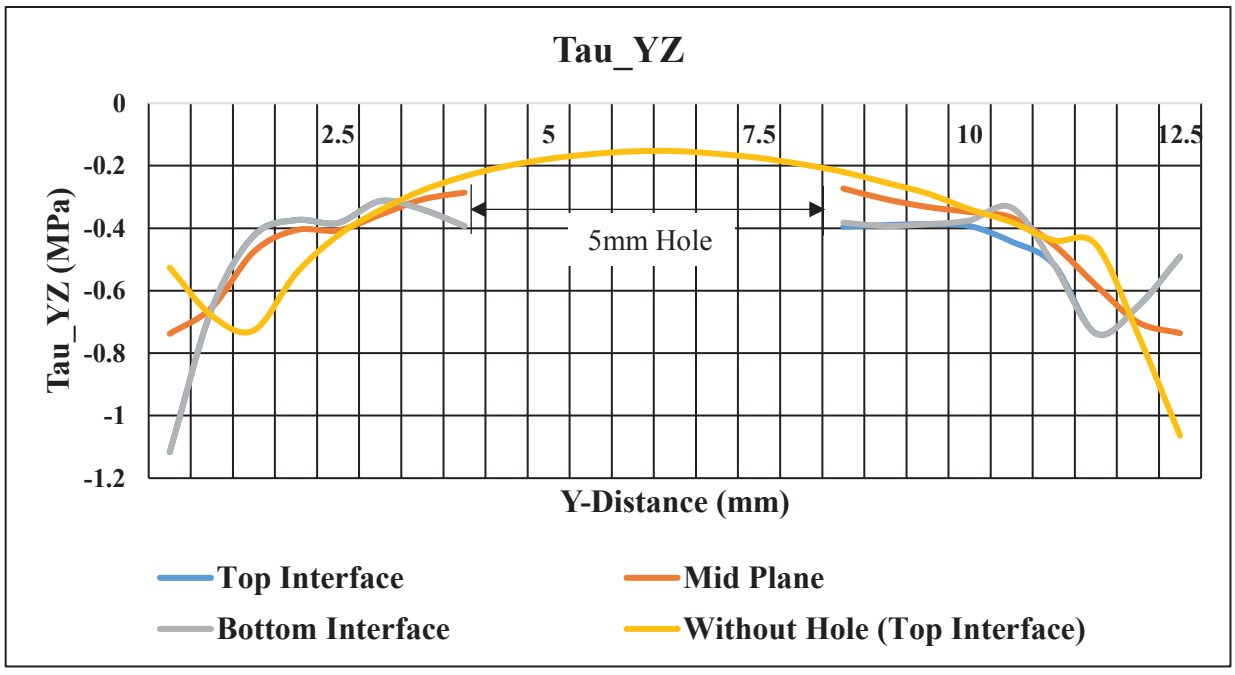

(d) In-plane shear stress τ_{yz} along CC

Figure 3.7: Stress distributions in the length direction at 'Section C-C' at a tensile load of 100 N

3.3.3 Effect of Hole Diameter on Maximum Stress

Table 3.1 compares the maximum stress values in the adhesive layer at a 100 N load for the different hole diameters. It can be observed in this table that the maximum values of all four stress components increase with increasing hole diameter. The longitudinal stress σ_{yy} and peel stress σ_{zz} are affected the most with the introduction of a hole in the overlap area. The increase in shear stress is relatively small.

Table 3.1: Effect of hole size on the maximum stresses at the mid-length of the adhesive layer at Section AA at a 100-N load

Hole Diameter	σ_{xx} **(MPa)**	σ_{yy} **(MPa)**	σ_{zz} **(MPa)**	τ_{yz} **(MPa)**
No Hole	-0.017	0.027	-0.022	-0.153
2 mm	0.059	0.107	0.090	-0.189
3 mm	0.076	0.158	0.118	-0.171
4 mm	0.085	0.166	0.134	-0.171
5 mm	0.089	0.170	0.139	-0.177

3.4 Effect of Hole Offset on Stress Distributions and Maximum Stress

This section examines how the stresses are affected when the hole is located off-centered. The 3-mm hole is located 2.5 mm off-centered in the overlap area and it is closer to Section BB, the reaction-side end of the overlap. The distance between the hole edge and Section BB is 2.25 mm compared to 4.75 mm for the centered hole.

All stress components are relatively larger near the hole in the adhesive layer. Near the reaction and loading sides, the stresses are similar to the specimen with the hole in the center. At Section B-B, all the normal stress components σ_{xx}, σ_{yy} and σ_{zz} are positive, i.e., tensile in nature; however, near the hole, all three stress component values have decreased to negative values;

compressive in nature. In comparison to the above, the in-plane shear stress (τ_{yz}) is negative in nature and decreases towards the positive values as we go near the center from the edges.

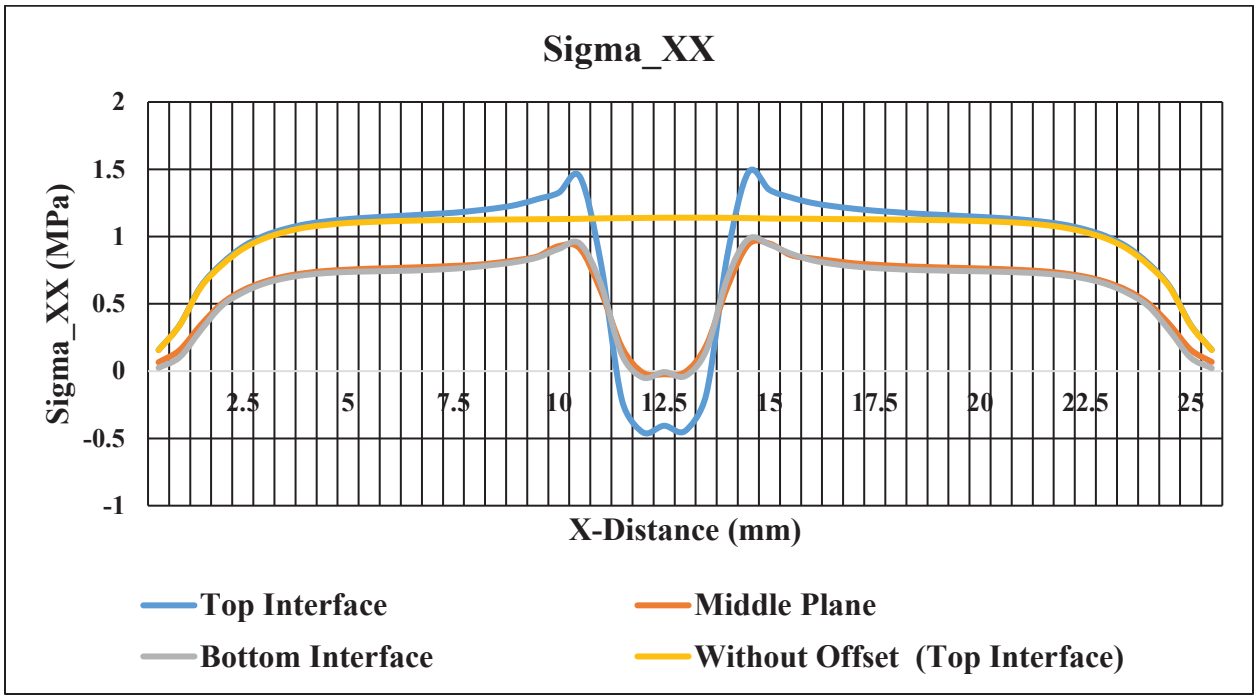

(a) Width-direction stress (σ_{xx}) along BB

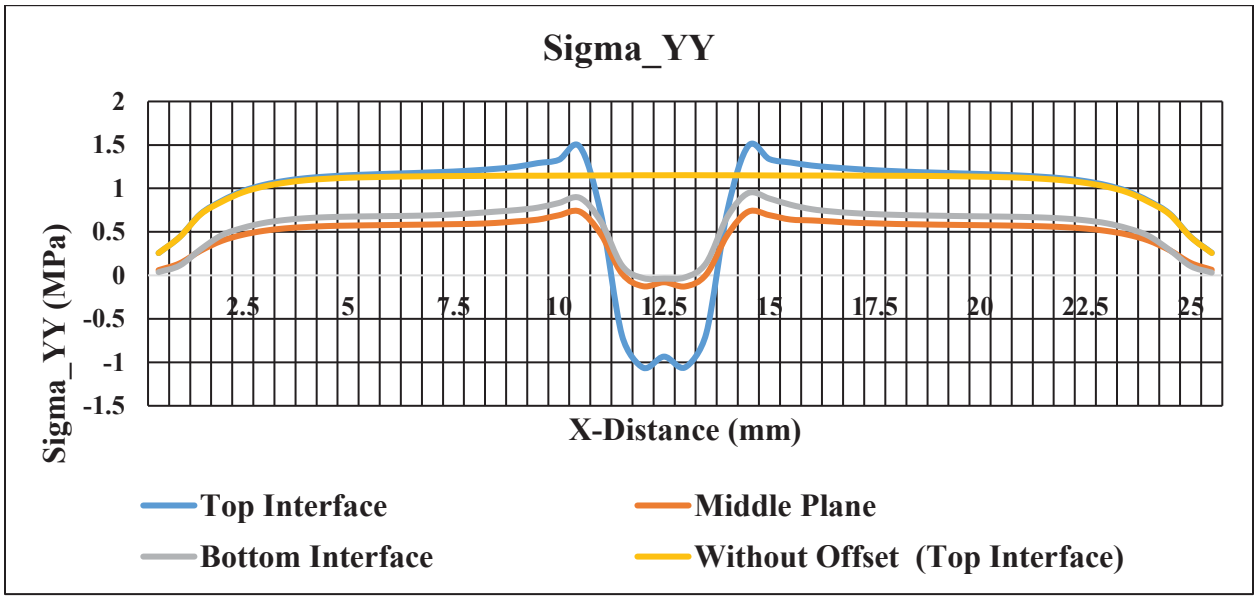

(b) Longitudinal stress (σ_{yy}) along BB

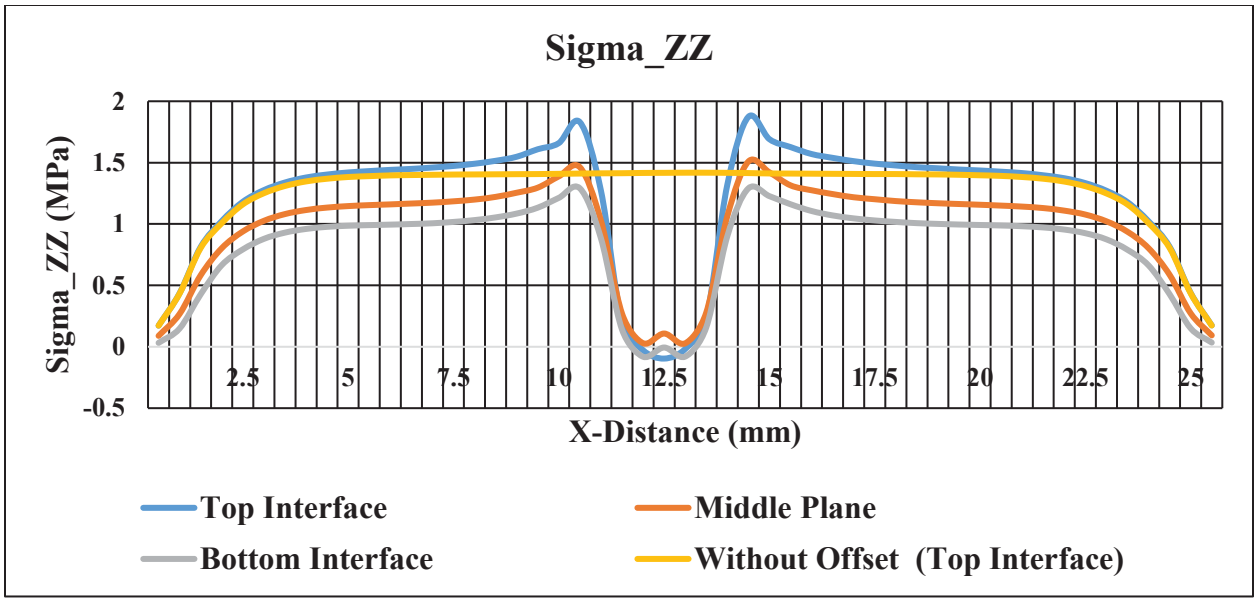

(c) Peel stress (σ_{zz}) along BB

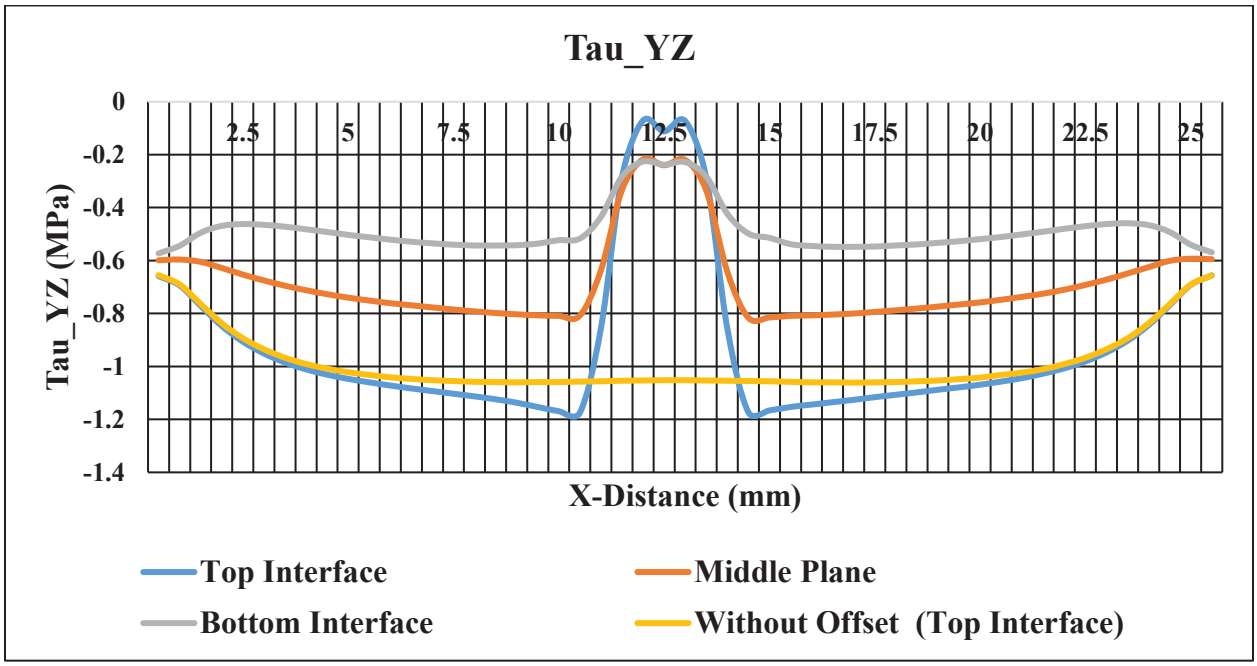

(d) In-plane shear stress (τ_{yz}) along BB

Figure 3.8: Stress distributions for the hole offset to the center of the adhesive at a tensile load of 100 N

3.5 Effect of Clamping Pressure on the Stress Distributions in the Adhesive

This section deals with the stress distributions in the adhesive layer of combined bolted-adhesive joints. However, instead of using an actual bolted connection, the clamping pressure needed for tightening the bolt is imposed on the substrates around the hole. It was observed in Section 3.3 that the presence of a hole can generate high tensile normal stresses at the hole edges. The interest here is to examine the nature of stress mitigation around the hole boundary as a clamping pressure is imposed.

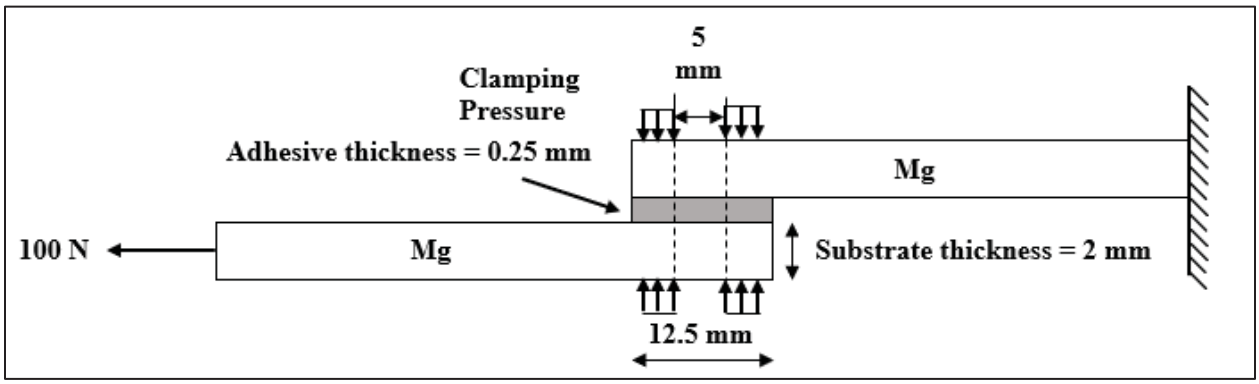

Figure 3.9: Single lap adhesive joint with clamping pressure

In this study, three different hole diameters are considered, namely 2. 3 and 5 mm. The applied clamping pressures on the top and bottom substrate are 1, 2, 5 and 10 Mpa on the top and bottom substrate. The circular areas of pressure application around the holes are 16.5 mm^2 for the 2-mm hole, 31.5 mm^2 for the 3-mm hole and 59 mm^2 for the 5-mm hole. The 5-mm hole configuration is shown in Figure 3.9.

Figure 3.10 shows the distributions of all four significant stress components along Section at the top interface, mid-thickness and bottom interface for a specimen with 5-mm hole and 2 Mpa clamping pressure. This figure also includes the stress distributions along Section AA with no clamping pressure. It can be observed in Figure 3.10 that with 2 Mpa clamping pressure, all three normal stresses are compressive over a distance of 5 mm from the hole edges their peak values occur at about 2 to 3 mm distance away from the hole edges. At the hole edges they are still compressive, but decrease to lower values. Without the clamping pressure, the normal stresses are tensile at the hole edges. The compressive normal stresses due to the clamping pressure are much

higher in magnitude than the tensile normal stresses without any clamping pressure. The in-plane shear stress is slightly higher than that without the clamping pressure.

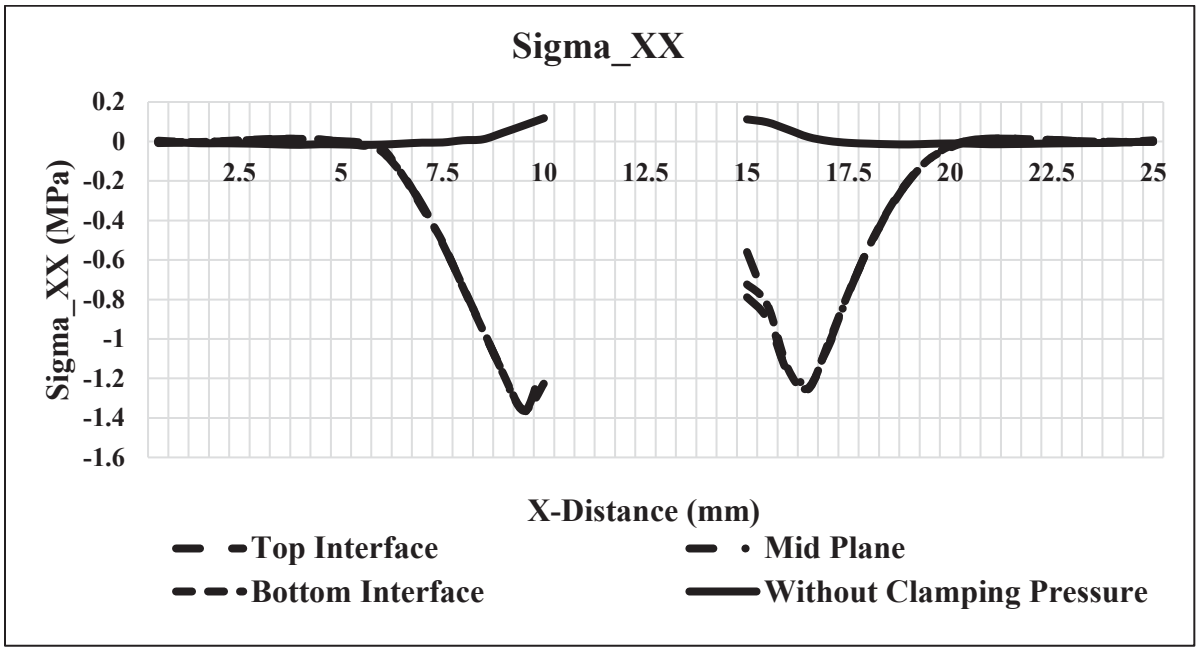

(a) Width-direction stress (σ_{xx}) along AA

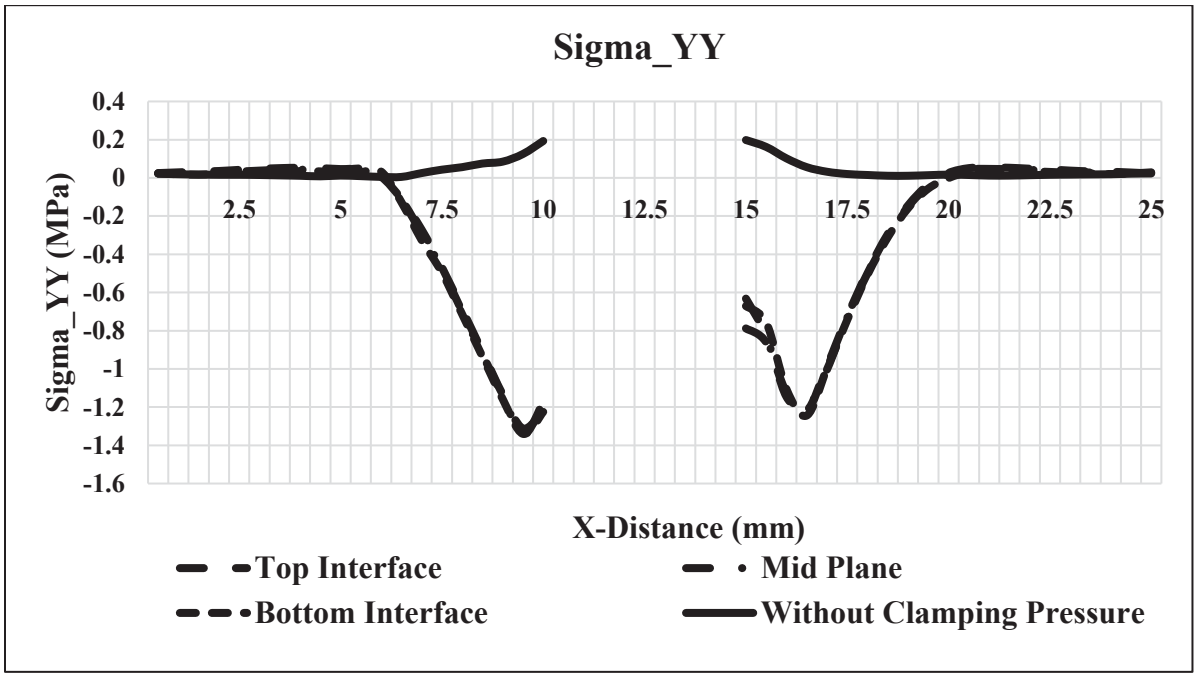

(b) Longitudinal stress (σ_{yy}) along AA

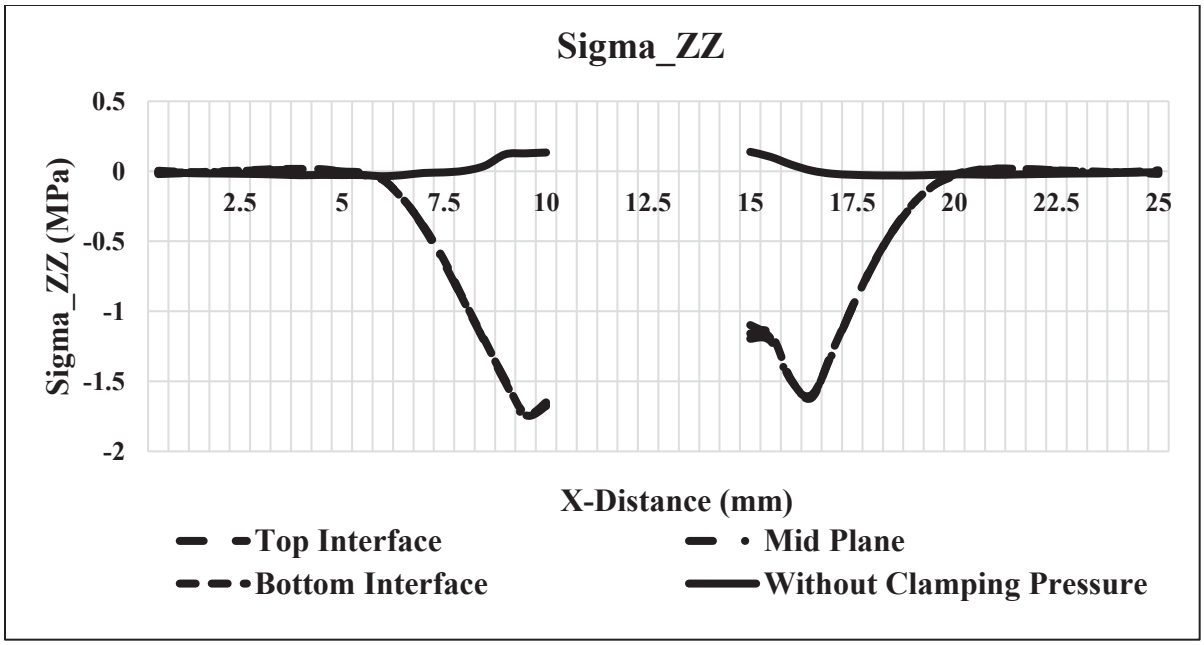

(c) Peel stress (σ_{zz}) along AA

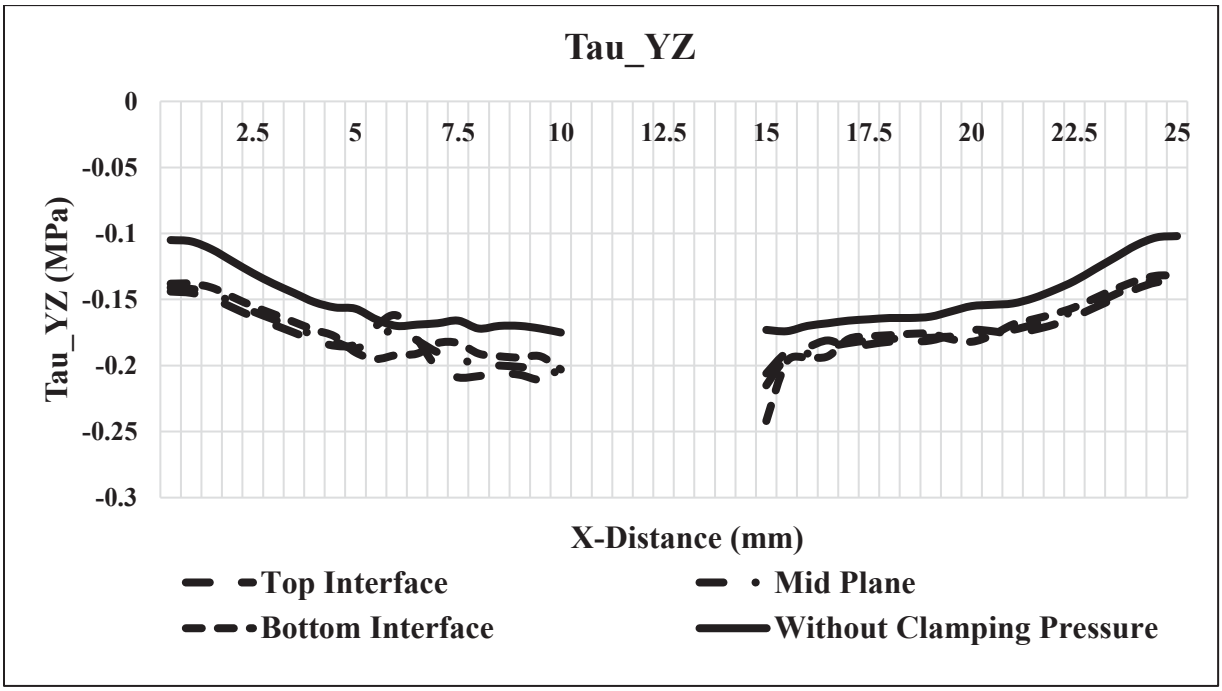

(d) Shear stress (τ_{yz}) along AA

Figure 3.10: Stress distributions in the adhesive layer at Section AA with a 5-mm hole and 2 MPa clamping pressure

Figure 3.11 shows the stress distributions for all four significant stress components along Section CC, i.e, in the adhesive length-direction at the top interface, mid-thickness and bottom interface for a specimen with a 5-mm hole and 2 Mpa clamping pressure.

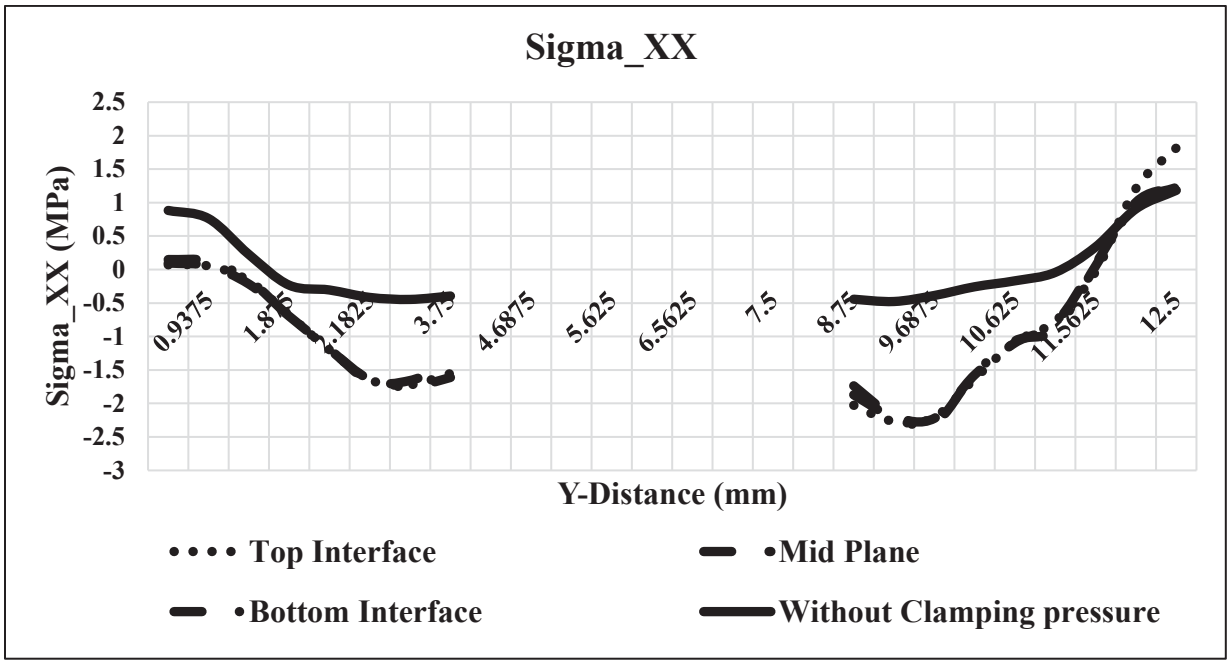

(a) Width-direction stress (σ_{xx}) along CC

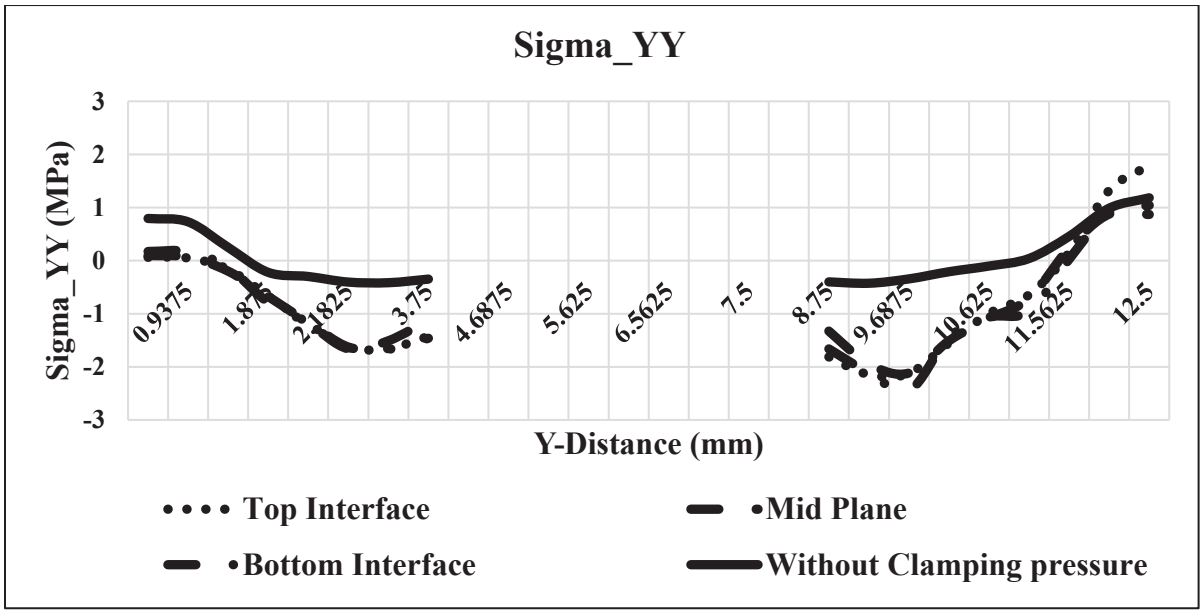

(b) Longitudinal stress (σ_{yy}) along CC

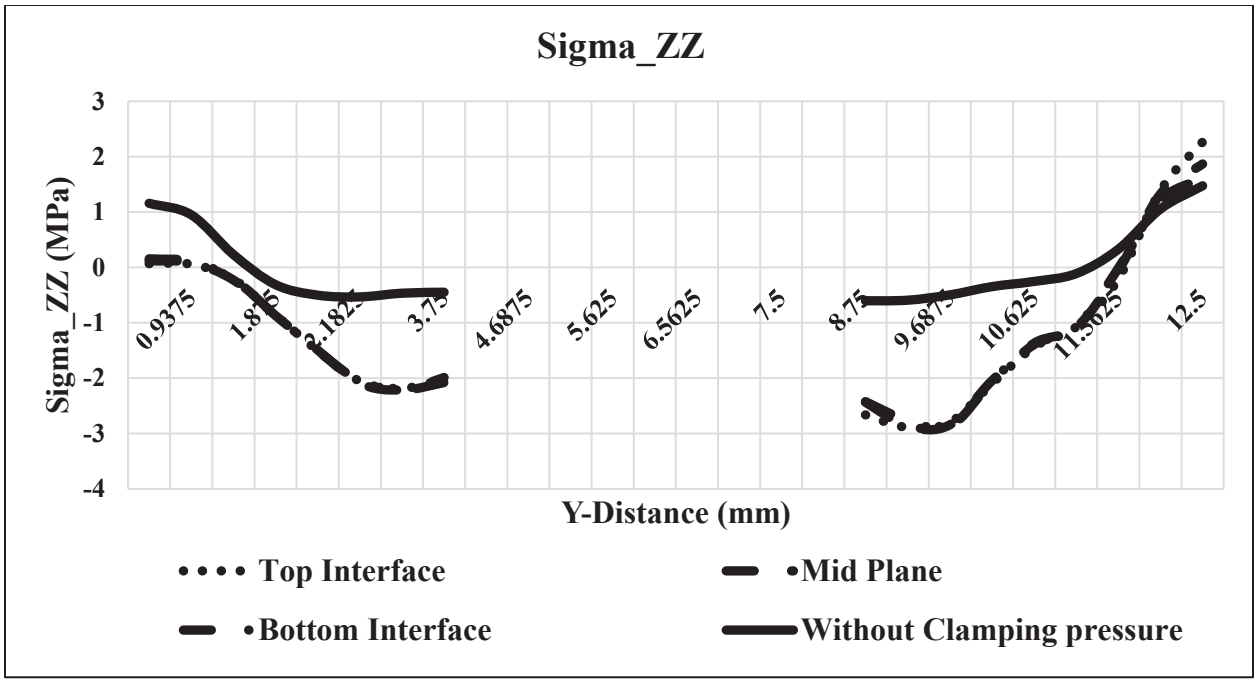

© Peel stress (σ_{zz}) along CC

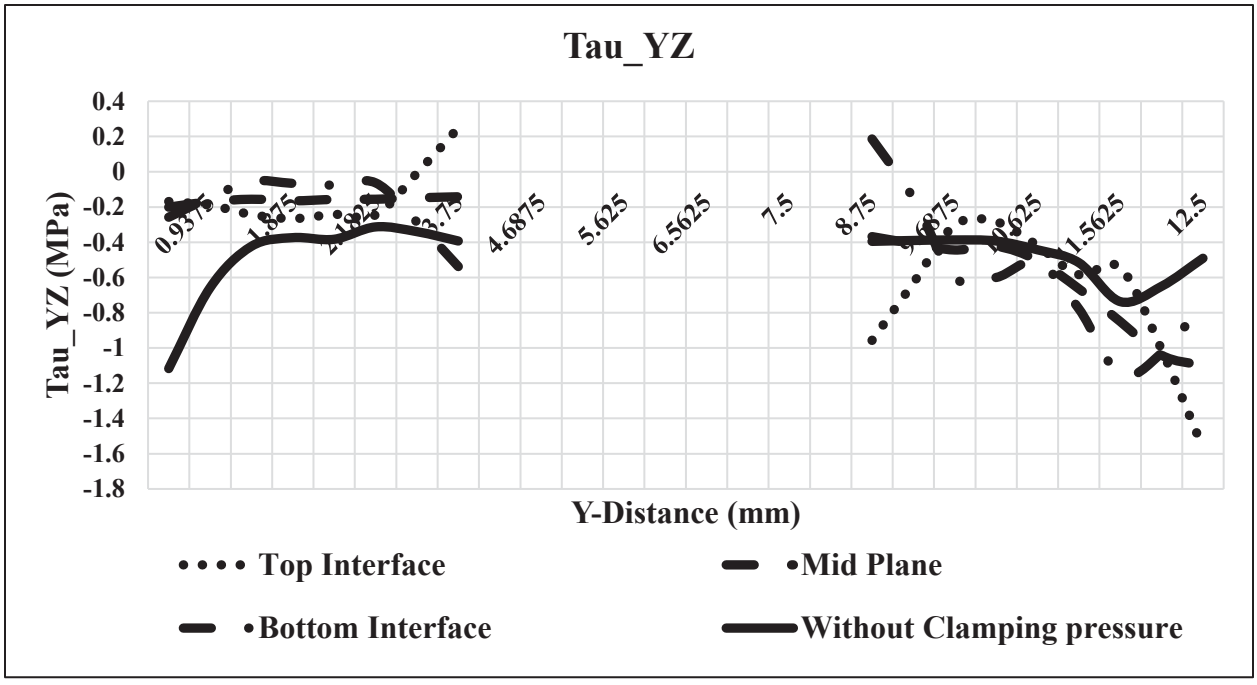

(d) Shear stress (τ_{yz}) along CC

Figure 3.11: Stress distributions in the adhesive layer at Section CC with a 5-mm hole and 2 MPa clamping pressure

Table 3.2 shows a comparison of the maximum stresses for different specimens corresponding to four different values of lateral pressure. It can be seen from the results that all six components of stresses would increase if the hole diameter is increased. However, if the clamping pressure is increased, there is decrease in the stress values. The normal stresses, instead of being tensile, are now compressive in nature. The higher the clamping pressure, the lower are the normal stresses. Among all the stress components, the peel stress (σ_{zz}) has the highest value and is compressive in nature. The other two normal stresses (σ_{xx} and σ_{yy}) are lower than the peel stress values but they are comparable to each other. The in-plane shear stress (τ_{yz}), although still very low, increases compared to the specimen with no clamping pressure.

Table 3.2: Comparison of the maximum stresses near hole in the adhesive layers due to clamping pressure

Hole Diameter	Lateral Load	σ_{xx} (Mpa)	σ_{yy} (Mpa)	σ_{zz} (Mpa)	τ_{yz} (Mpa)
No Hole(1)	**0 MPa**	1.144	1.160	1.423	-1.069
	0.5 MPa	-0.631	-0.617	-0.799	-0.148
	1 MPa	-0.924	-0.894	-1.160	-0.146
	2 MPa	-1.846	-1.814	-2.314	-0.143
	5 MPa	-4.608	-4.571	-5.771	-0.196
	10 MPa	-9.212	-9.164	-11.531	-0.304
2 mm	**0 MPa**	1.457	1.488	1.831	-1.192
	0.5 MPa	-0.464	-0.453	-0.581	-0.195
	1 MPa	-0.470	-0.445	-0.635	-0.193
	2 MPa	-0.972	-0.958	-1.302	-0.200
	5 MPa	-2.475	-2.495	-3.297	-0.234
	10 MPa	-4.979	-5.055	-6.620	-0.288
3 mm	**0 MPa**	1.411	1.551	1.779	-1.190
	0.5 MPa	-0.559	-0.498	-0.699	-0.057
	1 MPa	-0.538	-0.515	-0.732	-0.140
	2 MPa	-1.222	-1.196	-1.550	-0.138
	5 MPa	-3.105	-3.181	-4.140	-0.123
	10 MPa	-6.311	-6.508	-8.395	-0.246
5 mm	**0 MPa**	1.495	1.858	1.797	-1.184
	0.5 MPa	-0.680	-0.614	-0.848	-0.076
	1 MPa	-0.575	-0.534	-0.793	-0.190
	2 MPa	-1.359	-1.312	-1.714	-0.217
	5 MPa	-3.218	-3.263	-4.325	-0.210
	10 MPa	-6.523	-6.676	-8.741	-0.385

(1) Overlap area = 12.5 mm x 25 mm =312.5 mm^2.

3.6 Stress Distributions at the Interface in a Single Lap Joint with a Central Hole, but without the Adhesive

The final study in this chapter involves stress determination in a lap joint in which the two substrates are joined directly without the adhesive. There is a 5-mm diameter central hole in the overlap area. The loading and boundary conditions are the same as in the case of adhesive joints studied previously. The finite element model of this direct joint is shown in Figure 3.12. The mesh pattern and the material properties are the same as before. The top and bottom substrates share common nodes at the interface where a stick type contact condition was also imposed.

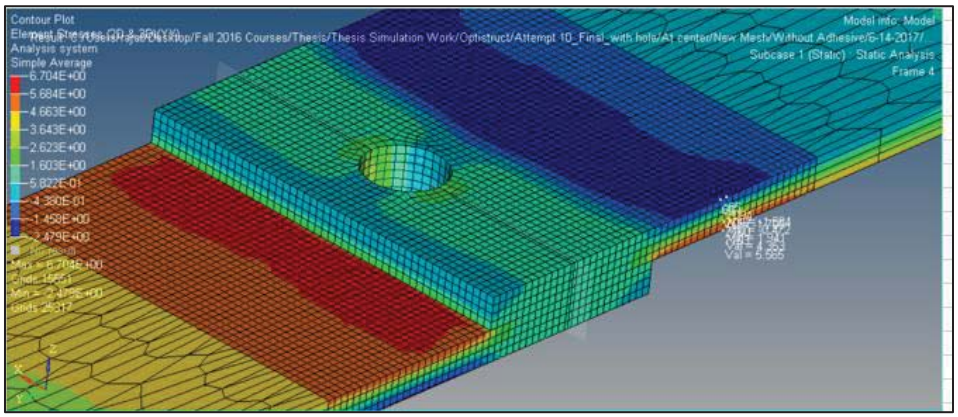

Figure 3.12: *FEM* Model of the Single Lap Joint without the Adhesive

Figure 3.13 shows the distributions of all four significant stress components in the adhesive length (y-direction) at top interface and bottom interface of a magnesium-magnesium direct single lap joint at a load of 100 N. The width-direction stress σ_{xx}, increases sharply near the hole; however, its peak value occurs at 1.5 mm away from the hole edges. There is a decrease in its value while approaching the edge of the hole. The peel stress σ_{zz} is tensile at the hole edges and decreases rapidly to near-zero values within a distance of 1.5 mm from the hole edges. The behavior of the longitudinal stress σ_{yy} is similar to that of the peel stress σ_{zz}. It can also be observed that all three normal stresses are significantly lower when a 0.25 mm adhesive layer is present between the substrates in the overlap area. The highest value of the in-plane shear stress τ_{yz} occurs at the ends of the width. At the hole edges, their values are lower and they have also changed signs, meaning that there is change in direction of the shear stress. The in-plane shear stress is higher in

magnitude and does not change in direction when there is an adhesive layer present between the substrates.

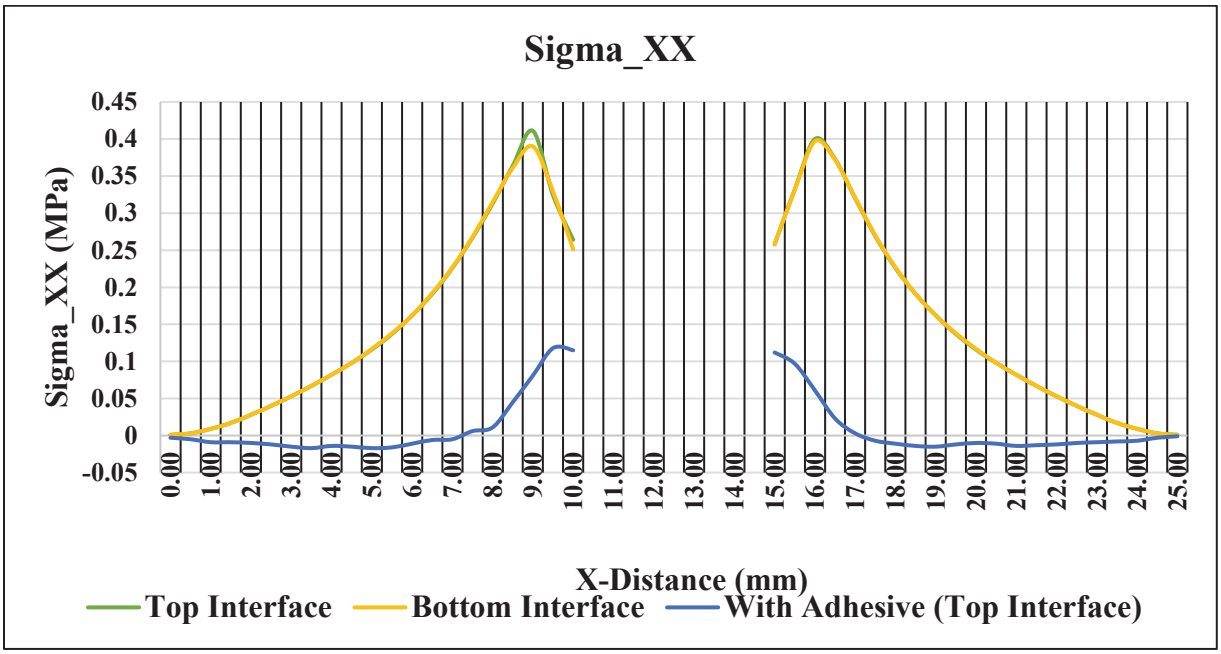

(a) Width-direction stress (σ_{xx}) along AA

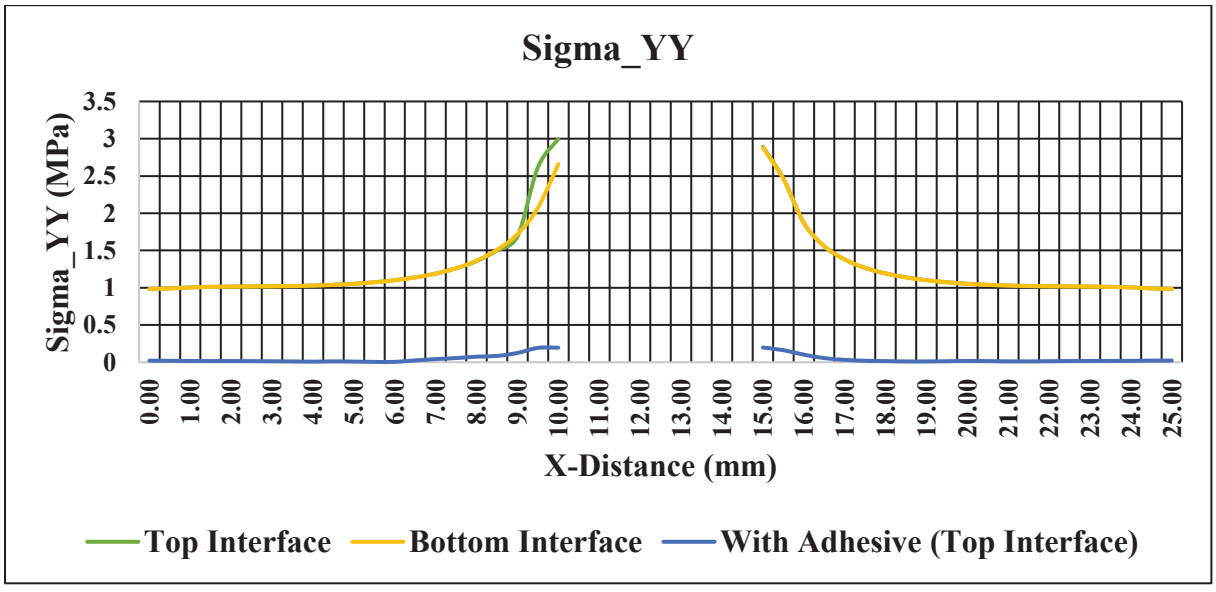

(b) Longitudinal stress (σ_{yy}) along AA

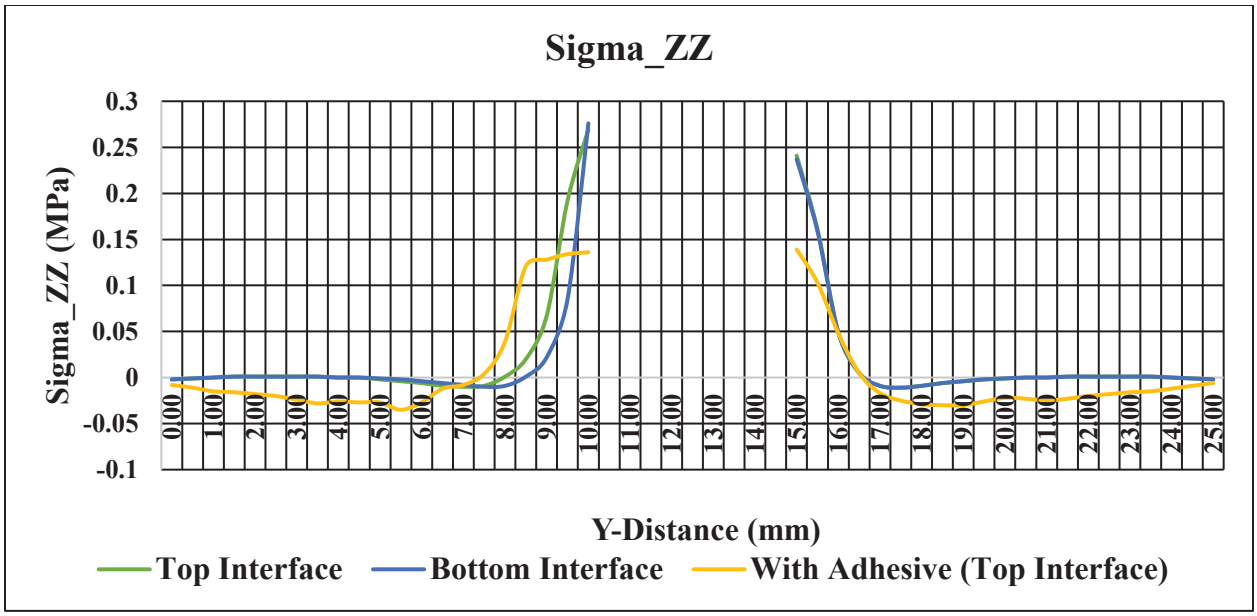

(c) Peel stress (σ_{zz}) along AA

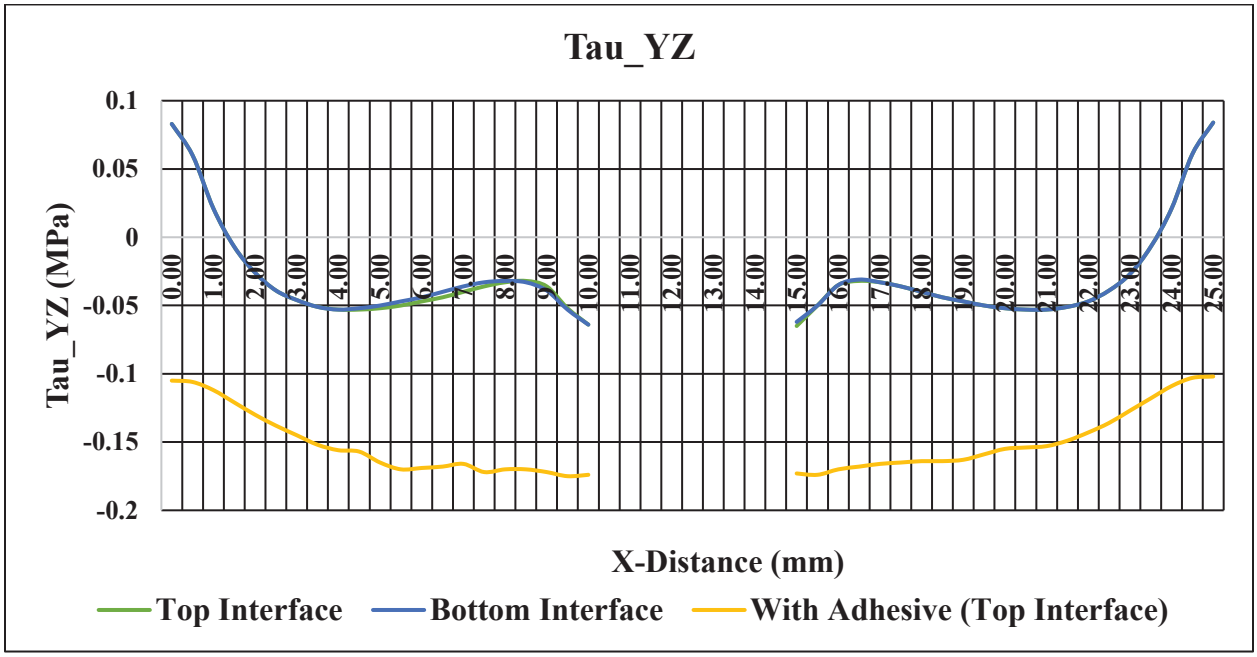

(d) In-plane Shear Stress (τ_{yz}) along AA

Figure 3.13: Comparison of stress distributions along the adhesive with direction at 'Section A-A' for a single lap joint with and without the Adhesive

3.7 Conclusions

In this chapter, the stress distributions and maximum stresses were determined for a single lap joint with a hole locate centrally at the mid-length of the overlap. It is shown that the normal stresses at the hole edges are not only tensile, but also much higher in magnitude compared to the stresses if there was no hole present in the joint. Increasing the hole size increases these stresses, while the in-plane shear stress is not affected significantly. A centrally located hole does not influence the stresses at the overlap ends; however, if the hole is off-centered, the stresses at the overlap end closest to the hole edges are modified. The application of clamping pressure significantly decreases the maximum normal stresses at the hole edges and changes them from tensile to compressive stresses. The in-plane shear stress, however, is increased. Finally, it is shown that a layer of adhesive between the substrates has a very beneficial effect on the maximum normal stresses at the hole edges, since they are much lower than the two substrates are directly joined.

References

1. Adams RD and Wake WC, Structural adhesive joints in engineering. London: Elsevier Applied Science Publishers Ltd.; 1984.

2. Shigley, J. E. and Mischke, C. R., Mechanical Engineering Design, 5th Ed., New York: McGraw-Hill Publishing Co.;1989.

CHAPTER 4

Conclusions

4.1 Conclusions

Following conclusions can be derived upon the three-dimensional stress analysis of a single lap adhesive joint between two magnesium substrates.

The stress analysis along the width, length and thickness directions of the adhesive layer in case of a specimen without a hole shows that σ_{xx}, σ_{yy}, σ_{zz} and τ_{yz} have significantly higher values at the reaction and loading sides of the overlap, while τ_{xy} and τ_{xz} have comparatively lower values. The distributions of σ_{xx}, σ_{yy}, σ_{zz} and τ_{yz} are symmetric about the mid-width, whereas the distributions of τ_{yz} and τ_{xz} are anti-symmetric about the mid-width.

- In addition to the longitudinal and peel stresses, there is a significant width-direction normal stress at the top and bottom interfaces. Thus, the stress state in the adhesive layer is tri-axial in nature, which a two-dimensional stress analysis will not exhibit. All three normal stresses have their highest values at the overlap ends where the in-plane shear stress also has its highest value.
- The difference in substrate thickness is shown to cause significant difference in bending deformation and joint rotation. As the ratio of the bottom and top substrate thicknesses is increased, both bending deformation and joint rotation are decreased. The peel stress and in-plane shear stress values have their lowest values when the two substrate thicknesses are equal and therefore, their bending stiffness values are also equal.
- Application of lateral pressure on the overlap area of the substrates can cause significant reduction in the maximum peel stress. With increasing values of the lateral pressure, the peel stress at the lap ends becomes increasingly compressive, which can be beneficial in terms of preventing joint failure due to high tensile peel stress which ordinarily exists at the overlap ends without the lateral pressure. However, there

is also an increase in in-plane shear stress with increasing lateral pressure. This can contribute to shear failure at the joint.

- If the single lap joint contains a hole located centrally at the mid-length of the overlap, the normal stresses at the hole edges are not only tensile, but also much higher in magnitude compared to the stresses if there no hole is present in the joint. Increasing the hole size increases the normal stresses, while the in-plane shear stress is not affected significantly.
- A centrally located hole does not influence the stresses at the overlap ends; however, if the hole is off-centered, the stresses at the overlap end closest to the hole edges are modified.
- The application of clamping pressure significantly decreases the maximum normal stresses at the hole edges and changes them from tensile to compressive stresses. The in-plane shear stress, however, is increased.
- A layer of adhesive between the substrates has a beneficial effect on the maximum normal stresses at the hole edges, since they are much lower with the adhesive than when the two substrates are joined directly.

4.2 Recommendations for Future Work

The present work lays the foundation for future studies for the analysis and research in the field of adhesive bonded joints.

- The finite element analysis performed in this thesis was a linear static analysis and does not consider either the geometric non-linearity or the material non-linearity that may occur at high loads. There may also be a variation in properties due to temperature change, which was also not considered. Thus, future analytical work may consider non-linear analysis with material property variation as a function of temperature.
- This study has shown that lateral pressure, whether applied directly on the overlap area or by clamping a bolted joint, has a beneficial effect in reducing peel stresses in adhesive joints. Experimental verification of this observation is another possible future work that can provide a better understanding of the stresses.